Integration of Distributed Energy Resources in Low Voltage Electricity Networks

Peter Richardson B.E.

A thesis submitted to
University College Dublin
in fulfilment of the requirements
for the degree of

Philosophiæ Doctor

College of Engineering and Architecture
School of Electrical, Electronic and Communications Engineering

Supervisor: Dr Andrew Keane
Co-supervisor: Dr Damian Flynn
Nominating Professor: Prof. Mark O'Malley
Head of School: Prof. Tom Brazil

January 2012

Abstract

The introduction of distributed energy resources (DER) is leading to significant changes in the way in which power systems are planned, operated and maintained. DER includes many different types of technology, ranging from producers of electricity such as microgeneration units to consumers of electricity such as heat pumps and electric vehicles. High penetrations of these new technologies are introducing new challenges for power systems as existing electricity networks were not originally designed to accommodate them.

This thesis investigates the potential impact of DER in distribution systems, in particular low voltage residential networks, in terms of end-user voltage levels and thermal loading of network equipment. Deterministic and stochastic methods are used to analyse low voltage residential test networks. Acceptable penetration levels of various DER technology are assessed while maintaining the network within permissible operating limits. A stochastic assessment of the network with various penetration levels of DER is also performed to incorporate a number of the uncertainties associated with DER, such as time-of-use and energy requirements.

In order to accommodate high penetrations of DER on existing low voltage distribution networks, a method for controlling their operation in a coordinated manner is proposed. The method controls the operation of DER units in order to fully utilise the available capacity of the network while maintaining acceptable operating limits. While the method is applicable to other forms of DER, electric vehicle technology is chosen to demonstrate the potential benefits. The technique is based on linear programming and determines the optimal charging rate for each electric vehicle in order to maximise the total power that can be delivered to all of the vehicles. The results show that high penetrations of electric vehicles can be accommodated on existing residential networks, thereby avoiding unnecessary network upgrades.

The method for controlling DER operation described above is based on a centralised control scheme where a third-party operator has real-time knowledge of operating conditions at all points of the network. Implementing such a scheme would require a significant investment in communication infrastructure in order for the controller to receive and transmit charging rate commands to all electric vehicles on the network. As such, a distributed control technique is proposed whereby individual electric vehicle charging units attempt to maximise the charging rate for their vehicle while maintaining local network conditions within acceptable limits. The method would require less communications infrastructure than the centralised control method. Results demonstrate that the method is not as accurate as the centralised control technique at maintaining the network within acceptable operating limits and that distributed control charging schemes may only be sufficient for dealing with lower penetrations of electric vehicles or other forms of DER.

Contents

Acknowledgements

I would like to thank all those whose help and support have contributed to this thesis. In particular, there are a number of people to whom I owe special thanks:

Firstly, my supervisor, Dr Andrew Keane, for his guidance, support and encouragement throughout my PhD. Despite the growing number of students coming under his supervision over the last number of years, he has always had time to discuss my work and provide advice. Without all of his hard work and dedication, I have no doubt that completing this thesis would not have been possible. He has truly been an excellent mentor and to him, I express my most sincere thanks.

My co-supervisor, Dr Damian Flynn, for all of the help and advice that he has provided during my PhD. He has always been a fantastic sounding board for any of my ideas or thoughts and I am most grateful for all of the effort and commitment that he has put into this thesis.

Dr Jason Taylor of the Electric Power Research Institute for his collaboration on the work involving the stochastic scenario analysis method.

Professor Mark O'Malley for providing me with the opportunity to undertake a PhD in the ERC. His commitment to the growth and development of the ERC is immense and I am privileged to have been a part of it.

All of the staff in the ERC, in particular to Magdalena Szczepanska for all of her help over the past number of years.

ESB Networks and ESB Ecars. In particular, I would like to thank Teresa Fallon, Ellen Diskin, James Gallagher, Anthony Walsh, and Declan Moran for their help and advice throughout my PhD.

The Electric Power Research Institute for my visit to their research centre in Knoxville. In particular, I wish to thank Mark McGranaghan and Roger Dugan for organising the visit and for their fantastic hospitality.

Science Foundation Ireland who have supported my research over the last four years through the Charles Parsons Energy Research Awards Scheme.

All of the students in the ERC for making the research centre such an enjoyable place to study over the past four years, not to mention some of the great extracurricular group activities that were had along the way. At this stage, there are too many people to thank individually. However, I would like to mention Eknath Vittal, Aonghus Shortt and Niamh Troy who have been there with me since the beginning of my PhD. They have not only been great craic during that time but great friends as well. Particular thanks are also due to Alison O'Connell for proof reading this thesis.

My family, Paul, Fionnuala, Eimear and Niamh. In particular, I would like to thank my parents for their constant support and encouragement throughout not only my education but my entire life.

My grandparents, extended family and friends. In particular, to my uncle, Michael, who inspired me to pursue a career in engineering.

Finally Christina, for the endless encouragement, support and belief in me which have been of enormous help to me over the last number of years. Thank you for everything.

List of Publications

Journal Publications:

P. Richardson, D. Flynn, and A. Keane, "Local vs. centralised charging strategies for electric vehicles in low voltage distribution systems," *IEEE Transactions on Smart Grid,* Special issue on "Applications of smart grid technologies on power distribution systems". In press.

P. Richardson, D. Flynn, and A. Keane, "Optimal charging of electric vehicles in low voltage distribution systems," *IEEE Transactions on Power Systems,* vol. 27, no. 1, pp. 268-279, February 2012.

Conference Publications:

P. Richardson, J. Taylor, D. Flynn and A. Keane, "Stochastic analysis of the impact of electric vehicles on distribution networks," *CIRED 21st International Conference on Electricity Distribution,* Frankfurt, Germany, 2011.

P. Richardson, D. Flynn and A. Keane, "Impact assessment of varying penetrations of electric vehicles on low voltage distribution systems," *IEEE PES General Meeting,* Minneapolis, MN, USA, 2010.

P. Richardson and A. Keane, "Impact of high penetrations of micro-generation on low voltage distribution networks," *CIRED 20th International Conference on Electricity Distribution,* Prague, Czech Republic, 2009.

List of Acronyms

Technical Acronyms:

AC	Alternating Current
AMI	Advanced Metering Infrastructure
BSOC	Battery State of Charge
CCC	Centralised Control Charging
CHP	Combined Heat and Power
CPOC	Customer Point of Connection
DC	Direct Current
DER	Distributed Energy Resource
DG	Distributed Generation
DLC	Direct Load Control
DSM	Demand Side Management
DSR	Demand Side Response
EV	Electric Vehicle
GHG	Greenhouse Gas
kV	Kilovolt
kVA	Kilovolt-ampere
kW	Kilowatt
kWh	Kilowatt Hour
kW_e	Kilowatt (Electric)
LCC	Local Control Charging
LV	Low Voltage
MV	Medium Voltage
P	Active Power
PDF	Probability Distribution Function
pu	Per Unit
PV	Photovoltaic
RER	Renewable Energy Resource
SOF	Standard Objective Function
STAR	Short Term Active Response
V	Volt

V2G	Vehicle-to-Grid
V2H	Vehicle-to-Home
VPP	Virtual Power Plant
WOF	Weighted Objective Function
WPDRS	Winter Peak Demand Reduction Scheme
Z	Impedance

Organisation Acronyms:

CER	Commission for Energy Regulation
DCENR	Department of Communications, Energy and Natural Resources
DSO	Distribution System Operator
DTI	Department of Trade and Industry UK
EC	European Commision
EEI	Edison Electric Institute
EPRI	Electric Power Research Institute
ESB	Electricity Supply Board
EU	European Union
IEA	International Energy Agency
IEEE	Institute for Electrical and Electronic Engineers
NHBC	National House Building Council UK
PSERC	Power Systems Engineering Research center
RAE	Royal Academy of Engineering
SEAI	Sustainable Energy Authority of Ireland
SONI	Systems Operator for Northern Ireland
TSO	Transmission System Operator
UNFCCC	United Nations Framework Convention on Climate Change

List of Figures

List of Tables

CHAPTER 1

Introduction

ELECTRIC power systems across the world are experiencing significant changes to the way in which they are planned and operated. Uncertainty over the price of oil, coal and gas together with increasing concerns over the security of supply of fossil fuel imports have forced governments and policy makers across the world to rethink their energy policies. In addition, the Kyoto Protocol (UNFCCC, 1997) requires participating nations to reduce their collective greenhouse gas (GHG) emissions by 5.2% from 1990 levels. The protocol was formally adopted in 1997 and has been in force since 2005. In adherence to the protocol, member states have set out their own individual, legally binding targets for GHG emission reductions.

The evolution of electric power systems across the world has led to a situation whereby electricity is typically generated by large synchronous generators and then delivered via a system of power line networks to geographically dispersed loads (EEI, 2011). Over the past decades there has been an increasing requirement for more electricity generation in order to meet the growing demand (IEA, 2011a). As large scale synchronous generators are typically based on GHG emitting fossil fuel technology, meeting the growing demand for electricity while adhering to emission reduction targets will prove to be a challenging task for governments and energy policy makers alike.

One solution to the problem of generating non-GHG emitting electricity, which is being actively pursued, is the use of distributed energy resources (DER) (EU, 2009; EC, 2004). The term DER can describe many different types of technology, including distributed generation (DG), flexible load, and energy storage devices. Many types of DG technology are designed to utilise renewable energy resources (RER) in order to generate electricity. While generation from renewable based DER can produce electricity with virtually zero GHG emissions, there are certain inherent characteristics that must be taken into account in order to successfully incorporate such technology into existing power systems. For example, the electricity output from wind generation based DG can be quite variable and as a result the units can operate at less than full capacity for significant periods of time. More significantly, from a security of supply point of view, it also means that there must be adequate generating reserve available in case of a reduction in the DG output.

DG units tend to be geographically spread out over large areas and have relatively low generating capacities. This is in contrast to the more traditional form of electricity generation from large-scale centralised power stations. Due to better resource availability and large space requirements, DG tends to be located in relatively non-populous areas which are usually located far from major load centres. Therefore, additional network infrastructure may be required in order to transfer the electricity from the DG units to the transmission network. It is typical, however, for DG to be connected to existing distribution networks in order to transmit electricity onto the transmission grid. For the most part, existing distribution networks were designed to deliver electricity from the transmission grid to the load, and not for bi-directional flow of electricity to and from the transmission grid. This has led to a number of issues arising in relation to the installation and operation of variable generation on primary distribution systems. For example, excessive voltage rise and reverse power flows. Investigating these issues as well as exploring new methods and solutions in order to successfully integrate DG into power systems has been the subject of many studies. A summary of some of the key work in this area is provided in Alarcon-Rodriguez et al. (2010).

Energy policies are not only focused on ensuring that generating technologies meet the growing electricity demand. Many countries are pursuing initiatives on the demand side also. These include introducing schemes to incentivise energy efficiency as well as demand side management (DSM) strategies. The widespread implementation of either, or both, of these schemes would see a reduction in the generation requirements of large-scale electricity generators (IEA, 2008).

The concept of a DSM scheme is not a new one and they have been in use in many countries for a number of years (SEAI, 2005). DSM schemes can take many forms and are typically tailored depending on the type of load and the response that may be required by the system operator, e.g. fast-acting response, peak load reduction (SEAI, 2005). Historically, the aim of any DSM scheme has been to reduce certain load on the power system in order to avoid excessive stress on system components, e.g. power lines, transformers. Such situations may occur during times of high power demand on the network or in the event of a system fault. Reducing the system load via DSM before, or in response to, the occurrence of such scenarios prevents overloading of system components and maintains equipment operating levels within their capability.

Typically, DSM schemes have been implemented with large industrial customers that have the ability to reduce or switch off their load in a short space of time. With the advent of advanced metering infrastructure (AMI) and Internet Protocol technology, new methods of DSM could potentially become available to system operators. Domestic customers as well as small-to-medium enterprises could also participate in DSM schemes. Customer participation could be achieved via demand side response (DSR) or by direct load control (DLC) or a combination of both. DSR could be implemented by providing customers with real-time system information, via intelligent metering devices, regarding the price of electricity and allow individual customers to take advantage of time-of-day prices by scheduling their electricity usage (Sæle and Grande, 2011). DLC, on the other hand, would allow system operators or load aggregators to directly control the operation of certain loads or generating units within a household. While DSR is more of a passive method for shifting load from peak periods to off peak periods, DLC would allow system operators to actively control a portion of the total load demand on a network. For example, such capability would allow operators to avoid the potential overloading of local network components during periods of high demand by temporarily reducing non-critical load such as charging electric vehicles.

In future years, the use of small-scale DER, or micro-DER, technology will also increase. Micro-wind turbines, solar photovoltaic (PV) cells and micro-combined heat and power (micro-CHP) units are some examples of micro-generation DER devices. However, the term DER is not only used for devices that generate electricity. Energy storage units as well as those with flexible load capability can also be described as DER devices (IEA, 2008). One example of a flexible load that will potentially see widespread implementation in future years is heat pump technology. As a result of the European Union directive on the energy performance of buildings (EU, 2010), the use of sustainable energy technologies, such as micro-generation and heat pump devices, will become more prevalent within domestic households and other buildings.

Another example of a technology that could potentially be utilised as a flexible load is the electric vehicle (EV). EV technology is seen as a means of potentially increasing use of renewable energy in the European transport sector in order to reduce GHG emissions (Bradley and Frank, 2009; Doucette and McCulloch, 2011; Element Energy, 2009; EPRI, 2007; Parks et al., 2007; RAE, 2010). However, any GHG emission reduction would be very much dependent on the source of the electricity used to charge the vehicles (Doucette and McCulloch, 2011; RAE, 2010). Nevertheless, various studies have been commissioned to investigate the potential barriers that need to be overcome in order to successfully introduce EV technology (Element Energy, 2009; PSERC, 2009; RAE, 2010). National targets for the implementation of EVs in the transport sector have been established, while many major car manufacturers are investing heavily in the research and design of the technology also (IEA, 2011b). EV technology could also offer owners and power system operators the opportunity to exploit the on-board batteries of the vehicles for use as flexible loads on the demand side. By scheduling the charging of their EV, owners could avail of cheaper off-peak electricity tariffs. System operators could manage the charging rates of EVs by using DLC methods in order to avoid overloading network components during periods of high demand. Potentially, the stored energy in the EV batteries could also be used to supply the electricity network using vehicle-to-grid (V2G) techniques (Kempton and Tomić, 2005; Tomić and Kempton, 2007). As the occurrence of EV charging increases in distribution systems, the implementation of any or all of these control methods could contribute to successfully accommodating this technology in existing distribution networks.

For the most part, micro-DER devices are usually located at the low voltage (LV) network level of distribution systems. Some forms of DER technology are designed to operate in a passive manner, such as micro-wind turbines or PV cell arrays. The output from these devices is dependent on the energy resource availability and they have no control capability apart from disconnection from the network due to wind overspeed. Operation of other forms of micro-DER are entirely dependent on user settings, e.g. scheduling the operation of a heat pump unit. User operated micro-DER technologies, together with DSM, offer the opportunity for system operators or load aggregators to manage certain loads and devices in a coordinated manner which would make the most efficient use of existing networks and delay the need for infrastructure upgrading. This could be achieved using either DSR methods, such as time-of-day pricing, or DLC, whereby operational commands are issued by the system operator to certain DER units as required.

In power systems with high penetrations of mega-watt sized DG based on RER technology, the introduction of DSM schemes together with micro-DER technology could prove to be beneficial in terms of power system operation. The potentially high levels of variability from large-scale DG could be offset by coordinating micro-DER devices at the distribution system level (Ekman, 2011; Pillai and Bak-Jensen, 2011). If the output from DG is high during periods of low demand then energy storage based micro-DER devices, such as EVs, could be used to store the excess energy. Alternatively, a reduction in the output from large-scale DG could also be offset by controlling micro-generation devices or storage devices to export electricity to the local grid until sufficient replacement plant can be brought online. As a result, the requirement for expensive, fast-acting generation could be reduced significantly (Kiviluoma and Meibom, 2010). Another benefit from the coordinated use of DSM and DER would be the local consumption of locally generated electricity, thus reducing power flows at the higher voltage levels and making more efficient use of network capacity. In the event of a fault or other similar scenario, DER units could also potentially permit a section of network to operate in an islanded mode as a micro-grid (Hatziargyriou et al., 2007).

While there are a number of potential benefits to the introduction of DER at the distribution level, the ability of existing networks to accommodate such technology must be assessed. Small-scale DER technologies are expected to be most prevalent at the LV distribution network level. However, this type of network was not designed for accommodating high penetrations of micro-generation, flexible loads or storage devices. Utilising DSM schemes will aid in accommodating these new technologies while making more efficient use of the network and postpone the need for widespread upgrading of existing infrastructure.

1.1 Thesis Objectives

As the adoption of DER technology increases, existing network infrastructure may not be able to support high penetrations of DER if operated in an uncontrolled manner. The simultaneous use of DER units could lead to voltage levels exceeding permitted limits or overloading of network components. Therefore, the first goal of the research presented in this thesis was to investigate the technical impact on existing distribution systems, specifically LV residential networks, from increasing penetrations of DER devices. Such analysis allows for a determination of the maximum permissable penetration limits of specific DER technologies with no control capability available. As the operation of many types of DER technology is actively controlled by the user, the level of coincident use of the devices on the network will be an important factor in determining their potential impact. This aspect of the widespread use of DER technology was also addressed in this thesis.

The main objective of this thesis is to investigate possible coordinated control techniques for DER devices in distribution systems. With the widespread implementation of both DER technology and more sophisticated DSM schemes, distribution systems will see a shift from traditional passive operation to a more active approach. This will be facilitated through the introduction of AMI and increased communications links between system operators/load aggregators and customers. As a result, one of the potential benefits that may arise will be the ability for the DSO or a third party to actively control the operation of certain devices within customer households. A method for the coordination of DER operation is proposed in this thesis, whereby the optimal operating set point of each unit is determined in order to utilise network capacity to its fullest. The method allows for high penetrations of DER devices to operate simultaneously while maintaining acceptable operating conditions on the network. The control technique can be implemented in either a centralised or decentralised manner and evaluating the advantages and disadvantages of both methods is the final objective of this thesis.

1.2 Thesis Contributions and Outline

The focus of this thesis is on the integration of DER technology into existing distribution systems. Chapter 2 presents a review of DER technologies currently in use on the Irish power system. A literature review of some of the more recent research investigating the potential impact from DER as well as methods for coordinating the operation of such devices is also provided. Understanding how DER devices will affect the operating conditions of the network will be crucial to determining acceptable penetration levels in a business-as-usual scenario of passive network operation. As such, Chapter 3 investigates the potential impact of DER technology on residential LV networks using two methods of analysis. Firstly, a deterministic analysis method is used in order to determine how increasing penetrations of DER devices affect the voltage levels and thermal loading of a test network. This analysis is performed for the worst case operating scenario of the network in terms of the underlying residential load already present on the network. As DER technology can include both micro-generation and flexible load devices, the analysis is performed using examples of each type of technology. The effect of the location of the DER units is also examined, as is the impact from an uneven distribution of the units across the network phases. The second method developed a stochastic based technique to generate operating profiles for both DER devices and household loads on a test network. The method takes account of the uncertainty and variability inherent with DER units and household loads by using probability distribution functions (PDFs) based on real network data obtained from DSO led field trials. By doing so, the method accounts for the spatial and temporal diversity of DER operation. Performing time-series load-flow analyses of a network using the stochastically generated profiles enables a much enhanced understanding of the severity of the impact from DER technology and the likelihood of network operating limits being exceeded.

With high penetrations of DER units on residential networks, passive operation may no longer be sufficient to ensure acceptable power quality at the customer point of connection (CPOC). Chapter 4 introduces a method for the coordinated operation of DER units in order to make optimal use of available network capacity. Here, it is assumed that a central controller has the ability to send control signals remotely to the DER units installed at the customer households. The method utilises the interdependency of the network sensitivities to the addition of DER devices and assigns each individual device with an optimal operating set point, determined using a linear programming tool. As the impact from large flexible load is demonstrated to have a more significant impact than micro-generation units in Chapter 3, the optimal coordination method is demonstrated for high penetrations of EV load in a residential LV test network. The results demonstrate that by optimising the charging rate of each EV using this technique, significantly higher penetrations can be accommodated than would be the case in a scenario with uncontrolled charging. The implementation of such a strategy allows for more efficient use of existing network capacity, which would benefit the DSO by deferring the need for costly network upgrading.

In order to implement a centralised technique across a power system, sufficient communications infrastructure is required to send bi-directional signals between the controller and individual DER devices. However, such a system may be costly to implement and it may not make economic sense until very high penetrations of DER units are present. As such, Chapter 5 presents a local control based optimisation method which differs from the centralised control method in that each DER unit determines its optimal operation set point based on local network information only. This is achieved by utilising the voltage and thermal loading conditions at the CPOC. Using these measured values, together with predetermined sensitivity values for the additional generation/demand from the DER device, an optimal operating set point is assigned for each time period. The method is once again tested for high penetrations of EV charging and results are compared to those from the centralised control method described in Chapter 5.

Conclusions for the thesis are presented in Chapter 6 together with a scope for future research work in this area.

CHAPTER 2

Distributed Energy Resources

2.1 DSM and DER in the Irish Power System

DSM schemes have been implemented on the Irish power system for many years. At present, various schemes in use involve both active and passive approaches to reducing the energy demand. The peak demand period on the Irish power system typically occurs during the winter months (EirGrid and SONI, 2010). During such periods, the potential exists for certain system components (i.e transformers, overhead lines) to exceed their rated operating capability and for generators to operate at or near maximum capacity. In order to prevent such situations from arising, there are a number of peak demand reduction schemes in place to reduce the load on the system (EirGrid, 2011). Typically the schemes involve agreements between the transmission system operator (TSO), and commercial and industrial businesses, who are financially compensated for their load reduction capability. In some cases, a reduction in demand is prearranged to occur at specific times of day during the winter season (WPDRS, 2011). In other situations, certain demand can automatically be reduced with the occurrence of a contingency event on the system (STAR, 2011). These schemes have been in use by the TSO for as long as 20 years and have proven to be an important service for maintaining system security.

Measures for increased energy efficiency on the demand side are deemed to offer significant potential benefits in terms of overall energy savings (SEAI, 2008). For residential electricity customers, government policies have seen initiatives set up to improve end-use energy efficiency by incentivising electricity customers to use more energy efficient appliances as well as improving the energy rating of their buildings (DCENR, 2009). Various campaigns have also been established to create awareness about efficient energy use amongst electricity customers (SEAI, 2011a,c). Domestic customers also have the ability to sign up to a basic dual-period time-of-use tariff which allows them to avail of cheaper electricity prices during nighttime hours (Electric Ireland, 2011). For example, this scheme is particularly beneficial to customers that utilise storage heating due to the high energy requirement and typical nighttime operating hours of the devices.

In future years, widespread introduction of a smart metering program will allow residential customers to play an even bigger role in actively managing their electricity usage. To this end, the Irish Government together with the energy regulator of Ireland commissioned smart metering trials (CER, 2011b), whereby various types of AMI with differing DSM capabilities were installed in residential households. In general, the trials concluded that the introduction of time-of-day tariffs had a positive impact on how customers managed their electricity usage, with up to 82% of participants adapting their electricity usage as a result of the new tariff structure. It is envisaged that the AMI will not only have the ability to display time-of-day electricity prices but also record electricity exported to the grid, for example from micro-generation. Over the trial period the customers response to various levels of information from the AMI regarding their energy usage, was measured to gauge the effectiveness of the technology and the different DSM schemes. Widespread introduction of smart meters to domestic electricity customers is intended to commence shortly after 2012 (CER, 2011a). Beyond this time, AMI or a similar technology will potentially facilitate the control of certain flexible load within the household. Such capability would provide system operators with a means of utilising DLC on certain loads within the customer household, e.g. storage heaters, refrigeration.

Micro-generation technology remains in the early stages of adoption in Ireland (SEAI, 2010). This is, in part, due to the high initial investment costs required for the devices. Other factors which contribute to the lack of uptake include insufficient primary energy resources for technology such as solar PV cells and micro-wind turbines. Due to its location on the edge of the Atlantic Ocean, Ireland experiences some of the best wind energy resources in Europe (SEAI, 2011b). However, unless micro-wind turbines are located in high areas with a very good wind resource and their installation costs have been heavily subsidised, they can struggle to generate enough electricity to pay back the investment cost over their life time (NHBC, 2008). The same can be said for PV cell technology due to insufficient levels of irradiance year round. Other forms of DER that are also being introduced include solar heating and heat pump technology. These forms of technology contribute to the heat energy requirements of buildings and while they can reduce heating costs, retrofitting these devices into existing buildings can cost up to 30% more than would be the case for installation in new build (NHBC, 2008). In order to continue the uptake of DER technology, government grants will remain necessary into the future until economies of scale bring initial investment costs down. Various other policies have also been introduced to increase the use of DER devices. For example, regulations have been put in place to ensure that all new domestic buildings have a minimum level of renewable technology installed (DCENR, 2009), while owners of DER units that export electricity back onto the grid can now be financially reimbursed for doing so (CER, 2010).

Another form of technology that is expected to see increased use over the coming years is the electric vehicle. Government policies have set a target of 10% of all passenger and light commercial vehicles in Ireland to be electric by 2020, while there are also financial incentives available to motorists for owning an EV (DCENR, 2009). Initiatives for the distribution system operator (DSO) to install EV charge points in residential households as well as fast-charge points along major intercity routes have also been introduced (ESB, 2011) to encourage the uptake amongst motorists.

The implementation of these various policies to encourage the use of DER technology, along with the introduction of advanced metering technology, will potentially lead to significant operational changes at the distribution network level. As customers begin to take a more active approach to managing their electricity usage in order to maximise their benefits, system operators must adapt to these new technologies while still maintaining acceptable operating levels across the entire system.

2.2 Impact of Distributed Energy Resource Technology

It is considered that micro-DER devices will mainly be located at the LV distribution network level of a power system. When LV distribution networks were originally designed and built they were only required to deliver electricity from the transmission grid to the residential loads. Investigating how micro-DER devices will impact on the traditional operation of the networks will be key to maximising the potential benefits of such technology.

Traditionally, LV distribution networks were rated to deliver electricity depending on the number of customers in any given area and their historical electricity demand (Willis, 2004). Once built, such networks were mainly operated in a passive manner with little or no system monitoring equipment past the LV transformer. However, the introduction of DER technology will alter traditional demand patterns and may result in adverse effects in terms of power quality and overloading of network components. Therefore, the largely passive operation of these networks may no longer be adequate. Understanding the potential impact that DER may have on existing networks will be crucial for ensuring safe and secure network operation.

Each type of DER technology will have a different impact on the network to which it is connected. While a single unit will most likely have a negligible impact in terms of power quality or loading, the combined effect from clusters of DER located on the same network may have quite significant impacts. The potential for such negative impacts increases even more if the majority of the units were to operate at the same time. In the case of micro-generation, studies have shown that while existing LV networks may be able to accommodate high penetrations of PV and micro-CHP, the potential exists for the reverse flow of power back up to the feeder transformer during times of low demand (Thomson and Infield, 2007a,b). Other studies of the impact from micro-CHP units on existing network have also determined that high penetrations could be accommodated without the need for network upgrading (DTI, 2003, 2004). These studies were conducted for very conservative scenarios with a high coincidence of operation at full output. Voltage and thermal loading levels appear to remain within acceptable operating ranges, and especially so for networks with tap changing capability at the feeder transformer (Silva and Strbac, 2008). Similar results were also found during field trials with a feeder of 500 houses, each with a 1 kW_e micro-CHP unit (Beddoes et al., 2007). The study noted that the introduction of high penetrations of micro-CHP could have a significant impact on the daily network voltage profile. Electricity is generated as a by-product of heat energy production from micro-CHP units. As a result, the coincident heat demand by customers at certain times of day leads to the simultaneous generation of electricity from the units. This can lead to the creation of new peak voltage levels during periods of high heat energy demand. In general, previous work investigating the impact of micro-generation has shown that existing LV networks should be able to accommodate significant penetrations of micro-generation in all but the most extreme case of simultaneous generation during low demand periods. For the most part, micro-generation tends to offset the electricity demand by load on the same network, thereby reducing the overall demand requirement of the feeder.

Flexible load DER will have a very different impact on network conditions compared to micro-generation. Typically, distribution networks have radial topologies, which result in lower voltage levels at network extremities when compared to sending end voltages at the feeder transformer. Based on historical demand data and an assumed level of coincident electricity use, networks are rated to ensure that the voltage at every customer connection point on the network is within an acceptable range under normal operating conditions (Willis, 2004). However, flexible load DER, such as EVs, will introduce a new type of demand, which will alter the typical customer load profile. The extent to which these new technologies may impact on the operating conditions of existing networks, such as voltage and loading levels, has been the subject of much research.

Investigations into the potential impact of EVs on load patterns and the need for load management at the distribution network level have been conducted since as early as the 1980s (Heydt, 1983; Rahman and Shrestha, 1993). Various system wide studies have been carried out to assess whether future power systems will have the required generating capacity and infrastructure to accept large penetrations of EVs (Denholm and Short, 2006; Hadley and Tsvetkova, 2008; Kintner-Meyer et al., 2007; Hadley, 2006; Short and Denholm, 2006). They conclude that, for the most part, existing and planned generation plant should be sufficient to meet the added demand from EVs. However, this may not be the case when this added demand coincides with existing peaks.

Some studies have also investigated the limitations from large numbers of EVs on network infrastructure in terms of increased loading, impacts on efficiency and loss of life for network assets (Gerkensmeyer et al., 2010; Putrus et al., 2009; Schneider et al., 2008; Shao et al., 2009; Taylor et al., 2009). These studies examined varying scenarios, such as unrestricted charging, peak and off-peak charging, diversified charging, and charging at varying power levels. The general consensus from these studies is that existing distribution networks should be able to accommodate substantial penetration levels of EVs if the majority of charging is restricted to low charging rates at off-peak times. Uncoordinated charging, especially fast, 3-phase charging, will lead to an increase in the number of occurrences of component overloading and excessive voltage deviations if it coincides with existing peaks from the residential load. Staggering the charging start times for localised groups of EVs is also shown to help avoid these adverse effects, as well as reducing spikes in demand due to simultaneous commencement of charging.

A review of the various studies above, which investigate the impact of DER technology on existing distribution systems, suggests that the impact from high penetrations of flexible load type DER devices will be greater than that from micro-generation devices. The following section provides a review of previous studies which have investigated intelligent control methods for accommodating flexible load devices, in particular EV load.

2.3 Intelligent Control of Distributed Energy Resource Technology

Strategies for managing the operation of DER devices will become increasingly important when high penetrations of DER units are reached. Implementing such schemes could allow for more efficient use of existing network assets while delaying the need for costly infrastructure upgrading. Other potential benefits include the use of DER for the operation of microgrids in order to allow the networks to operate in an islanded mode (Katiraei et al., 2008). In Pudjianto et al. (2007) a concept for the coordination of DER devices for use in a virtual power plant (VPP) is proposed. The VPP concept would allow DER owners to participate in the electricity market either for bulk power supply or to provide ancillary services. The system operator also benefits as the VPP can be viewed as a single market participant as opposed to many individual units. In the event of a section of distribution network becoming isolated from the main grid, in either planned or unplanned circumstances, it has been shown in Peças Lopes et al. (2006) that safe and secure operation of the network can be maintained by controlling the operation of DER units and storage devices. Similar results are found in Peças Lopes et al. (2010, 2011) where the authors propose management strategies for EV charging/discharging in LV microgrids. By allowing network control devices to respond to voltage and frequency levels, it is shown that the EV load can enable LV microgrids to be operated in a stable manner.

The use of EVs as flexible load has been the subject of much recent research. This is, in part, due to the expected increase in the future uptake of EV technology in the transport sector (IEA, 2011b). The introduction of AMI devices in residential housing, be it for real-time pricing or active DSM, or both, will aid the control/predictability of the load patterns on residential networks. With high penetrations of EVs connected to the network, it is envisaged that EV charging could potentially be controlled to gain certain benefits in other aspects of power system operation. For example, shifting the majority of EV charging to off-peak periods through the use of DSR or DLC methods would reduce the system peak demand while increasing the use of more efficient base-load plant (Camus et al., 2009; Mullan et al., 2011; Perujo and Ciuffo, 2010). Similarly, in Shortt and O'Malley (2009), it is demonstrated that by controlling the charging of EVs to operate at off-peak times, significant savings to the average cost of electricity can be achieved due to the increased use of cheaper base-load plant. Various studies have also been undertaken to assess the potential benefits from using flexible EV load in conjunction with high penetrations of wind generation (Ekman, 2011; Pillai and Bak-Jensen, 2011; Wang et al., 2011). Results from these studies indicate that, by coordinating the charging of EVs, system operators can more easily achieve a balance between generation and demand on systems with high amounts of variable generation.

Much research into the coordination of EVs to improve the operational performance of distribution networks has also been conducted. In Sortomme et al. (2011), the charging schedule of EVs on a network is optimised with the objective of minimising losses. Results show that minimisation of losses can achieve a 20% reduction for 50% EV penetration and a 30% reduction for 100% penetration. Work described in Deilami et al. (2011) also demonstrates the potential reduction in network losses from the use of controlled EV charging. In this work, a charging strategy designed to operate in real-time is proposed in order to schedule EVs on a network with the objective of minimising costs. Results show that loss reductions in the region of 70% are achievable for EV penetrations of approximately 50%. In Acha et al. (2010), a technique is employed to minimise power losses and on-load tap changes for the network transformer, mainly due to the charging/discharging of EVs located far from the slack bus. In Clement-Nyns et al. (2009, 2010) the authors use quadratic and dynamic programming techniques to minimise the impact from EV charging on network losses and deviations from nominal voltage on residential networks. By controlling and optimising individual EV charging rates, network losses and voltage deviations are reduced for all penetration levels examined.

2.4 Summary

Much of the previous work on intelligent control of DER focused on developing techniques for reducing the potential network impact from DER devices, for example, minimising losses and peak loading reduction. This thesis proposes new methodologies for the coordination of DER devices with the aim of maximising the use of existing network capacity while maintaining acceptable network operating conditions. Demonstrations of the methods show that, by employing such methods, higher penetration levels of DER can be accommodated on existing networks compared to scenarios with uncontrolled DER, thus deferring the need for costly reinforcement of network infrastructure.

CHAPTER 3

Impact of Distributed Energy Resources on Low Voltage Networks

3.1 Introduction

DISTRIBUTION networks are rated (kVA limit) to deliver electricity depending on the number of customers in a given area and the historical electricity demand data for each of those customers. Widespread adoption of DER technology will introduce new customer demand and generation patterns, and high penetrations could result in adverse effects on the network. Such effects include excessive voltage variations and overloading of network components (e.g. power lines and transformers). Maintaining network operating conditions within acceptable limits is necessary to ensure adequate power quality for electricity customers.

A number of previous studies have investigated the impact from the introduction of micro-generation into distribution systems. In Thomson and Infield (2007a) and Thomson and Infield (2007b), the authors use an unbalanced load-flow tool to analyse the impact from micro-CHP units and PV cell arrays on a test network, in terms of voltage levels and network losses. They conclude that, under normal operating conditions, distribution networks should be able to accommodate large penetrations of both technologies. It is noted, however, that the ability of a particular network to accommodate micro-generation is very much dependent on the existing voltage control practices of the DSO. Similar results were found in DTI (2003), where a test distribution system was found to be able to accommodate a 40-50% penetration of micro-generation units without exceeding voltage limits. These results were determined under a conservative scenario of minimum network load with a high coincidence of micro-generation operation. The study also concluded that the location of the units on the network had a significant influence on the node voltage levels with some scenarios permitting a maximum penetration level of less than 40%.

The impact on voltage levels and component loading from high penetrations of heat pumps on LV distribution systems is examined in Akmal et al. (2011). Results show that penetration levels of up to 20% can be installed before potentially overloading LV transformers. The study also shows that the high starting current of heat pump devices operating simultaneously can lead to transient voltage drops which can exceed acceptable limits. A number of studies have also investigated the potential impact from EV charging on existing networks. In Taylor et al. (2009); Maitra et al. (2010); Schneider et al. (2008), the impact on network infrastructure is assessed in terms of increased loading and loss of life for network assets. Other work has assessed the impacts on LV transformers in terms of efficiency and overloading, and concluded that large penetrations of EVs can create new peak loads from an LV transformer's point of view (Shao et al., 2009). The work described in Putrus et al. (2009) examines the impact of EVs on distribution networks in terms of supply/demand matching, voltage deviations and power quality. The general consensus from these studies is that existing distribution networks should be able to accommodate early penetration levels of EVs if the majority of charging is restricted to low charging rates at off-peak times.

This chapter investigates the extent to which DER could impact on existing distribution networks, with a specific focus on residential LV networks. Two particular types of technology are considered in order to analyse the potential impact from DER. These are micro-CHP units and EVs. These technologies were chosen as they represent examples of both an electricity generating and flexible load form of DER. Micro-generation units can be expected to cause a rise in the voltage at their point of connection to the network. In contrast, EV charging may result in excessive voltage drops and overloading of network assets. The sensitivity of these impacts to changes in the point of connection of the DER is also analysed as a potential indicator for determining permissible levels of DER penetration.

Residential households are connected to the distribution system via a single-phase connection. This has the knock-on effect of creating voltage and current unbalance at the 3-phase level of the network. Uncontrolled charging of EVs or generation of electricity from micro-generation units could lead to levels of unbalance which exceed acceptable network limits (Shahnia et al., 2011). Results from investigations into the interdependency of network phases are also outlined in this chapter.

3.2 Deterministic Analysis

3.2.1 Methodology

In order to assess a network's ability to accommodate DER technology, two types of analysis are carried out here on LV test networks. Firstly, a deterministic steady-state analysis is performed in order to assess network limitations. The analysis is carried out by introducing DER to a test network for a given worst case scenario. Depending on the particular type of technology under investigation, a worst case scenario can be defined as a period of time whereby the demand on the network is at either its lowest or its highest level. The method investigates the effects of increasing DER penetration, as well as the effect of the location, on the network and is assessed in terms of the resulting network voltage levels and thermal loading of components. The method provides insight into the limitations of a given network's capability to accommodate DER without the need for active control on the demand side or upgrading of the network.

When assessing the limitations of a distribution system, it is normal practice to test models of the system for a worst case scenario. For LV residential distribution networks, this typically implies that the network is examined under conditions of maximum load. However, this may not be the case in future networks where there is a large penetration of local micro-generation units. The maximum, or minimum, system demand is usually determined from historical load data. The main concern from a distribution system operator's point of view is that a network operates in a safe and reliable manner under all loading conditions. With an increase in DER on the network in future years, the level of electricity demand that will define a network's 'worst case scenario' will undoubtedly change significantly.

This method assesses the potential impact on the distribution network due to the introduction of DER. This is achieved by incrementally adding DER units to the network for a given time period, i.e. maximum or minimum demand. In order to perform this analysis, a model of a section of LV distribution network was developed using power system analysis software (DIgSILENT GmbH, 2011). Details of the model are given in Section 3.2.2. Steady-state analyses were performed using unbalanced load-flow calculations, with the changes in voltage and thermal loading levels at various parts of the network recorded. The load-flow solutions were calculated using the Newton-Raphson method employing 3-phase current injection equations (Garcia et al., 2000).

3.2.2 Test Network 1

The deterministic impact assessment is performed using Test Network 1, which is based on a LV residential distribution feeder in a suburban area in Dublin, Ireland. A simplified version of the feeder is given in Fig. 3.1. The network supplies 134 residential customers through a total of 1.2 km of 3-phase copper mains cables and a total of 980 m of single-phase copper service cables. A lumped load model, representing a similar number of residential customer loads is included to represent another feeder being supplied from the same transformer. In the actual test feeder model, each household, DER unit and service cable are modelled separately. In Ireland, the LV distribution network

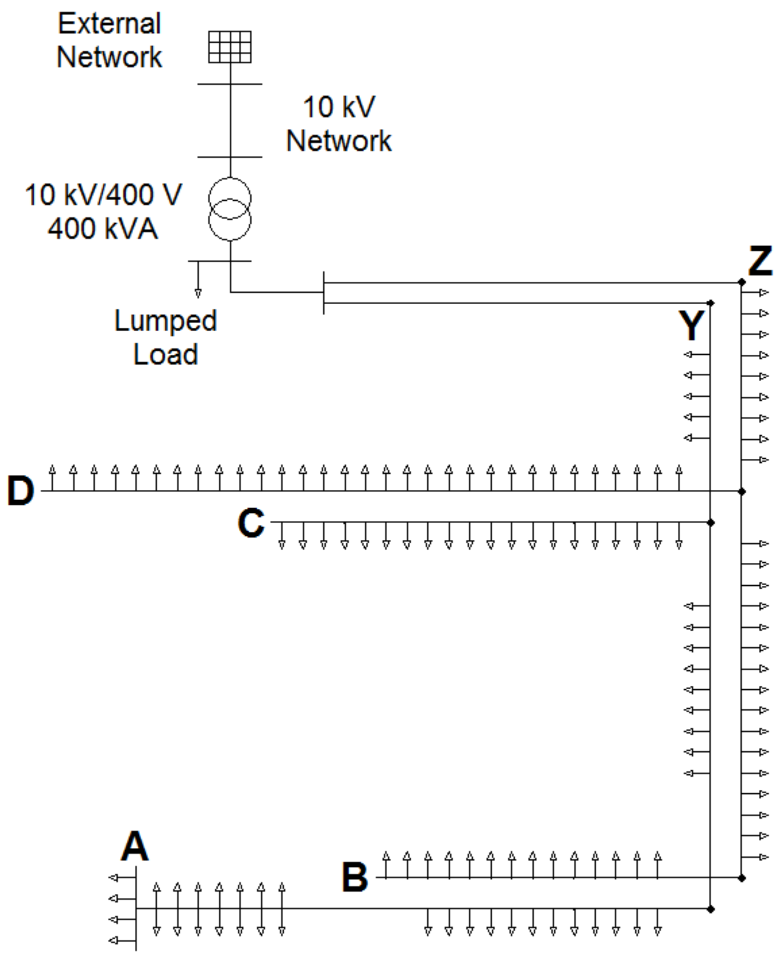

Figure 3.1: Single line diagram of Test Network 1

is operated at a nominal voltage of 230/400 V with a voltage range tolerance of +/-10% (ESB Networks, 2007). The model incorporates a 400 kVA, 10/0.4 kV step-down transformer. For the most part, LV substation transformers in Ireland do not have tap-changing capabilities, which is the case for the transformer modelled in this test network. As such, the medium voltage (MV) network supplying the LV transformer is included as an equivalent impedance in order to take account of the voltage drop at this network level. The MV network is modelled such that at maximum residential load the voltage at all points of the network does not exceed -10% of nominal assuming residential load only. Specifications for the network model components were supplied by the DSO for the Republic of Ireland.

3.2.3 Residential Customer Load

Typical load data for domestic electricity demand customers was obtained from the DSO. It consists of 15-minute time-series demand data for high, medium and low use customers over a one year period. This data was used to generate both the deterministic and stochastic household load profiles, which were assigned based on the annual energy demand of each customer.

For the deterministic analysis, different electricity demand profiles were randomly assigned to each of the houses in the test network. An example of a typical 24 hour load profile for a residential customer is given in Fig. 3.2. In order to confirm that these load profiles portrayed an accurate representation of the power demanded by a real distribution feeder, the coincidence factor, (3.1), of the test network was determined to ensure a realistic load diversity.

$$\text{Coincidence Factor} = \frac{\text{Maximum Diversified Demand}}{\text{Maximum Non-coincident Demand}} \tag{3.1}$$

The maximum diversified demand is defined as the maximum demand imposed by a group of loads over a certain period, while the maximum non-coincident demand of a group of loads is defined as the sum of the individual maximum demands, without the restriction that they must occur at the same time (Kersting, 2002). From assessing the yearly load profiles for each of the households on the network, the coincidence factor was found to be 0.32. This value compares favourably with coincidence factors for similar residential load networks (Willis, 2004).

Following the assignment of load profiles to each house in the test network, the minimum demand period for the network was determined. This is considered to be the worst case scenario for the micro-CHP study. Similarly for the EV investigation, the maximum demand period for the network was determined. This assessment is restricted

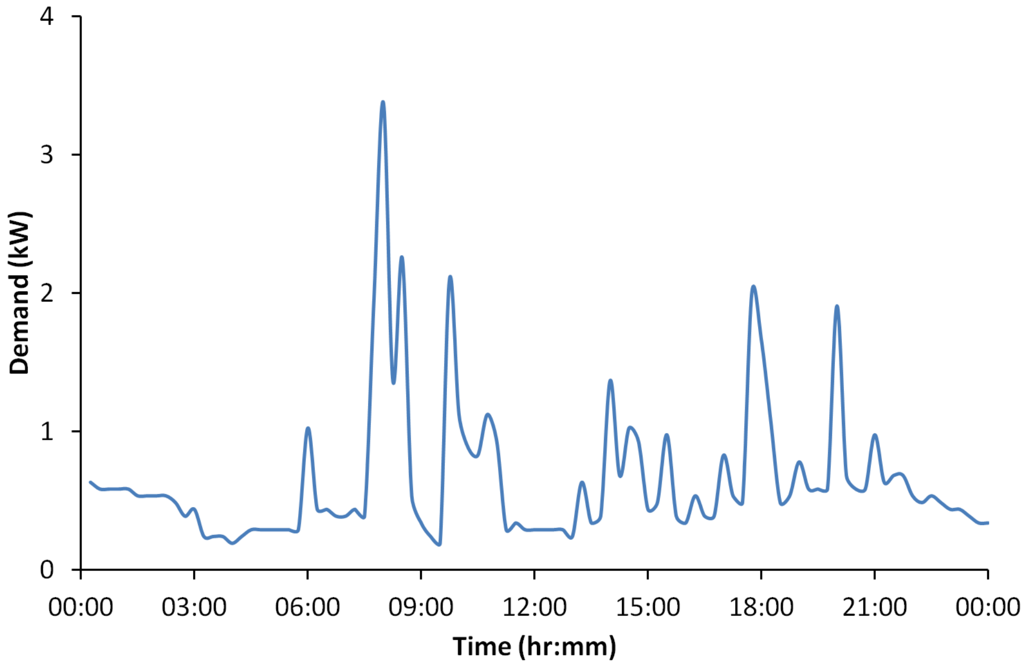

Figure 3.2: Typical 24 hour load profile for a residential customer

to times of day when there would be a higher probability of simultaneous EV charging, i.e. between the hours of 4 pm and 8 am. Each of the houses in the test networks are modelled as a constant power load with a power factor of 0.97 inductive.

3.2.4 Micro-generation

Domestic micro-CHP units can be switched on by the owner/operator as required. However, they usually operate at times of day when heat, usually for hot water, is required in a building. This normally occurs during the morning period, between 6 am and 10 am and to lesser extent again in the evening, between 6 pm and 10 pm (Thomson and Infield, 2007b). Electrical energy is only produced as a byproduct of the heat energy and as such will only be produced when heat is demanded in the building. In the network models, individual micro-generation units are rated with electrical outputs of 1-1.2 kW. This is similar to the rated capacities of micro-CHP units that are currently available on the market (Pehnt et al., 2006). The units are modelled with a power factor of 0.98 and are each connected to the feeder via a single-phase connection at the same point of connection as the household.

3.2.5 Electric Vehicles

The vast majority of privately owned EVs can be expected to charge at the owner's household. Although the possibility exists for fast, 3-phase charging, for the most part, EV charging at customer households will do so by means of a standard single-phase AC electrical socket. Therefore, it is assumed that EVs will be connected to the network at the same point of connection as the residential household. Charging profiles for EVs can vary depending on the particular technology employed: battery type, charging equipment and the electricity supply network can all affect the EV charge profile. For the purposes of this work, it was not necessary to consider the energy required by the EV batteries. Instead, the main focus here is on voltage levels and the thermal loading of network components. Therefore, only the power demand for charging EV batteries is considered. Depending on the type of charging equipment used, the level of power that can be delivered to a battery can vary considerably, e.g. 3-phase charging, DC fast charging. A demand of 3.5 kW per vehicle is assigned as a typical EV charging power demand. This value is appropriate in terms of the power delivery capabilities of existing LV distribution networks in Ireland (ESB Networks, 2007). EV batteries are assumed to have unity power factor.

3.3 Deterministic Analysis Results

3.3.1 Voltage Impact

Unbalanced load-flow analyses were carried out at various levels of DER penetration for the worst case scenario of residential load. Micro-CHP and EVs are added to individual households in the network in 10% increments with respect to the total number of households. Two cases are examined for each level of penetration: case (i) locates the units at households which are furthest from the substation bus, while case (ii) locates the units at households nearest to the transformer bus. Performing the analysis in this manner indicates the boundaries of possible values recorded due to the point of connection to the network.

3.3.1.1 Impact on 3-Phase Voltage Levels

Test network 1 was examined for increasing penetrations of micro-CHP units for both cases (i) and (ii). Fig. 3.3 shows the recorded voltage levels at node A, which is a 3-phase mini-pillar supplying 4 customers at the extreme of the network. Due to the network being modelled for the extreme scenario of minimal residential demand, this results in a particularly high voltage at node A even with no micro-generation operating. Here, micro-CHP units were incrementally added to the network branch ending at node A. The second branch, ending at node B, has no micro-generation units present. It can be seen that even with 100% micro-CHP penetration, the voltage at node A is within the upper voltage limit (1.1 pu) regardless of whether the units are located near or far from the transformer.

Fig. 3.4 shows a similar result to Fig. 3.3 except in this case there is a 100% penetration of micro-CHP on the second branch of the network. While the overall voltage can be seen to have risen significantly, the upper limit is only exceeded in the extreme case of a 85-90% penetration of micro-CHP units across the entire network for both cases (i) and (ii).

Both Fig. 3.3 and Fig. 3.4 demonstrate how the location of micro-CHP on the network can have a significant impact on the voltage level at a particular node on the network. For a given voltage, the micro-CHP penetration can vary by as much as 30%.

Following the investigation into the potential impact from micro-CHP operation on 3-phase voltage levels, a similar analysis was performed to assess the potential impact from EVs. Simulated voltage levels were recorded at six points on the test network, marked A, B, C, D, Y and Z in Fig. 3.1. Four of these points are located at the end of branches where the voltage drop is likely to be greatest due to the radial nature of the

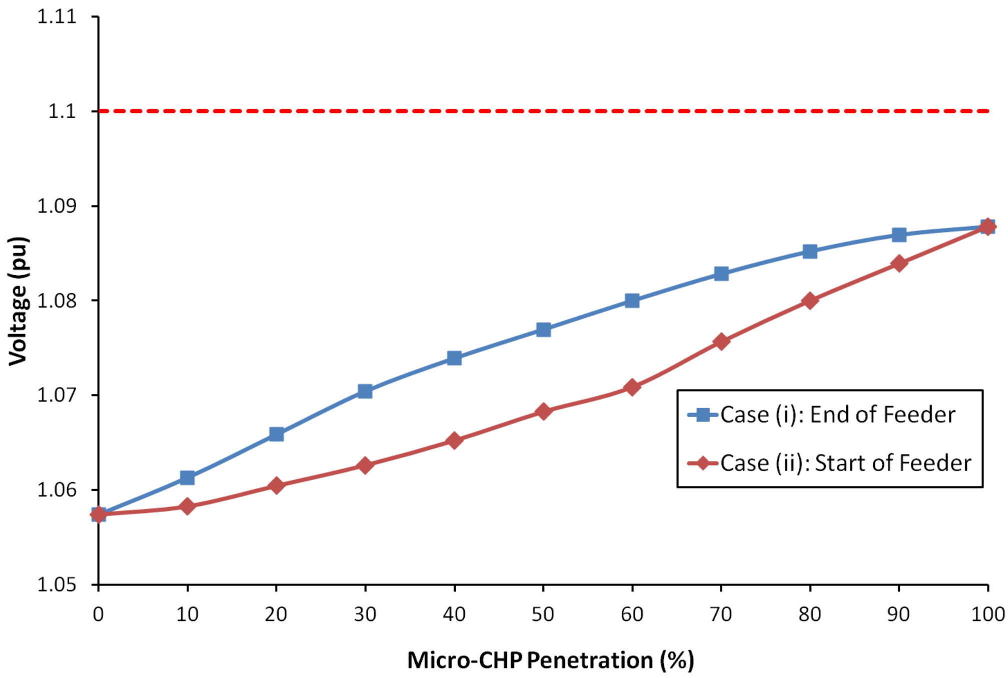

Figure 3.3: Line voltages for varying levels of micro-CHP penetration on line ending at node A

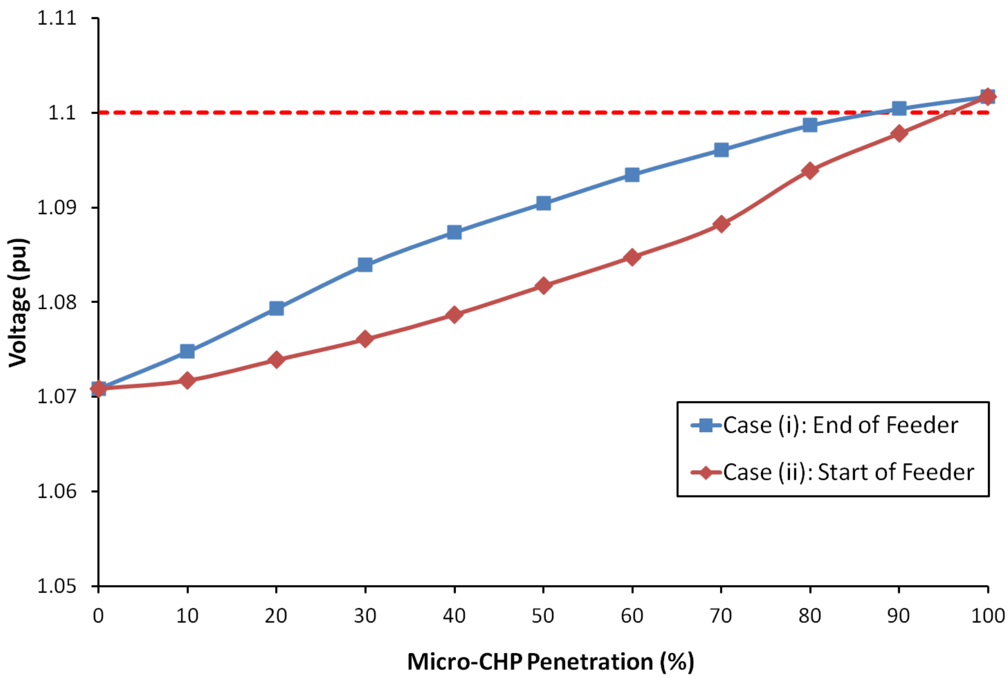

Figure 3.4: Line voltages for varying levels of micro-CHP penetration on line ending at node A with 100% micro-CHP penetration present on second line

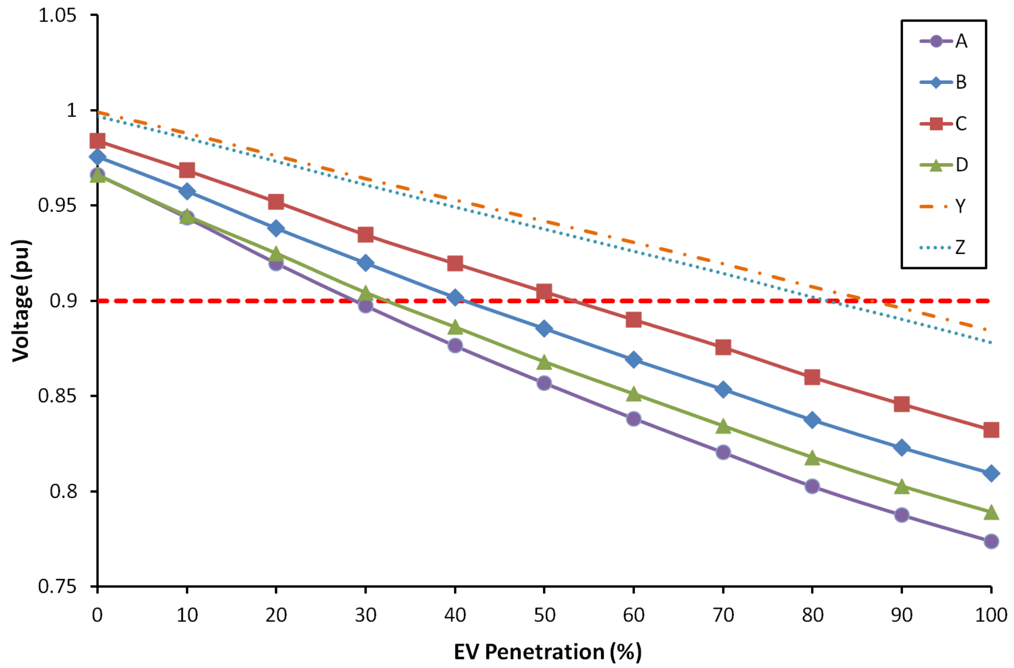

Figure 3.5: Line voltages for varying levels of EV penetration

network. The remaining 2 points are located at households nearest to the substation bus. Fig. 3.5 shows the voltage level at the 6 points of interest for various penetrations of EVs for case (i). Here, the initial voltage levels at 0% EV penetration are due to the high residential load demand on the network. It can be seen that point A experiences the most severe voltage drop and reaches the lower limit of 0.9 pu at an EV penetration level of approximately 28%. Fig. 3.6 compares the voltage level at point A for both cases with different amounts of EVs connected to the network. For case (ii), the voltage drop is not as severe, reaching the lower acceptable limit at an EV penetration of approximately 42%.

For the worst case scenario of maximum residential demand, these results indicate that, at best, for EV penetration levels greater than 42% that there will be sections of the network where the voltage level will have dropped below the acceptable limit. They also show that depending on the location of the points of connection, there can be a significant difference, i.e. 28% vs. 42%, in the amount of EVs that can safely be connected to this particular network before the voltage levels drop below safe limits.

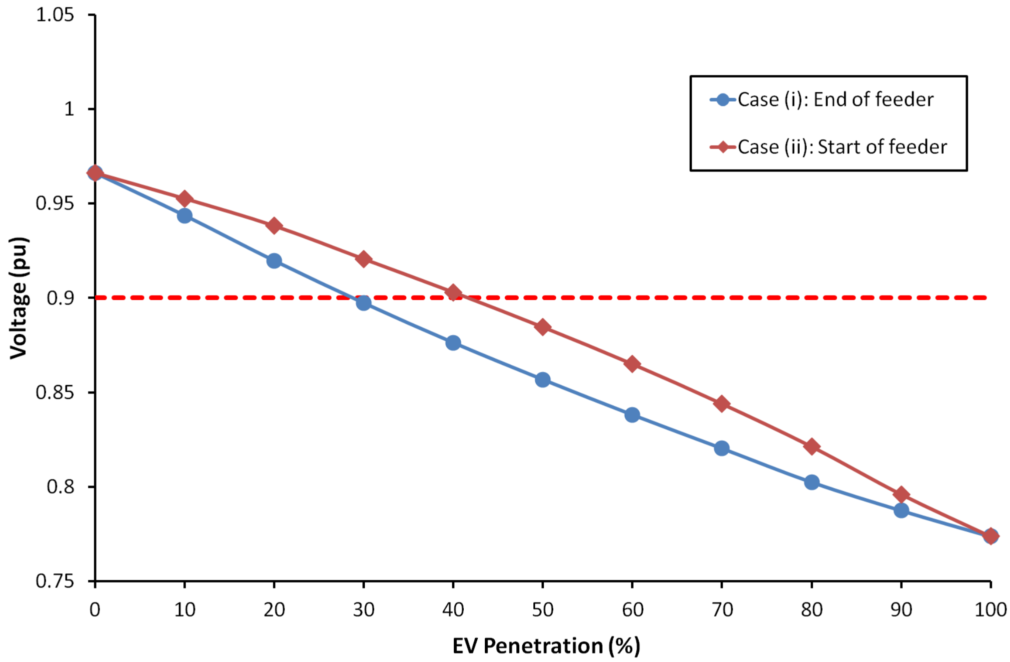

Figure 3.6: Line voltages for varying levels of EV penetration at node A for cases (i) and (ii).

From the 3-phase voltage analysis results, it is evident that the addition of EV load is more likely than micro-CHP to have a greater impact on the operating conditions of this type of network. As such, the following results focus on the impact from increasing penetrations of EV load only.

3.3.1.2 Impact on Single-Phase Voltage Levels

It is highly likely that there will be a certain amount of unbalance present on a distribution network at any given time due to the varying loads on each phase. Therefore, each of the phase voltages were examined separately for increasing levels of EV charging. Measurements were recorded at the connection point for one house on each phase at points of interest in the network. Fig. 3.7 compares each of the phase voltages at the most severely impacted point on the network for case (i). It can clearly be seen that the voltage level for each phase can vary greatly due to the connection of EVs to the network. The voltage recorded on phase ‘c’ reached the lower limit at an

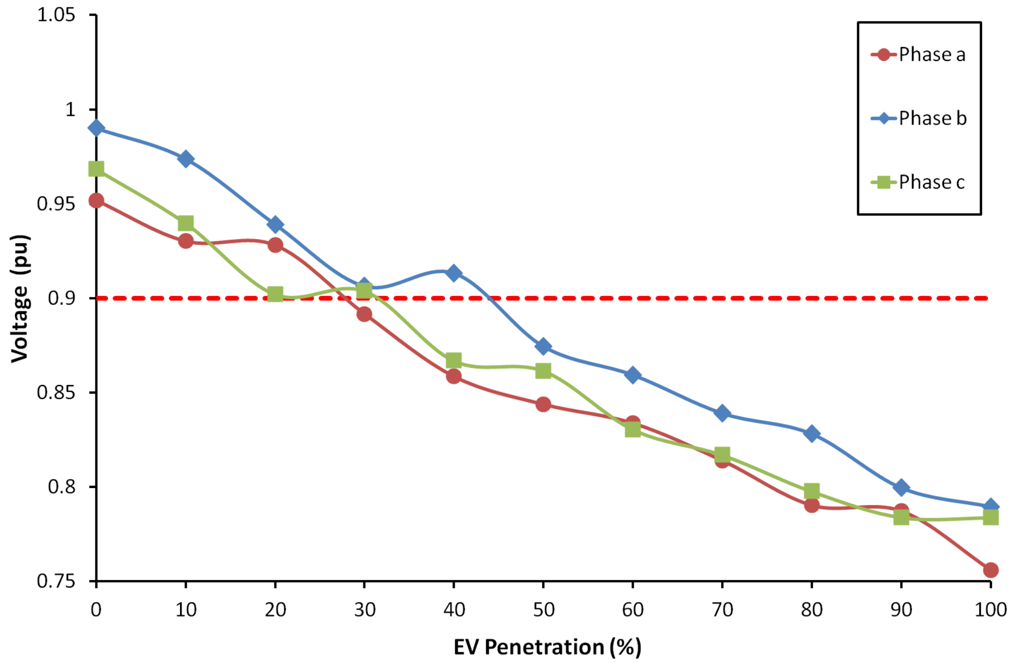

Figure 3.7: Phase voltages for varying levels of EV penetrations at point A

overall penetration of 20%, while the corresponding values for the ‘a’ and ‘b’ phases were 27% and 44% respectively. A different initial allocation of loads across the phases could, of course, alter the phase thresholds. While a certain portion of this unbalance can be attributed to the residential demand for each household, the results show that uncontrolled connection of EVs at single-phase points can significantly degrade this unbalance due to the additional load on the phase. It also demonstrates the need for voltage levels to be monitored at individual household connection points, as opposed to simply at the 3-phase supply level where the lower allowable limit was reached with an EV penetration of 28%.

The characteristics shown in Fig. 3.7 are not smooth due to the allocation of EVs at each penetration level. The location of EVs on the feeder is chosen as a result of their geographical position and is not dependent on which phase they are connecting to. As a result, it is possible that the additional load, for each increment of EV penetration, is not spread evenly across the phases. A slight voltage rise on some of the phases is also observed at certain EV penetrations. Reasons for this occurrence are explored in the following subsection.

3.3.2 Phase Interdependency

The level of influence that adding EVs on a particular phase can have on the other phases of a feeder was also examined. EVs were added incrementally, as before, but only to those houses connected to phase 'a'. Voltage levels were recorded at each point of interest in the network. It should be noted that such a scenario is highly unlikely to occur in reality. If such a scenario were to arise, the DSO would more than likely reconfigure the network in order to spread the load as evenly as possible across the phases before such a situation could occur. These results are shown as an indicator of the extent to which excessive loading of one phase in a network can affect the other phases.

Fig. 3.8 compares each of the phase voltages with increasing penetration of EVs at point A, which is the most severely affected point in the network, as seen in Fig. 3.5. As can be seen in Fig. 3.8, a certain level of unbalance across the phases already exists due to the residential load. Voltage levels are only shown for penetrations up to, and including, 50% as the load-flow calculations fail to converge for higher levels due to the extreme voltage unbalance and voltage drop on the network. This effect can be attributed to the modelling of household loads as constant power loads, which is unlikely to be the case in reality. A more realistic representation of the loads would be to model them as a mixture of constant power and constant impedance.

In order to investigate the importance of residential load modelling, the test was performed again with household loads modelled as constant impedances. Doing so allows for comparison with the other extreme case of modelling the households as constant power loads. Fig. 3.9 shows the voltages of the 3 phases at node A for varying EV penetration levels. There is a similar impact on the voltage levels, as in the previous test, although the scale of the effect is not as great. For the case where the households are modelled as constant power loads, the lower voltage limit is exceeded at a penetration level of approximately 13%, whereas for the case with constant impedance loads the penetration level is approximately 25%. It can also be seen that the voltage rise experienced on the remaining phases is not as severe in the constant impedance

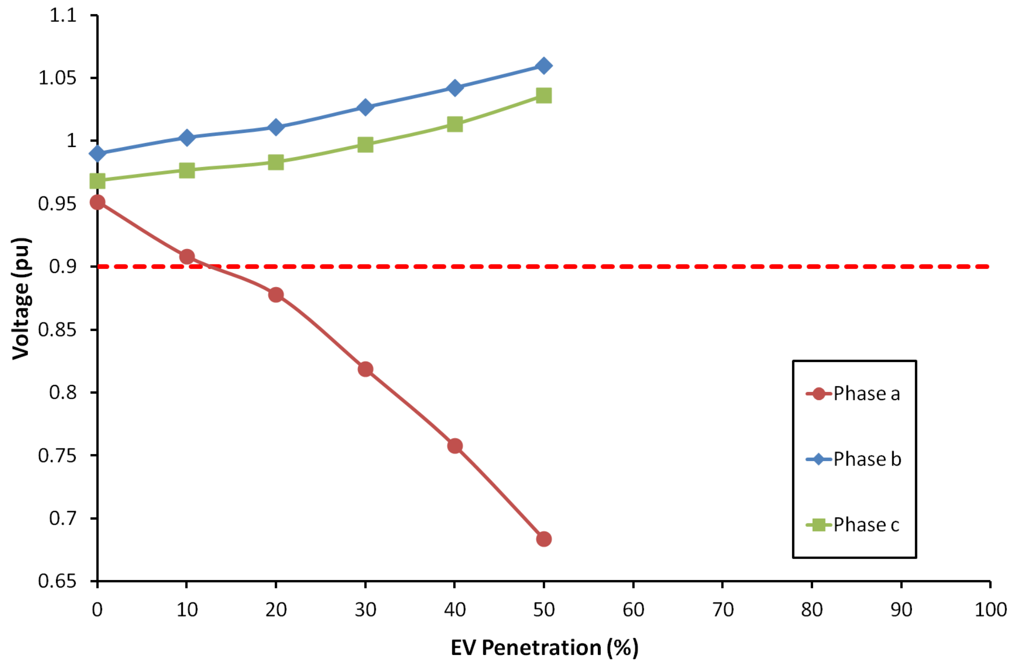

Figure 3.8: Phase voltages at point A for varying levels of EV penetrations applied to phase a only. Household loads are modelled as constant power loads

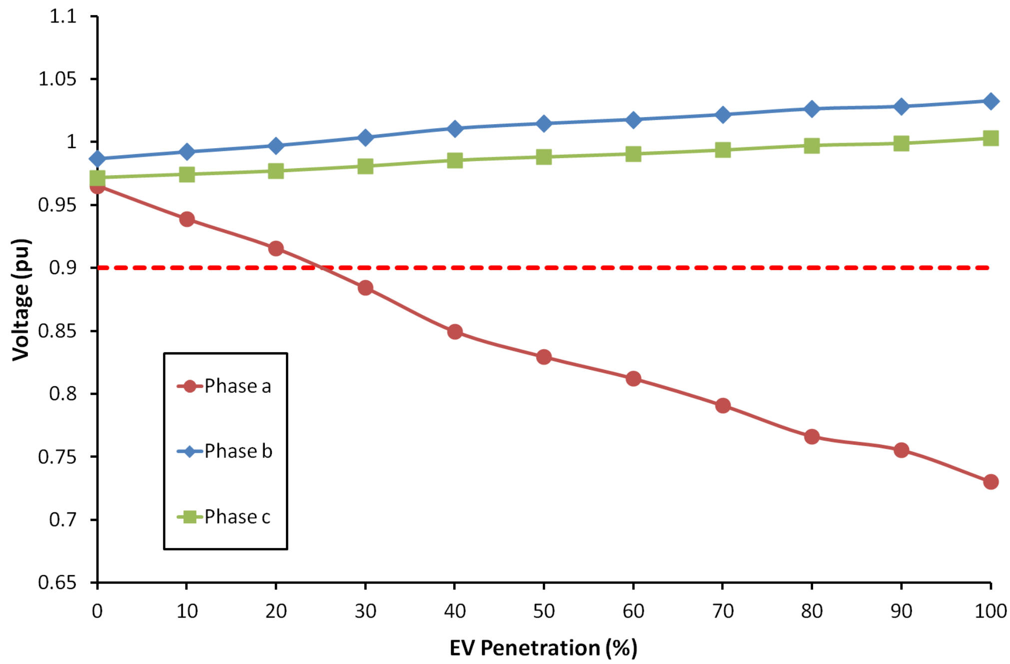

Figure 3.9: Phase voltages at point A for varying levels of EV penetrations applied to phase a only. Household loads are modelled as constant impedance loads

case as it is in the constant power case. This suggests that load composition is a significant factor in determining acceptable EV penetration levels and that accurate load modelling should form part of any EV impact study.

It should also be noted from Fig. 3.8 and Fig. 3.9 that the addition of EV charging to phase 'a' alone not only results in a severe voltage drop on that phase but also causes phases 'b' and 'c' to experience voltage rise. This may be attributed to the interdependency between each of the phases due to the sharing of a common neutral conductor and will be investigated further in future research.

3.3.3 Thermal Loading Impact

The thermal loading of certain parts of the test feeder were recorded for the same residential load conditions as applied in the previous tests. Both the transformer and the line connecting the substation busbar to the first terminal along the feeder were examined, as these were anticipated to be the network components which would experience the highest loading levels. Fig. 3.10 shows that the thermal loading of the transformer reaches 100% of its rated value with an EV penetration of approximately 25%. Similarly, Fig. 3.11 shows for the same conditions the loading of each of the phases of the substation line. The individual phases exceed their rated loading capability for EV network penetrations of approximately 23-30%, indicating that the thermal loading of network components must also be considered as a barrier to the number of EVs that can charge simultaneously on a particular network. As discussed in Section 3.3.1.2, the characteristics shown in both of these figures are not smooth due to the manner in which the EVs are allocated to the individual phases of the feeder.

3.3.4 Summary

Deterministic analysis methods can provide insight into the limitations of existing networks for particular loading scenarios. Here, the impact from increasing penetrations of micro-DER devices on network operating conditions was assessed for particular resi-

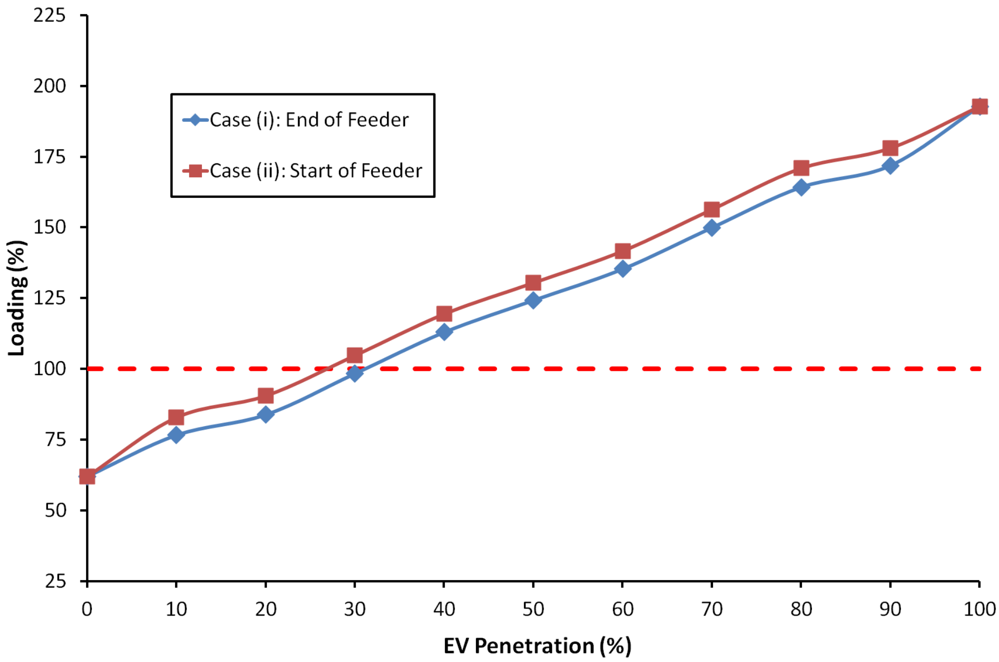

Figure 3.10: Thermal loading of feeder transformer for varying levels of EV penetration

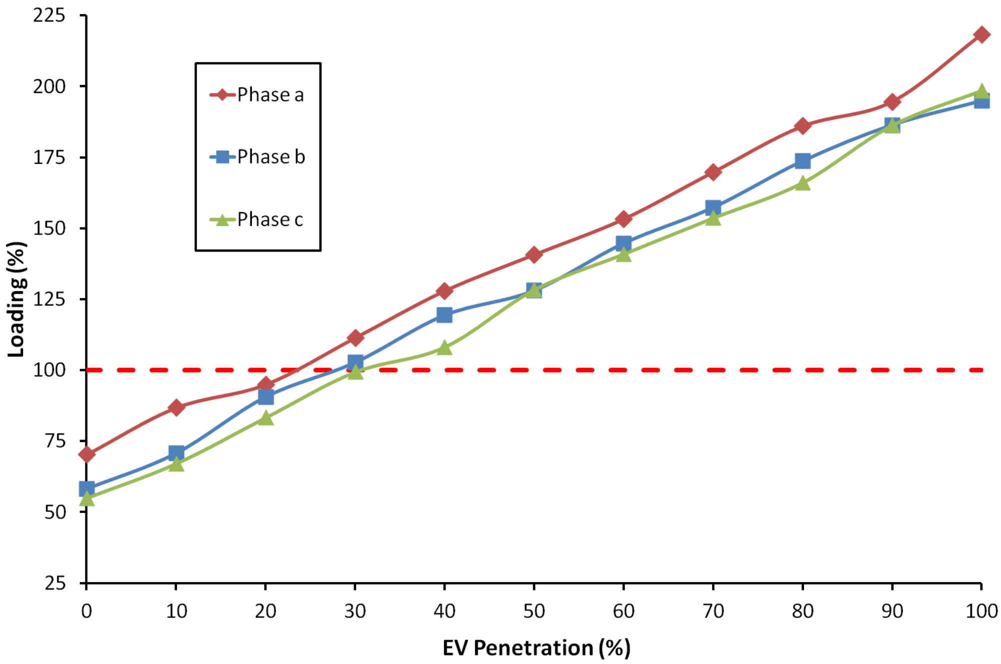

Figure 3.11: Thermal loading on each phase of substation line for varying levels of EV penetration

dential loading scenarios. By carrying out such analysis, it is possible to determine how individual network components are impacted due to increasing penetrations of DER units. While this method can prove to be useful for comparing operating conditions under various predetermined loading scenarios, it provides limited insight into the likely impacts that could be expected by taking account of the diversity of load and DER operation on the network. As such, a stochastic based time-series analysis technique is developed in the following section to assess the likely impact from the use of DER on LV networks.

3.4 Stochastic Scenario Analysis

3.4.1 Methodology

Stochastic scenario analysis involves the use of stochastically generated load profiles to assess the impact of DER while incorporating a number of uncertainties inherent with DER technologies, e.g. start time, duration of operation, network location. Taking account of such uncertainties, as well as the uncertainty in the underlying residential load, provides a more reliable insight into the potential effects of DER on LV networks and the likelihood of network operating limits being exceeded as has been shown in Fluhr et al. (2010); Gomes and Pires (2010); Papadopoulos et al. (2010).

A stochastic analysis technique has been developed to incorporate specific uncertainties inherent with DER operation on a LV residential network. These include uncertainties which would be predetermined before each simulation (e.g. location, battery capacity) and uncertainties which would be determined throughout the simulation (e.g. start times, duration of operation). The method adopts predefined PDFs to determine the behaviour of both the residential load and the DER units on the network. These PDFs are based on real data obtained from DSO led field trials (ESB Ecars, 2011). The sources of uncertainty are outlined in Sections 3.4.3 and 3.4.4 along with their respective PDFs. The program has the ability to generate both residential customer demand profiles as well as DER profiles for a one year period. PDFs representing likely time-of-day, weekday/weekend or seasonal operating levels for the residential load and DER profiles are converted to cumulative distribution functions. Following this, a monte-carlo based algorithm is employed to generate the profiles depending on the particular DER scenario and time period to be analysed. A summary of the method for producing residential and EV load profiles is given in Fig. 3.12.

Once the profiles for the residential load and DER units have been generated, an unbalanced, 3-phase, load-flow, time-series analysis is implemented on a test network in order to determine the impact from DER operation using power system analysis software (DIgSILENT GmbH, 2011). The impact on voltage levels and thermal line loading are then determined from this analysis.

3.4.2 Test Network 2

For the stochastic scenario analysis, a second test network was used. This network is based on a LV residential distribution feeder in a suburban area in Dublin, Ireland which was chosen by the DSO in order to conduct EV field trials. A simplified version of the feeder is given in Fig. 3.13. The network supplies 74 residential customers, each of which is connected via a single-phase connection to one of the feeder's 9 mini-pillars, numbered 2-10 in Fig. 3.13. Each of the mini-pillars are fed from the LV transformer via 3-phase mains cable. The network consists of a total of 432 m of 3-phase mains cables and 2.16 km of single-phase service cables. Specifications for the network transformer and nominal operating voltage are the same as those for Test Network 1.

3.4.3 Residential Load

Using the same load data as was used for the deterministic analysis, PDFs for residential customer load were developed for use in the stochastic program. They account for both seasonal and weekday/weekend variations in the load profiles. In Ireland, peak load for the electricity system occurs in winter time. An example PDF for a residential customer load in both winter and summer is shown in Fig. 3.14. Both PDFs represent

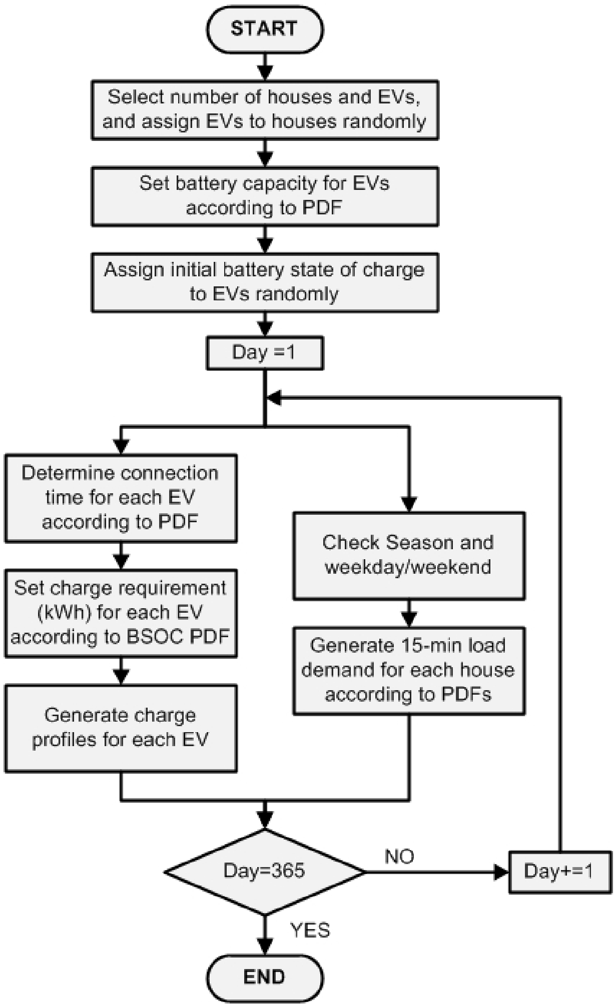

Figure 3.12: Flow chart for annual load profile generator for households and EVs

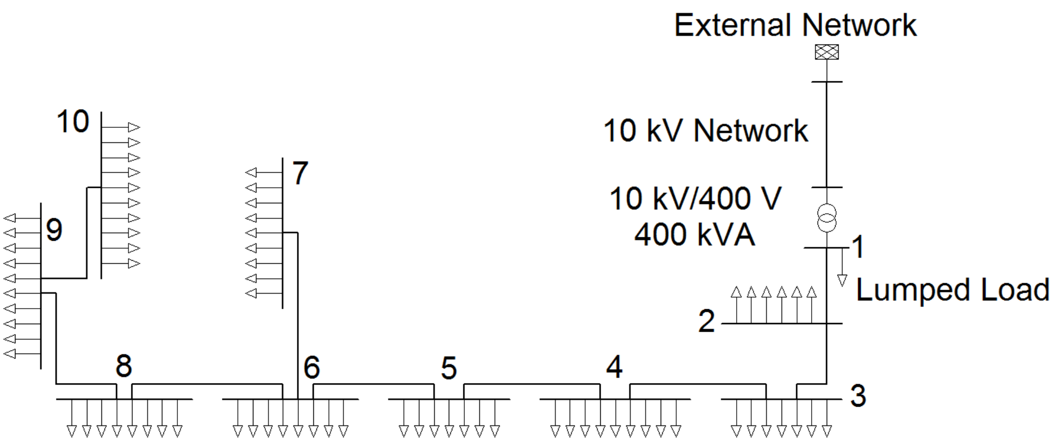

Figure 3.13: Single line diagram of Test Network 2

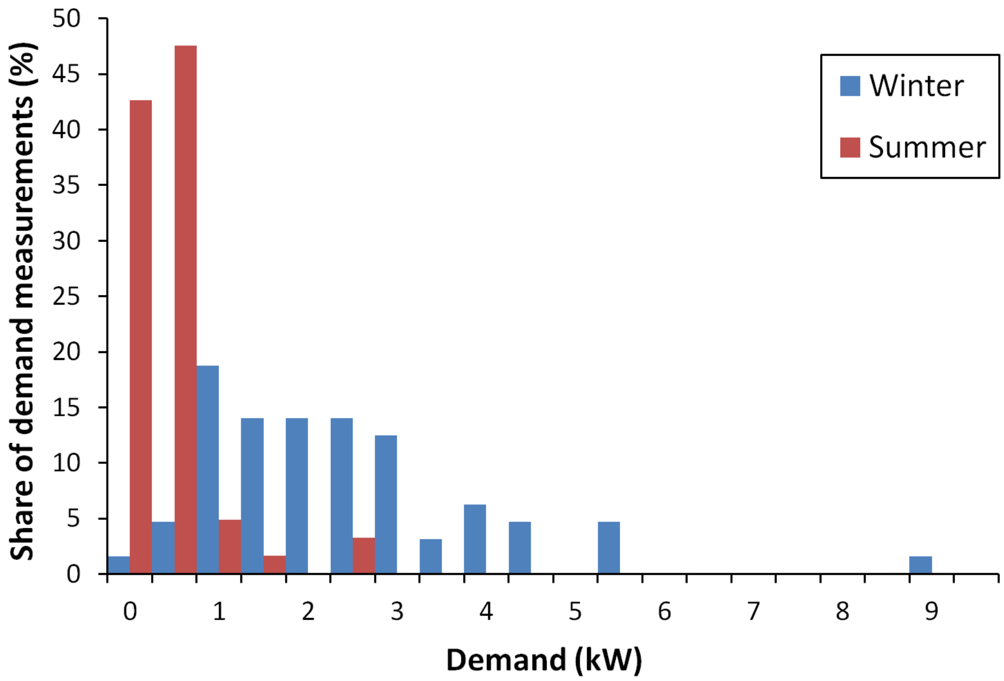

Figure 3.14: Example PDF of summer and winter customer demands at 6 pm on a weekday

the probable load at 6 pm on a weekday.

For modelling purposes, the power factor for each household load was set at 0.95 inductive throughout the year. Each load is modelled as a combination of 50% constant power and 50% constant impedance for voltage dependency purposes.

3.4.4 Electric Vehicle Load

When determining EV charge profiles, it was necessary to determine certain parameters prior to the creation of the charging profiles, including which households would own an EV. Depending on the particular penetration level of EVs to be investigated, vehicles would be randomly assigned across the network with the condition that only one EV could be assigned to a household for each simulation. The battery capacity for each EV in the model is determined a priori, based on the EV battery capacities of vehicles which are expected to be introduced to the automobile market in future years. They are based on both fully-electric (16/20 kWh) and plug-in hybrid EV (8 kWh) technologies. Each

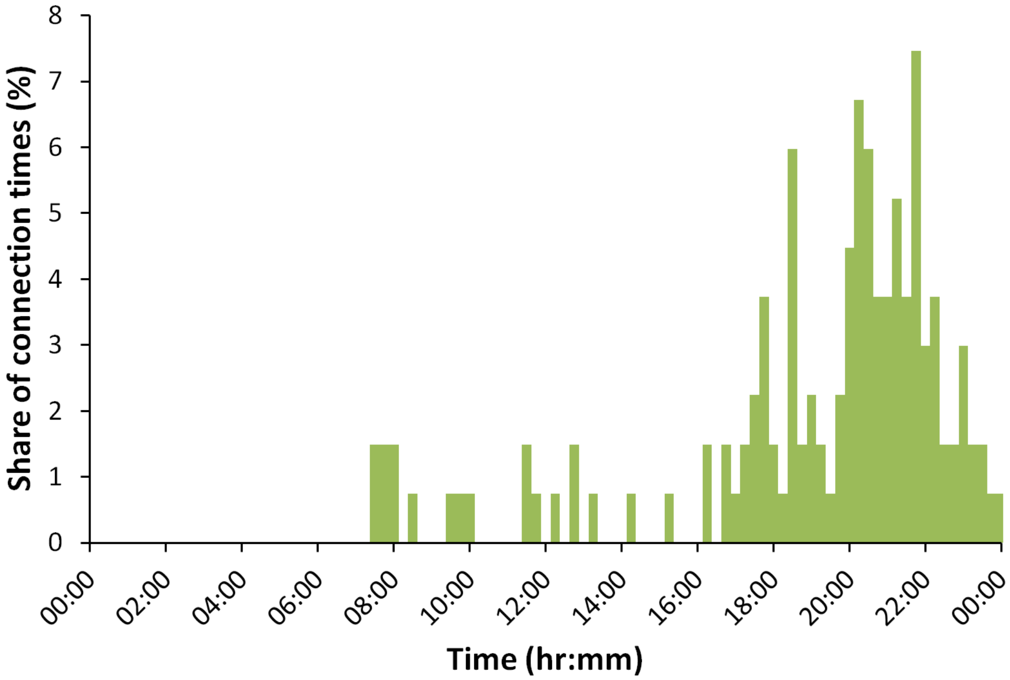

Figure 3.15: PDF of EV connection times over a 24 hour period

EV in the network is assigned a battery capacity based on a PDF of likely capacities. Each of the above parameters remain fixed for a one year period, but are redefined for each new year of load data.

At the start of each day, the connection time for each EV is determined using a PDF for typical connection times based on actual data collected from EV trials in Ireland. This data was collected from EV owners with no controlled charging capability and no time-of-day incentives. Fig. 3.15 shows the PDF for EV connection times over a 24 hour period. For this sample, the majority of connection times take place after 8 pm, which happens to avoid the typical winter residential daily load peak, which normally occurs between 5 pm and 7 pm.

The battery state of charge (BSOC) for each EV at the time of connection is determined in a similar manner to the connection time. The values obtained during the simulations compared well to those from the DSO led EV trials (ESB Ecars, 2011).

3.5 Stochastic Scenario Analysis Results

3.5.1 Voltage Impact

The stochastic technique is implemented for EV penetration levels of 10% and 50% on test network 2 (Fig. 3.13). Load control capability and financial incentives are not considered in this analysis. Load-flow simulations were subsequently performed, with voltage levels measured at each CPOC, along with cable loading and network line losses. Illustrative results given below compare simulation outputs for both summer and winter scenarios.

Voltage levels at the CPOCs for households at mini-pillars 9 and 10 were recorded, as they are located at the extremity of the network. Fig. 3.16 and Fig. 3.17 show the voltage probability distribution for both the summer and winter scenarios. While there is an overall decrease in the voltages experienced in the winter scenario, the lower acceptable limit (i.e. 0.9 pu) is exceeded less than 3% of the time in both scenarios. As expected, increasing EV penetration levels result in lower voltages being observed.

From the results of the deterministic and stochastic methods, it appears that the voltage drop for a 50% EV penetration is more severe in the deterministic case. This is due to the fact that the household load is modelled for the worst case scenario of maximum demand. However, in the stochastic method, the load profiles of the households and EVs are time varying and are, therefore, rarely representative of the worst case scenario shown in the deterministic case.

3.5.2 Thermal Loading Impact

The thermal loading of the mains cable supplying the feeder from the MV/LV transformer was recorded for both the summer and winter scenarios, Fig. 3.18 and 3.19. While a general increase in cable loading can be observed in the winter case when compared to the summer case, the cable exceeds its maximum rated loading less than 2% of the time. While the probability of exceedance is similar for both winter and summer, loading levels were recorded as high as 127%.

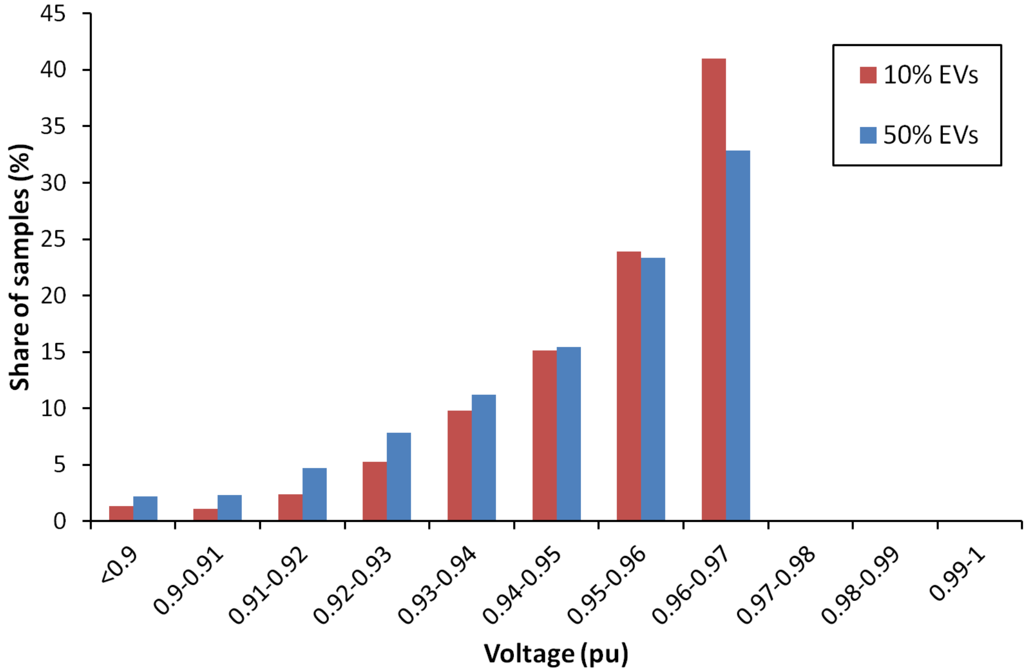

Figure 3.16: Probability of simulated voltage levels recorded at CPOCs connected at mini-pillars 9 and 10 for summer scenario

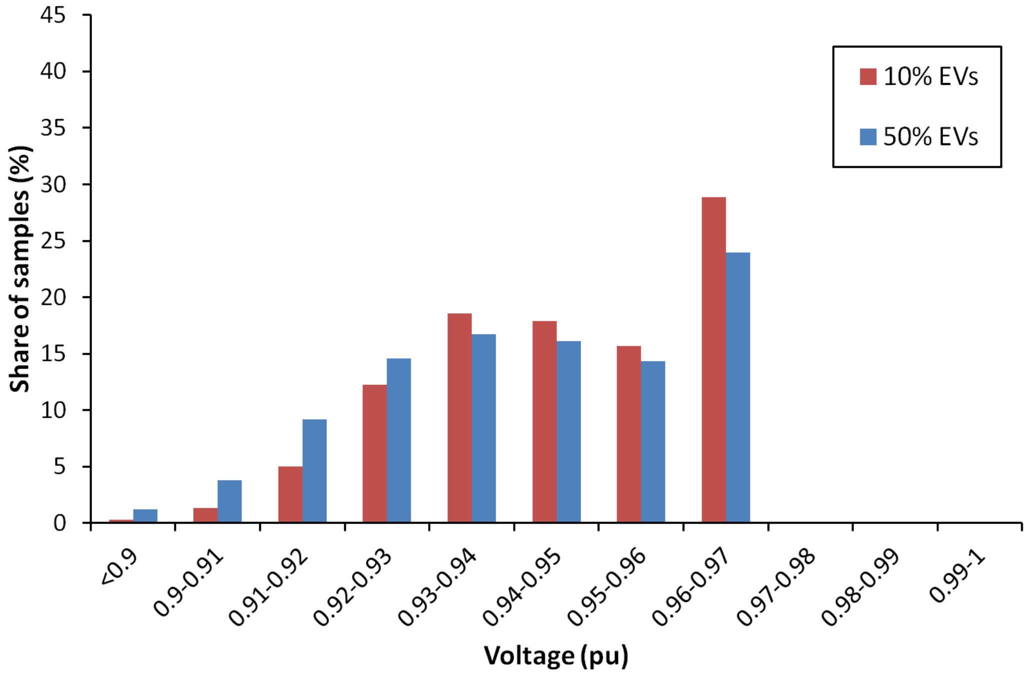

Figure 3.17: Probability of simulated voltage levels recorded at CPOCs connected at mini-pillars 9 and 10 for winter scenario

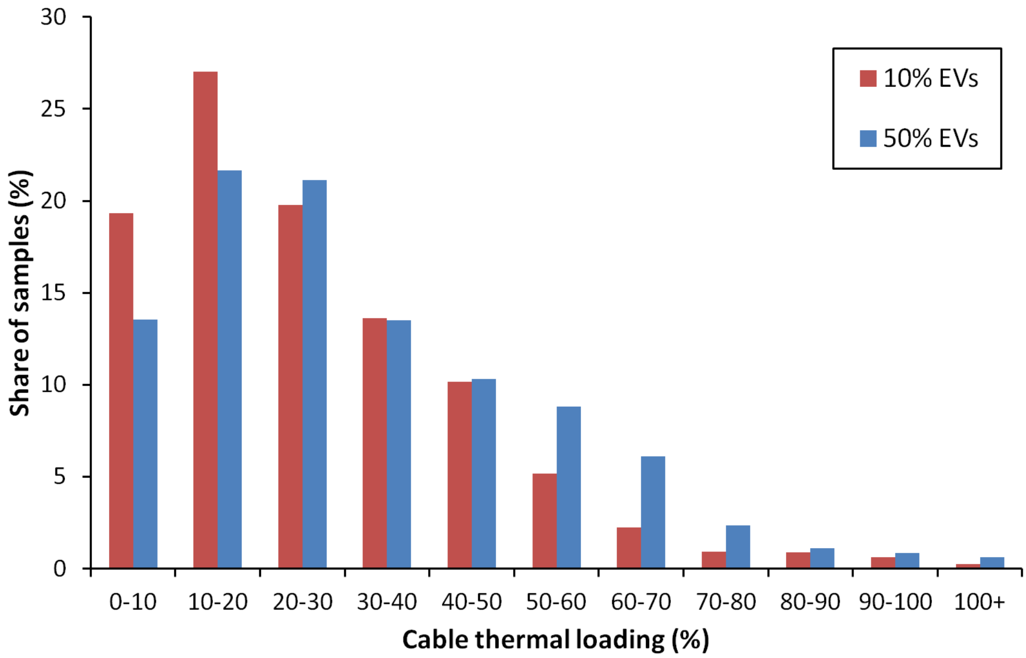

Figure 3.18: Probability of thermal loading on feeder cable for summer scenario

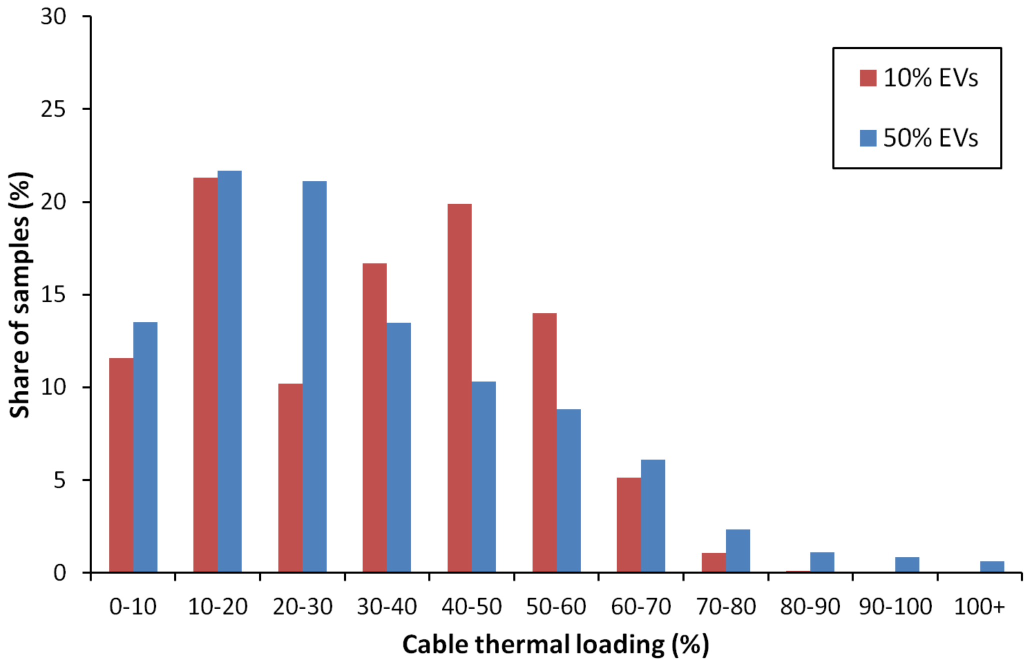

Figure 3.19: Probability of thermal loading on feeder cable for winter scenario

3.5.3 Summary

By using the time-series stochastic scenario analysis tool, the likely impact from the use of DER devices on network operating conditions can be determined. The method incorporates the inherent uncertainty in the residential load as well as the temporal and spatial diversity of the operation of multiple DER devices within a network. In doing so, the technique provides insight into how network operating conditions can be impacted based on varying levels of coincident operation.

3.6 Conclusion

This chapter presents an analysis of some of the potential impacts on existing distribution networks from DER. It has been demonstrated that the impact from micro-generation, specifically in the form of domestic micro-CHP units, may only be significant in the extreme scenario of minimum load and maximum generation with a 100% penetration of micro-CHP. For flexible load forms of DER, it has been shown that for a 20-40% penetration of EVs, the test network reached the limits of acceptable operation. In such a situation, DSOs would be forced to curtail the delivery of electricity to EVs, or other load, in order to maintain secure and reliable network operations. The work has also highlighted the significance of the location of the connection points of EVs to the network in terms of voltage impact. It has also been shown that due to the unbalanced characteristics of a distribution system, it is important to analyse each phase separately in order to capture the most extreme effects on voltage and thermal loading levels from the introduction of DER.

This analysis is performed for a worst case scenario, with the network impacts dependent on the amount and type of residential demand on the feeder. With the introduction of DER, the scale of coincident operation and the location of the points of connection also become significant factors. The stochastic scenario analysis results presented in this chapter show the likelihood of network limits being exceeded while taking account of some of the uncertainties associated with EV charging. While this technique provides a good indication of how network operating conditions can be affected from EV charging, the results are very dependent on the input data used (i.e. PDFs for operating times, duration of use etc.).

Given the variability in the physical and technical characteristics of distribution systems, the level of DER penetration attainable for any particular network could vary greatly. The findings of the work presented in this chapter serve as indicative results for typical suburban LV distribution feeders. For example, acceptable EV penetration levels may be much lower on rural networks. The extra demand from EV charging may result in a more severe voltage drop as a result of the typically longer line lengths on this type of network.

With the implementation of advanced metering devices in households, DER operation could potentially be controlled, and it will be critical to explore various techniques for implementing such strategies. Such technology would allow the electricity customer to take advantage of time-of-day electricity pricing by programming their units to operate at financially beneficial times, for example. They could allow DSOs to employ some form of control capability, which would allow large numbers of DER units to connect to the distribution system simultaneously. There are a number of potential benefits that could be achieved from the use of such technology. Alongside maintaining safe operation of the system, control of DER operation would allow DSOs to maximise network utilisation while reducing the need for costly network upgrades. The implementation and analysis of such a strategy is the focus of Chapter 4.

CHAPTER 4

Optimal Charging of Electric Vehicles

4.1 Introduction

CHAPTER 3 investigated the potential impact on LV network operating conditions from the introduction of DER. For the micro-generation study, it was shown that network limits are only likely to be exceeded in extreme scenarios of minimum residential load and 100% penetration of micro-CHP units. With the addition of EV load to the network however, operating limits were reached at penetration levels below 50%. An investigation of the potential impact from both types of DER was conducted for each technology's respective worst case scenario. While a worst case scenario is highly infrequent under normal operating conditions, the network must still be rated to accommodate the total load being demanded at that instant. As a result, the total network capacity may be underutilised for long periods of time. As shown in the previous chapter, the operation of DER, especially EV load at peak demand, could cause serious issues in terms of network voltage levels and component overloading. In such a situation, the DSO may be forced to curtail load on the network or limit the number of DER units in a given area. Alternatively, network infrastructure upgrading would be required to accommodate the DER units.

The introduction of AMI devices would allow customers to avail of time-of-day electricity pricing structures. From the system operators viewpoint, it would also provide an opportunity to improve the predictability of load patterns and potentially even the ability to control certain loads/DER units. Such capability would allow DSOs or third party operators to manage the operation of these devices in a coordinated manner. This would allow operators to schedule the operation of certain load/DER units, thereby utilising the available network capacity in a more efficient way. As a result, curtailment of network load could be avoided while prolonging the time before widespread network upgrading would be required.

In this chapter, a method for coordinating and optimising the operation of DER devices is proposed. The method is tested with high penetrations of EV charging as this form of DER is considered to have a significant impact on network operating conditions, as was shown in Chapter 3. The coordination of EV charging has been investigated previously, albeit with varying objectives. In Sortomme and El-Sharkawi (2011), optimal charging strategies are developed whereby aggregated EV load can be used for network regulation purposes. A number of optimisation methods for determining the EV charging rates are examined. Depending on the particular algorithm used, the techniques were shown to provide significant benefits in terms of cost savings for the customer and aggregator, and flexibility for utilities accommodating variable renewable energy sources. The work described in Su and Chow (2011) uses an 'estimation of distribution algorithm' to schedule charging for large numbers of EVs in a parking deck. The method optimises the energy allocation to the EVs in real time while considering various constraints associated with battery limits and utility limits. The method compares favourably to other optimisation techniques in terms of total energy delivered upon departure of the EVs. In Dyke et al. (2010), the ability of a large number of EVs to smooth the load profile of residential networks is investigated. By controlling the bi-directional flow of energy to and from the EV batteries, it is demonstrated that

EVs can supply power to meet residential load peaks while also creating more predictable load profiles. Utilising EVs for the smoothing of load profiles is also shown to be beneficial in terms of accommodating renewable DG. In Clement-Nyns et al. (2010), various techniques are utilised to investigate the impact of varying penetrations of EVs on residential networks. Quadratic and dynamic programming techniques minimise the impact from EV charging on network losses and voltage deviation in particular. By controlling and optimising individual EV charging rates, network losses and voltage deviations are reduced for all penetration levels examined. The methodology is examined using both deterministic and stochastic methods and concludes that while the difference in the results obtained using the quadratic or dynamic technique is negligible, the dynamic technique is more computationally intense. Work in Clement-Nyns et al. (2009) investigated the use of voltage control on EVs with charge/discharge capabilities. Here the objective was to minimise the charging cost to the EV owner while maintaining network voltage levels within acceptable limits. Results were shown to vary significantly depending on the initial state of charge of the EV batteries, with high dependence on the tariffs associated with charging and discharging.

The work described in this chapter differs in its approach to the coordinated charging of EVs described above. Instead of minimising power losses and/or voltage deviations, the objective of the optimisation technique employed here is to maximise the total amount of energy that can be delivered to all EVs over a charging period while ensuring that network limits are never exceeded due to high levels of coincident EV charging. Such an approach ensures that optimal use is made of available network capacity while avoiding excessive voltage drop and component overloading, which have been shown in the previous chapter to be potential issues with high levels of EV charging. The technique employs linear programming that takes advantage of the approximately linear characteristics of both the network voltages and component loading sensitivities to the addition of EV load.

The methodology for this work is presented in Section 4.2. Section 4.3 describes the modelling of the test network, the residential load and the electricity demand profiles for the EVs. Results and discussion for two specific charging periods are presented in Section 4.4 along with generalised results for a wide range of network scenarios. Conclusions are presented in Section 4.5.

4.2 Methodology

4.2.1 Assumptions

Coordinated charging of EVs could be achieved in a variety of ways. It is assumed here that EV owners are incentivised to charge their vehicles at off-peak times of day. For the purpose of clarity, once the off-peak period has begun, no additional EVs will connect for charging and no EVs will disconnect before reaching a full BSOC. Smart metering technology with load control capability is also assumed to be present in each household. It is assumed that this load control capability can be utilised by the DSO (or a third-party aggregator), from a remote location, in order to manage certain loads on the consumer side of the meter. Such a scheme would be subject to prior agreement by both the consumer and the DSO. For the purposes of this work, the ability to control the load extends to EV charging only and allows the operator to vary the charging rate of each EV on the feeder. Each EV can charge at any rate between zero and the maximum rated output, subject to certain restrictions, which are outlined later in this section. The ability to vary the charge rate of individual EVs in a continuous manner has been studied for use in optimal charging strategies previously (Clement-Nyns et al., 2010; Brooks et al., 2010; Sortomme and El-Sharkawi, 2011). While the possibility exists for fast, 3-phase charging, it is assumed that each EV will be connected to the network via a standard single-phase AC connection. In addition, although the concept of vehicle-to-grid for local system support or otherwise exists (Peças Lopes et al., 2010; Kempton and Tomić, 2005; Tomić and Kempton, 2007; Clement-Nyns et al., 2011), bi-directional flow of electricity to and from an EV battery is not considered in this work.

4.2.2 Standard Objective Function

The objective of the method is to maximise the energy delivered to all EVs within a set period of time. This is achieved by optimising the charging rate of each connected EV in order to maximise the total power that can be delivered for each 15 minute time interval, subject to network constraints. Doing so allows for the method to operate in real-time while not depending on previous or future network conditions. Coordinating the charging of EVs ensures that the network is utilised to its fullest extent in terms of energy delivered.

The standard objective function (SOF), F, is calculated at each time step and is given as

$$F = \sum_{i=1}^{N} x_i P_{\mathrm{EV}_i} \tag{4.1}$$

where N is the number of customers being served by the network, and P_{EV_i} is the power delivered, measured in kW, to the EV connected at the ith CPOC. It is assumed that P_{EV_i} is a continuous control variable that can vary between 0 kW and the maximum power output of the charger at node i. x_i is zero when an EV is not connected at the ith CPOC or the EV battery is fully charged, while x_i equals one when the EV at the ith CPOC is connected and the EV battery is less than fully charged.

4.2.3 Constraints

At each time step, the objective function, F, is maximised subject to certain constraints. The first of these is that the power demand of an EV cannot exceed the rated power output of the charger supplying that vehicle, (4.2).

$$0 \leq P_{\mathrm{EV}_i} \leq P_{\mathrm{EV}_i}^{max} \tag{4.2}$$

In order to avoid large variations in the charging rate over consecutive time steps, which is undesirable for current battery technology as it may reduce battery cycle life (Hoffart, 2008), a rate of change constraint is also imposed (4.3).

$$P_{\mathrm{EV}_i}^{\,t-1} - \Delta \;\leq\; P_{\mathrm{EV}_i}^{\,t} \;\leq\; P_{\mathrm{EV}_i}^{\,t-1} + \Delta \tag{4.3}$$

Here, t is the current time step and Δ is a defined limit, in kW, by which the charging rate can vary, compared to the charging rate at the previous time step, excluding on/off transitions.

The next constraint relates to the acceptable voltage range for the LV network. The addition of EV loads, for the most part, will cause the voltage at various points of the network to drop. The extent of the voltage drop can vary depending on a number of factors, which include the location of the EV and the rate of charge. The voltage at each CPOC must be maintained within the rated voltage range specified for the network, (4.4).

$$V_{min_i} \leq V_i \leq V_{max_i} \qquad i \,\forall\, N \tag{4.4}$$

Here, V_i (V) is the voltage at the ith CPOC, while V_{min_i} and V_{max_i} are the minimum and maximum allowable network voltage levels at node i respectively.

The thermal loading of network components refers to the ratio of the apparent power flowing through the component to its rated capacity. For this study, the thermal loading of both the network transformer and the mains cable connecting the transformer to the network are considered. These constraints are summarised in equations (4.5) and (4.6) respectively.

$$L_{\mathrm{TX}} \leq L_{\mathrm{TX}_{max}} \tag{4.5}$$

$$L_{\mathrm{MC}} \leq L_{\mathrm{MC}_{max}} \tag{4.6}$$

where L_{TX} and L_{MC} are the thermal loading (kVA) for the transformer and mains cable respectively, while $L_{\mathrm{TX}_{max}}$ and $L_{\mathrm{MC}_{max}}$ are the associated maximum loading of the components.

4.2.4 Network Sensitivities

A time-series, unbalanced, 3-phase load-flow analysis of the test network was performed in order to determine the network voltage and thermal loading levels as a result of residential household load. This was performed using power system analysis software (DIgSILENT GmbH, 2011) and applying residential load information. The voltage sensitivities at each CPOC were also calculated for both the addition of EV load at their own terminal and at each of the other household terminals on the network, i.e. the change in voltage due to charging demand from the EVs. For each time step, EV load is added incrementally at each CPOC in turn and the change in voltage at each CPOC is recorded. This data is then used to calculate the voltage sensitivities of the network to the addition of EV load. A summary of the methodology for calculating the network sensitivities is given in Fig. 4.1. The addition of EV load to any CPOC on the network causes variations in the voltage at each of the other CPOCs. Thermal loading sensitivities for the network components of interest were calculated in the same manner. The addition of EV load at any point of the network causes an increase in the thermal loading experienced by the transformer. Analysis of the load-flow results showed that the assumption of linearity for both the voltage and thermal loading sensitivity characteristics is sufficient. The constraint for the voltage level can be summarised as

$$V_{min_i} \leq V_{init_i} + \mu_i P_{\mathrm{EV}_i} + \sum_{j=1}^{N} \mu_{ji} P_{\mathrm{EV}_j} \leq V_{max_i} \qquad i \,\forall\, N \quad , \quad i \neq j \tag{4.7}$$

```
for each time step
    Update residential load and EV load;
    Perform load flow calculation;
    Determine node voltage and component loading margins;
    for each EV
        Incrementally increase EV demand;
        Perform load flow calculation after each increment;
        Calculate slope of incremental change in voltage and
        loading levels to determine sensitivity values;
    end
end
```

Figure 4.1: Methodology for calculating network sensitivities to the addition of EV charging

where V_{init_i} is the initial voltage at the ith CPOC of the network with no EVs charging, μ_i (V/kW) is the sensitivity of the voltage at the ith CPOC due to power demanded by the EV connected at the same CPOC, μ_{ji} is the sensitivity of the voltage at the ith CPOC due to power demanded by an EV connected at the jth CPOC.

The thermal loading constraints are summarised as

$$L_{\mathrm{TX}_{init}} + \sum_{k=1}^{N} \delta_k P_{\mathrm{EV}_k} \leq L_{\mathrm{TX}_{max}} \qquad k \,\forall\, N \tag{4.8}$$

$$L_{\mathrm{MC}_{init}} + \sum_{k=1}^{N} \beta_k P_{\mathrm{EV}_k} \leq L_{\mathrm{MC}_{max}} \qquad k \,\forall\, N \tag{4.9}$$

where $L_{\mathrm{TX}_{init}}$ and $L_{\mathrm{MC}_{init}}$ are the respective initial thermal loading levels of the network transformer and mains cable with no EVs charging, and δ_k (kVA/kW) and β_k (kVA/kW) are the sensitivities of the transformer and the mains cable loading to power demand (P_{EV_k}) from an EV at the kth CPOC.

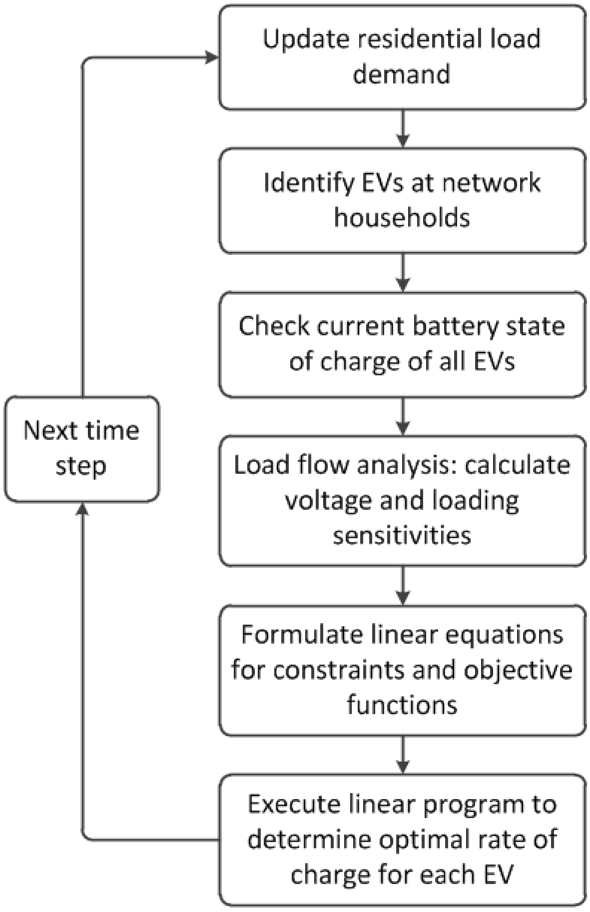

Figure 4.2: Methodology for optimising the charging rates of EVs

The voltage and thermal loading sensitivities are determined for each time step of the analysis. Subsequently, a linear programming tool in MATLAB (2009) determines the optimal charging rate for each connected EV for each time step, in order to maximise the total amount of energy that can be delivered over the considered period. A summary of the methodology is outlined in the flow chart presented in Fig. 4.2.

4.2.5 Weighted Objective Function

Due to the radial layout of the majority of LV residential networks, the standard optimisation technique could be expected to charge EVs connected near to the transformer at a higher rate than those located far from the transformer. This is due to the voltage levels being less sensitive to the addition of EV load near to the transformer. In order to provide a more even distribution of energy to the charging EVs and prioritise batteries with a low BSOC, a modified objective function was applied to the optimisation algorithm, which applies a weighting according to each individual EV's BSOC at the previous time step. It is assumed that the BSOC of each EV is known at the beginning of each optimisation time step. The weighted objective function (WOF), F, is summarised as follows:

$$F = \sum_{i=1}^{N} x_i \left(1 - \left(\frac{\mathrm{BSOC}_i}{\mathrm{BSOC}_{max_i}}\right)\right) P_{\mathrm{EV}_i} \tag{4.10}$$

where BSOC_i is the current BSOC(kWh) of the EV connected at the ith CPOC and BSOC_{max_i} is the maximum battery capacity of that EV.

4.3 Modelling of Test Network

4.3.1 Distribution Network

The test network is based on a LV residential distribution feeder in a suburban area of Dublin, Ireland, previously described as test network 1 in Section 3.2.2. A simplified representation of the feeder is given in Fig. 4.3. The black dots indicate those households where EVs are located for the analysis. This is described in further detail in Section 4.3.4 below. In the actual test feeder, each household, EV and service cable are modelled separately. The model incorporates a 400 kVA, 10/0.4 kV step-down transformer supplying a feeder of 134 residential customers. The transformer has no tap-changing capability. A lumped load model, representing a similar number of residential customer loads with no EV loads, is included to represent another feeder being supplied from the same transformer. The nominal voltage of the network is 230/400 V with a voltage range tolerance of +/-10% (ESB Networks, 2007). Specifications for

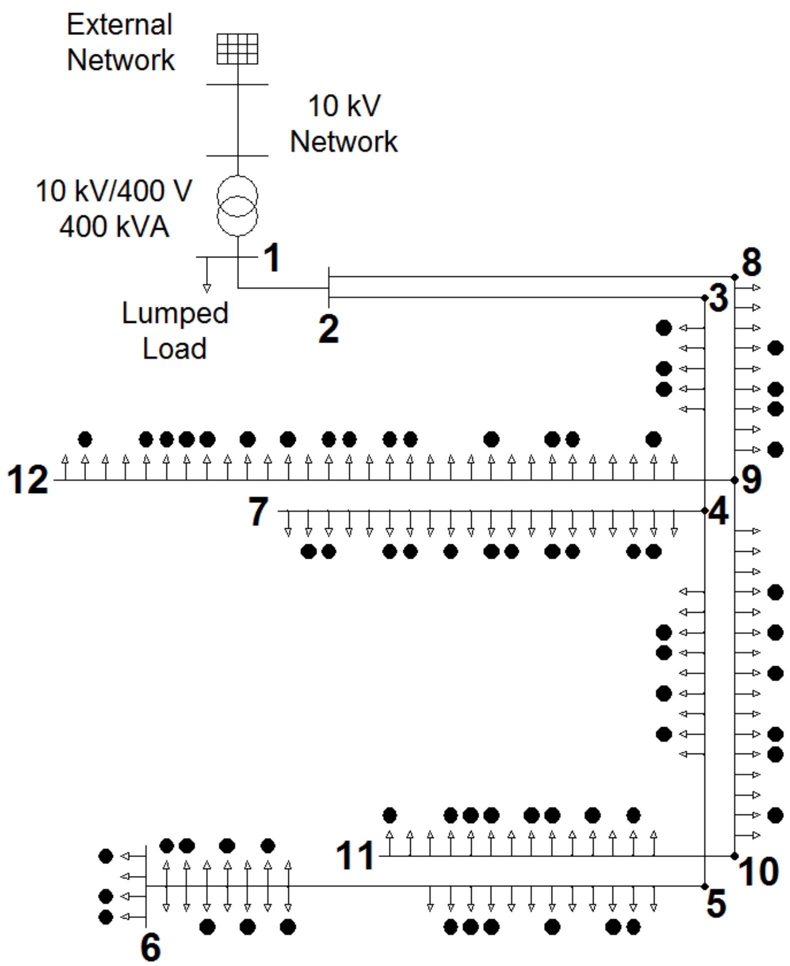

Figure 4.3: Single line diagram of test network 1. Dots indicate houses where EVs are connected for charging

the network model are given in Appendix A.

4.3.2 Residential Customer Load Modelling

Typical load data for domestic electricity demand customers was obtained from the DSO consisting of 15-minute time-series demand data for high, medium and low use customers. Different electricity demand profiles were randomly assigned to each of the houses in the test network. The coincidence factor for the test feeder was found to be 0.32, which compares favourably with similar residential networks (Willis, 2004).

For modelling purposes, the power factor for each household load was set at 0.97

inductive during the day and 0.95 inductive at night, in accordance with standard network modelling practises used by the DSO in Ireland. For the purposes of this study, daytime is specified as between 6 am and 10 pm, and nighttime as between 10 pm and 6 am. The load is modelled as a combination of constant power (P) and constant impedance (Z). From April to September inclusive, the load is modelled as 60% constant P, 40% constant Z. From October to March inclusive, the load is modelled as 40% constant P and 60% constant Z, due to an increase in electric heating load. It is common practice to model residential loads in this manner when exact information on the load type is not available (Willis, 2004).

4.3.3 Electric Vehicle Load Modelling

It is assumed that each EV is connected at the same CPOC as the household load through a single-phase connection. Charging profiles for EVs can vary depending on battery type, charging equipment and the electricity supply network. It is assumed that once connected, an individual EV with no charge controlling capability charges at a rate of 4 kW up to a BSOC of approximately 95%. After this point the vehicle charges at a rate of 1.5 kW until the battery has reached its maximum capacity. For this work, all EV batteries are modelled with a capacity of 20 kWh. The EV charging equipment is assumed to have a 90% efficiency rating. The charging rate of 4 kW is appropriate in terms of the power delivery capabilities of existing LV distribution networks in Ireland (ESB Networks, 2007). EV batteries are modelled as constant power loads with unity power factor.

4.3.4 Time Periods for Investigation

In order to demonstrate the benefits of the optimisation technique, two specific periods of time within the one year period of residential load data were chosen. For this study, the charging period occurs from 10 pm to 7 am the next day. One test period was chosen because it contained the highest 15-minute residential demand during the off-peak charging periods (winter scenario). The maximum 15-minute residential demand

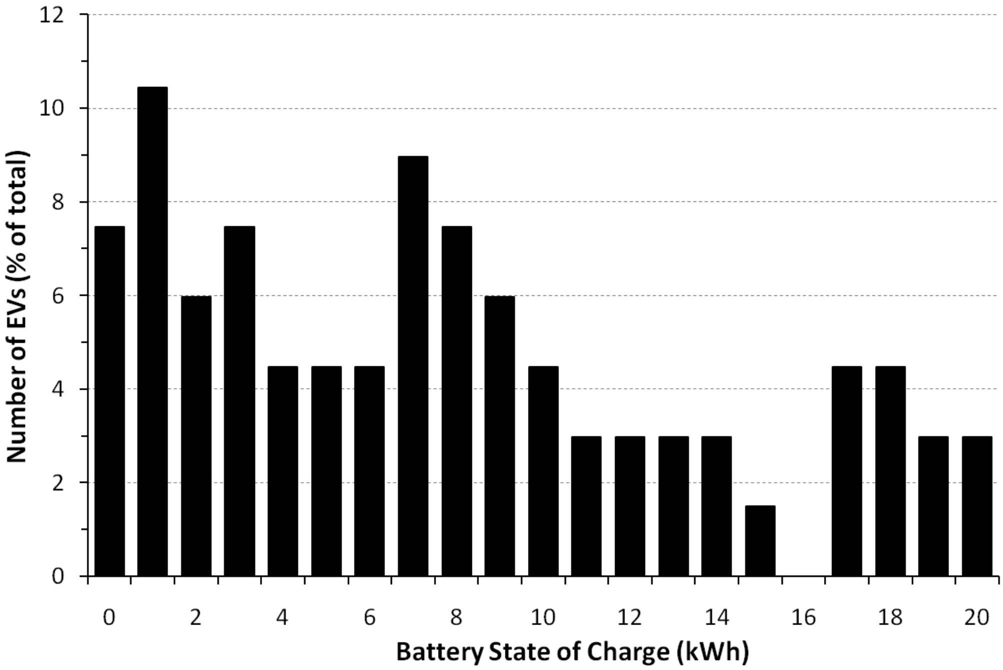

Figure 4.4: Distribution of the initial BSOC for each EV

for this time period was approximately 152 kW. The other test period chosen was a low-demand mid-week charging period in the summer (summer scenario).

For the simulations, half of the residential households were randomly assigned an EV, as shown in Fig. 4.3. This amounts to 67 EVs on the network with a potential combined maximum demand of 268 kW. It was assumed that all EVs remain connected to the network for the entire charging period, with each EV randomly assigned an initial integer valued BSOC. The distribution of the initial BSOC for each EV is shown in Fig. 4.4. The average initial BSOC of all the EVs was 7.8 kWh, or 39% of the maximum BSOC.

Table 4.1 shows the breakdown of EVs allocated to the network as well as the total energy requirement of these vehicles on a phase-by-phase basis. It is clear from this table that there is a greater number of EVs on phase c, and thus a larger energy requirement, compared to the other phases. While a 50% penetration of EVs on a distribution feeder may not be experienced in reality for many years to come, it was deemed appropriate to examine such a demanding scenario in order to fully capture the main benefits from controlled charging strategies compared to uncontrolled charging.

Table 4.1: Initial EV Conditions

	Number of EVs	**Combined Battery Capacity (kWh)**	**Combined Initial BSOC (kWh)**	**Total Energy Required (kWh)**
Phase a	19	380	139	241
Phase b	18	360	146	234
Phase c	30	600	236	344
Total	67	1340	521	819

4.3.5 Stochastic Scenario Analysis

The charging periods identified above were chosen to examine the optimisation technique for specific network scenarios. However, in order to demonstrate the benefits of the optimisation technique for a wider range of scenarios, a stochastic tool is developed to generate different residential load scenarios with probabilistic conditions for varying residential load, EV location and initial BSOC.

Probability distribution functions (PDFs) for the household load were created based on the residential load data provided by the DSO with PDFs for low, medium and high use customers. 15-minute household load profiles were then generated for each house for a 9 hour period from 10 pm to 7 am the next day, similar to the deterministic analysis. It is assumed that all EVs are connected for charging at the beginning of this period and remain connected until the end. At the beginning of each 9 hour charging period the EV locations on the network were randomly selected with each one then assigned an initial BSOC based on a PDF of BSOC data. The values for the initial BSOC obtained during the simulations compared well to those determined from the DSO led EV trials (ESB Ecars, 2011). For each charging period time step, network sensitivities were determined which are then used to optimise the charging rate of each EV. The load model and power factor for both the residential and EV load remain the same as for the deterministic analysis.

4.4 Results and Discussion

The optimisation technique is tested with the two different objective functions. The first objective function, (4.1), maximises the total energy delivered to the charging EVs according to network sensitivities while the second, (4.10), also applies a weighting based on the energy requirement of the individual EVs. The results for each approach are outlined below and are compared to scenarios with no EV charging present and with uncontrolled EV charging.

4.4.1 Network Sensitivities

For each 15-minute time interval, a series of three-phase, unbalanced load-flow calculations are performed using the customer demand profiles in order to determine the voltage and thermal loading sensitivities of the network due to the introduction of EVs. These sensitivities inform the optimal charging rate of each EV for each time step of the charging period. The voltage sensitivity at each CPOC is measured for varying charging rates and varying EV charging locations on the network. Fig. 4.5 demonstrates how the voltages measured at the CPOCs closer to the transformer (i.e. 3 and 8 from Fig. 4.3) are less sensitive to the addition of EV loads as compared to those located near the end of the feeder (i.e. points 6, 7, 11 and 12).

Since the household loads for this network are connected to individual phases of the network, the addition of EV load to a particular CPOC affects the voltage at that particular CPOC as well as the voltage on the other phases of the network, as demonstrated in Fig. 4.6. As can be seen, the addition of EV load on phase c only causes the voltage on that phase to decrease while the remaining phase voltages increase slightly. This effect is not uncommon in unbalanced networks (Kersting, 2002) and is captured in the voltage constraint equation, (4.7), where the sensitivity, μ, of the voltage at a particular CPOC can be either positive or negative depending on the phase to which an EV is connected.

The voltage sensitivities can vary due to changes in the domestic household load,

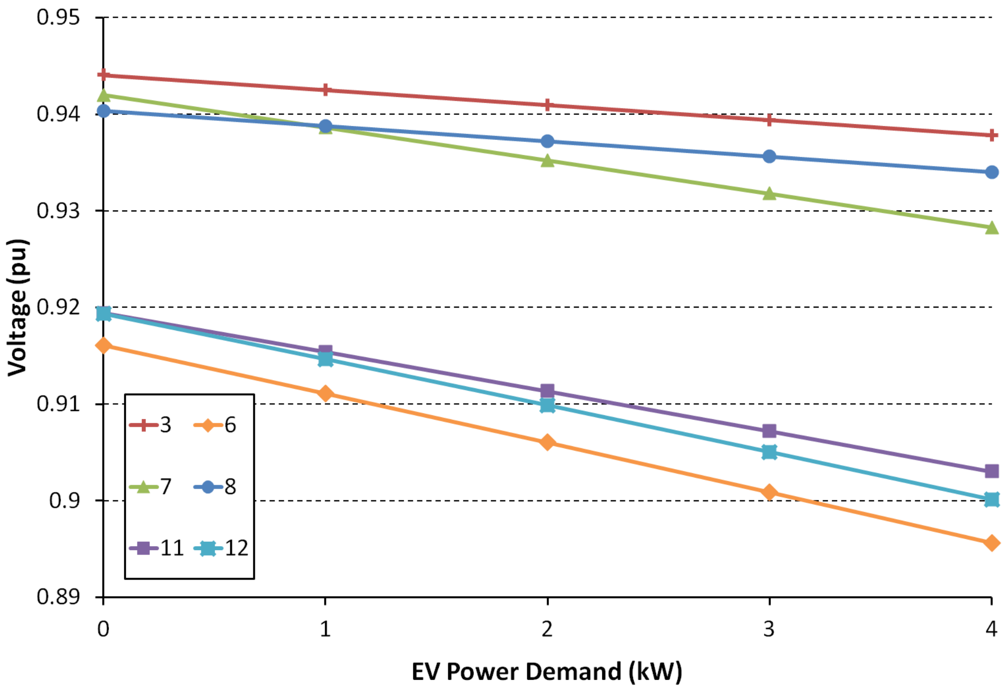

Figure 4.5: CPOC voltage levels at 6 network points for increasing levels of EV charging (winter scenario)

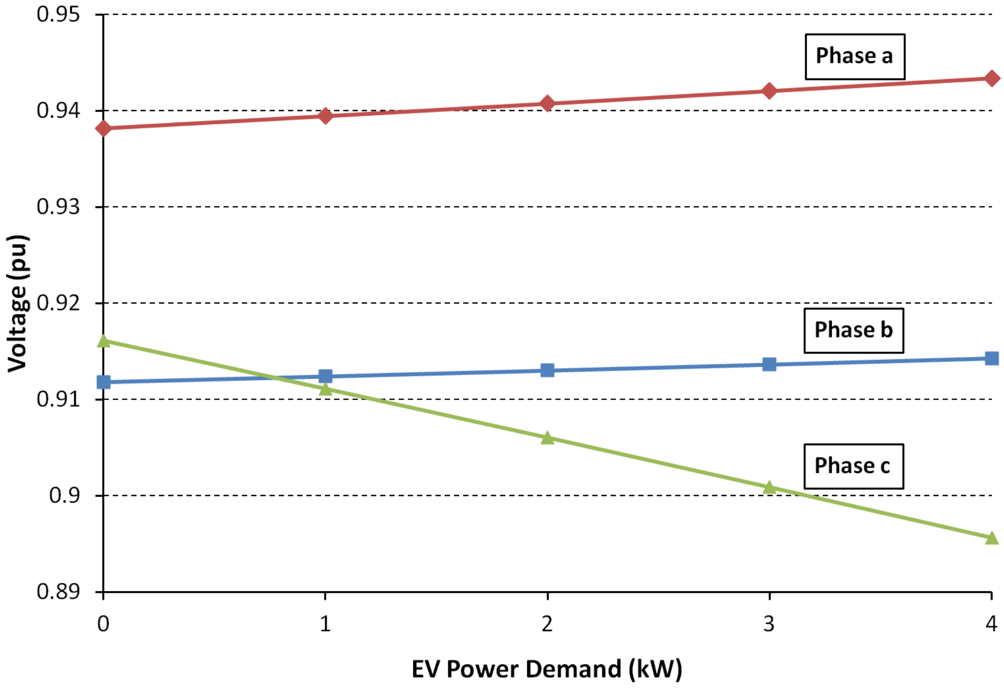

Figure 4.6: Interdependence of 3 CPOC voltages with EV charging on phase c (winter scenario)

and therefore they are calculated for each time step of the analysis. This information is then subsequently used to optimise the EV charging rates, the results of which are outlined in the following sections.

In order to determine the accuracy of the optimisation technique, error margins were calculated based on the difference between the predicted CPOC voltages from the optimisation algorithm and the CPOC voltages recorded from the subsequent load-flow calculations. The average maximum error margin over the summer charging period was found to be 1% for the standard and weighted objective functions. For the winter charging scenarios these values were recorded as 1.4% (standard objective function) and 1.5% (weighted objective function). As can be seen in the results presented below, the accuracy of the sensitivities, in combination with the included safety margins, is adequate to ensure that no operating limits are exceeded due to EV charging.

4.4.2 Uncontrolled EV Charging

With no active control over EV charging rates, all of the EVs would be expected to commence charging at the beginning of the charging time period at the maximum rate of charge. As the network is not rated for this high level of demand, the network operating conditions are severely impacted. Fig. 4.7 shows the voltage level at a CPOC at node 6 for the winter scenario base case. The charge profile for an EV connected at the same CPOC is also displayed. The initial BSOC of this EV was 3 kWh or 15%. While all EVs on the network would be fully charged by the end of the charging period, the lower voltage limit at this CPOC, i.e. 0.9 pu, would be exceeded for over 3 hours at the start of the charging period. The lowest voltage experienced at this node is approximately 0.68 pu. It is clear that such a scenario could not be permitted to occur and it is likely that the number of EVs on the network would be restricted to a predetermined limit. For the purposes of comparison, an uncontrolled charging scenario was created whereby there is a limit to the number of EVs that are allowed to charge simultaneously. This number was determined by incrementally adding EVs, charging at the maximum rate of charge, to the extremities of the feeder up to the point

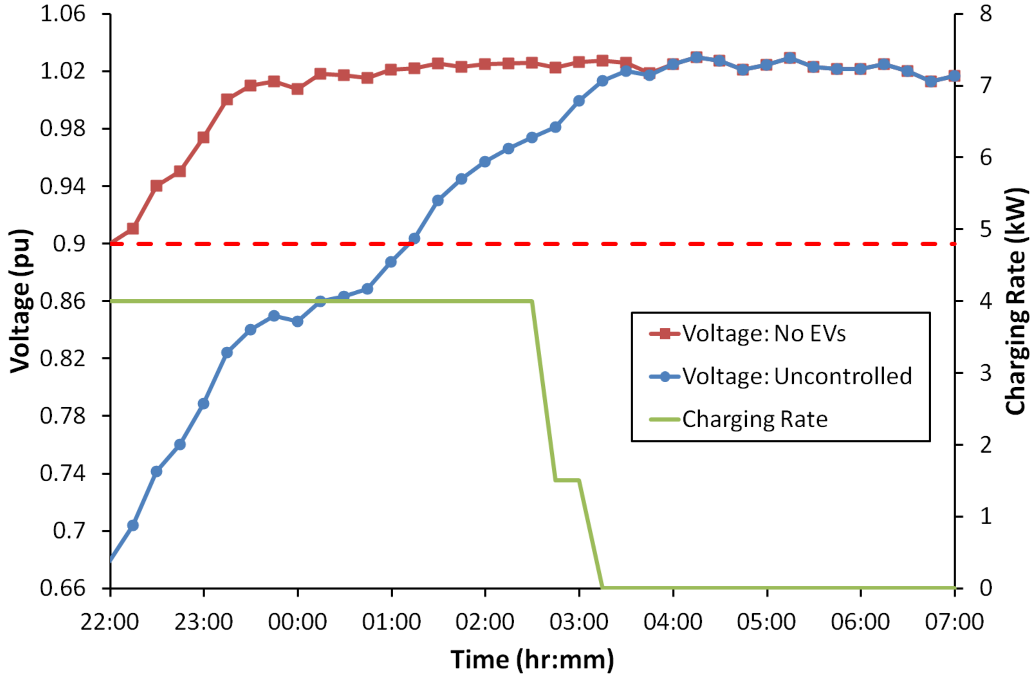

Figure 4.7: Voltage level for a CPOC at node 6 for base case and uncontrolled charging scenarios with charge profile for an EV charging at the same CPOC (winter scenario)

before the feeder exceeds an allowable operating limit. This test was performed with the residential load at the maximum annual expected nighttime demand. Charging was restricted to begin only after midnight to ensure that the residential load is off-peak. For the test network utilised in this work, the predetermined number of EVs that could be allowed to charge in an uncontrolled scenario was found to be 21.

4.4.3 Controlled EV Charging

By employing the methodology described in Section 4.2, the rate at which each EV charges is now optimised in order to deliver the maximum power to the EVs while maintaining all voltages and network flows within acceptable operating limits for each time step. At the beginning of the charging period, the total energy required to return all EVs to 100% BSOC is 819 kWh. For the optimisation, the lower voltage limit is set at 210 V or 0.913 pu, which allows for a margin of safety with respect to the lower voltage limit defined in the Irish distribution network code (ESB Networks, 2007). This ensures that any unexpected short term variations in the demand will not cause the network to exceed its operating limits. The maximum variation allowable for the rate of charge between time steps, i.e. Δ in (4.3), is set at 0.25 kW for each of the control strategies.

4.4.3.1 Standard Objective Function

From Table 4.2 it can be seen that using the SOF a total of 810 kWh in the summer and 798 kWh in the winter were delivered to the EVs by the end of the respective charging periods. Although this means that the total EV energy requirement (819 kWh) was not met, in both cases the network was maintained within normal operating limits for the entire duration of the charging period.

Table 4.2: Total Energy Delivered to EV Batteries

		Total Energy Delivered (kWh)	**% Energy Requirement**
Uncontrolled Charging (21 of 67 EVs)	Summer	238	29
	Winter	238	29
Standard Objective Function	Summer	810	98.9
	Winter	798	97.4
Weighted Objective Function	Summer	818	99.9
	Winter	815	99.5

The voltage profile of a CPOC at node 6 with an EV charging and the corresponding EV charge profile is given in Fig. 4.8. It is evident that the voltage here is a binding constraint for the optimisation technique as it is held just above the lower voltage limit for the majority of the charging period. It can also be seen that the EV connected to this CPOC does not truly begin charging until the third hour of the charging period and does not approach a maximum rate of charge until towards the end of the period. This particular EV had an initial BSOC of 3 kWh (15%) and had reached a BSOC of 15 kWh (75%) by the end of the charging period. Clearly, this would be an unacceptable outcome for an EV owner that desired a full BSOC.

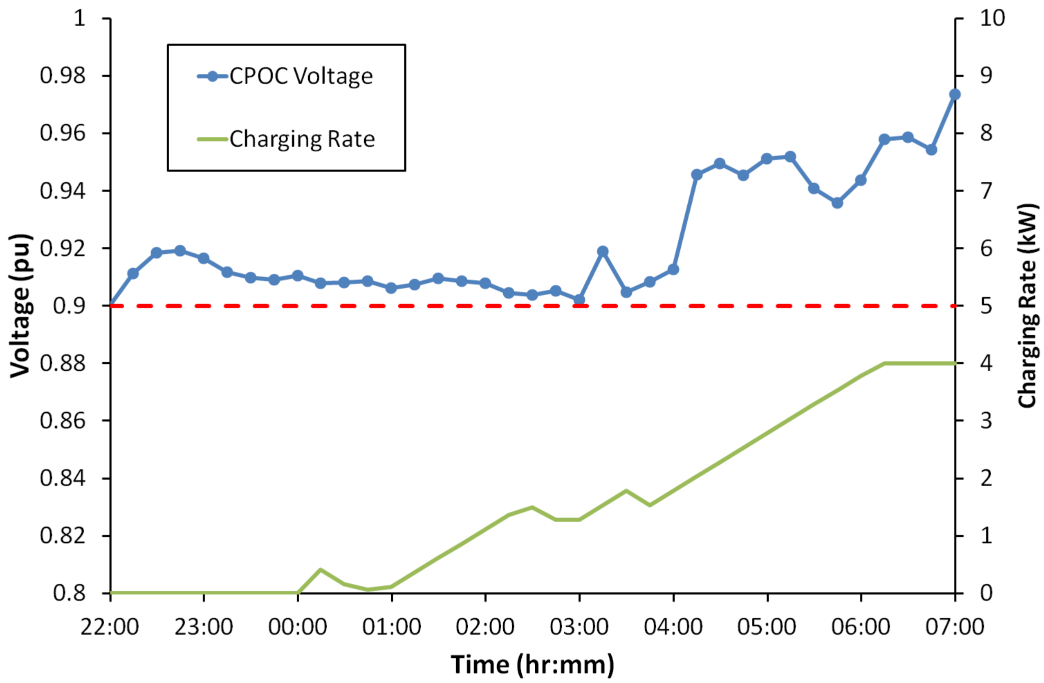

Figure 4.8: Voltage profile for a CPOC at node 6 and charge profile for EV charging at the same CPOC with optimised charging employing the standard objective function (winter scenario)

Fig. 4.9 shows the distribution function for the BSOC of each EV at the end of both the summer and winter charging periods. It is evident in both cases that a number of EVs, including the one shown in Fig. 4.8, have not reached a full BSOC by the end of the charging period. In the summer scenario, 64 of the 67 EVs were fully charged, while for the winter charging period, 63 EVs had a full BSOC. In both cases, the EVs with a BSOC of less than 100% are all located near the end of the branches of the feeder and are connected to phase c. From Table 4.1 it can be seen that a greater number of EVs are connected to phase c than either of the other phases, which results in a larger energy requirement. Additional load due to EV charging at CPOCs near the end of feeder branches will have a greater effect on network voltage levels than if located closer to the transformer. As a result, the optimisation method allocates low charging rates to these EVs until the other EVs are fully charged. The combination of both factors leads to a number of EVs not receiving a full BSOC by the end of the charging period. This outcome is displayed in Fig. 4.10, which shows the active power demand, with and without EV charging, on each phase of the network over the charging period. It is

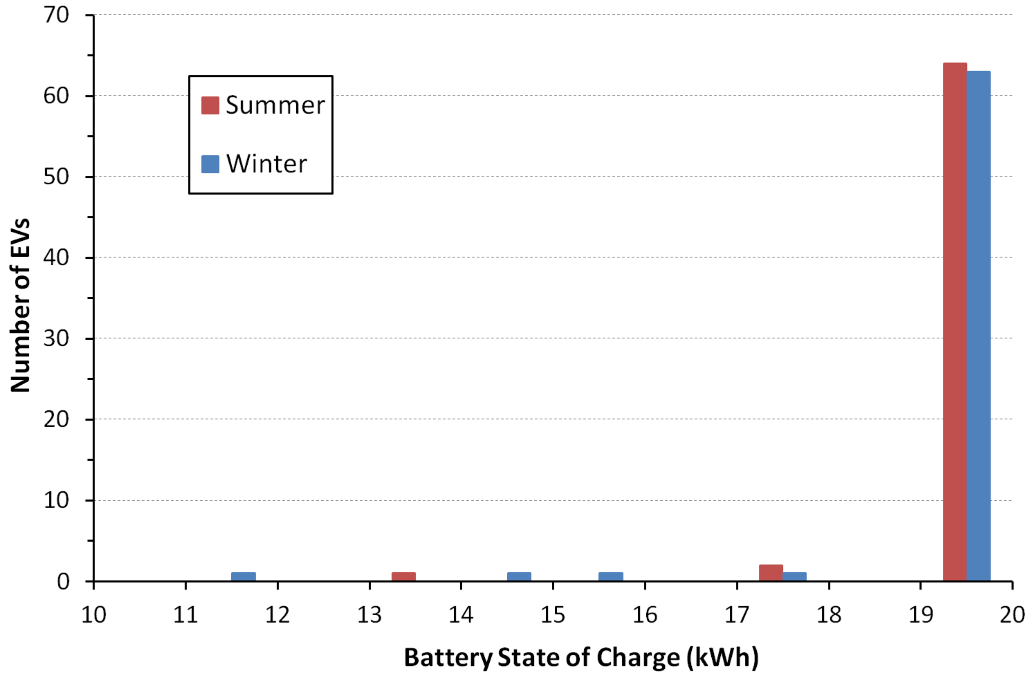

Figure 4.9: Distribution function of the battery state of charge for all EVs at end of the summer and winter charging periods: standard objective function

clear that, while the EVs connected to phase a and phase b have completed charging, power is still being delivered to some EVs connected to phase c. Also shown in this figure is the lowest CPOC voltage measured on each phase of the feeder for each time step. It is again clear that while power is being delivered to the EVs on the feeder, the voltage levels at each of the CPOCs are held above the lower voltage limit.

4.4.3.2 Weighted Objective Function

The standard objective function optimisation technique will consistently tend to assign low charging rates to EVs located further from the transformer. Such a situation would clearly be unacceptable. In order to overcome this, the optimisation process was repeated, as described in Section 4.2, with the objective function weighted according to the current BSOC of each charging EV (4.10).

By employing this method, 818 kWh of energy are delivered to the EVs for the summer charging period and 815 kWh are delivered in the winter charging period, which

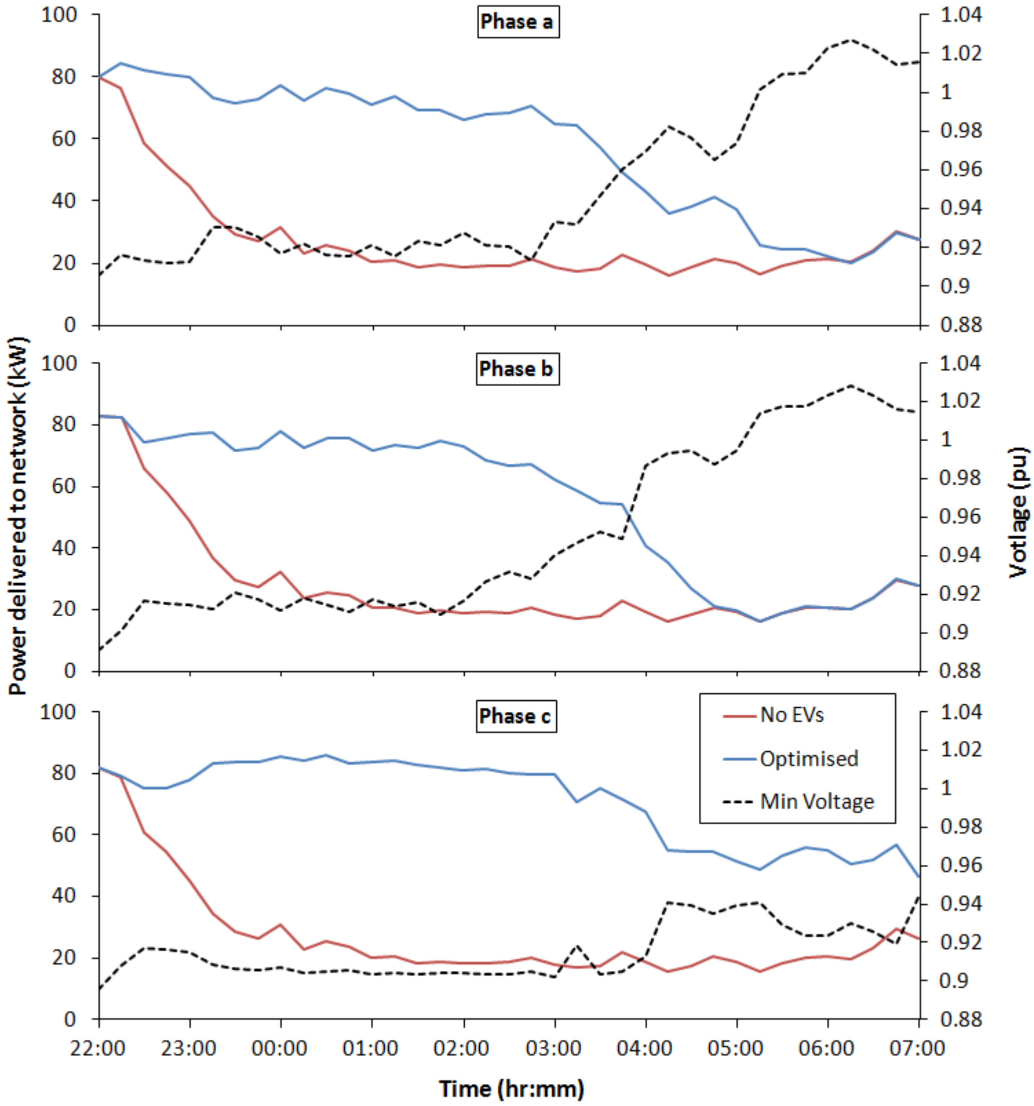

Figure 4.10: Power delivered to network on each phase for the case with no EVs charging and the optimised charging case employing the standard objective function (winter scenario). The lowest CPOC voltage for each phase at each time step for the optimised charging case is also shown.

represents 99.9% and 99.5%, respectively, of the total energy required to return all EV batteries to a full BSOC. The total power delivered to the EVs for the uncontrolled and optimised charging scenarios is shown in Fig. 4.11. While both objective function methods deliver similar energy totals by the end of the charging period, the individual EV charging patterns vary significantly across the network. During the early stages of the charging period, the SOF prioritises EVs that are located close to the transformer,

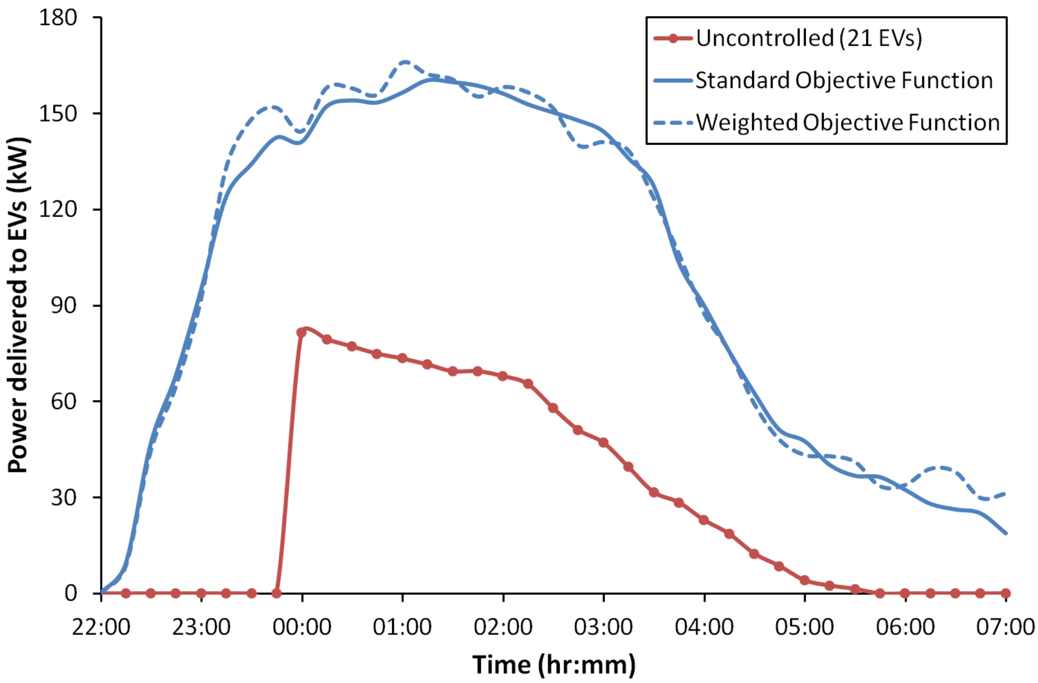

Figure 4.11: Total power delivered to EVs for uncontrolled and optimised winter charging scenarios

whereas the WOF assigns higher charging rates to EVs with a low BSOC, wherever they may be located in the network. Later in the charging period, applying the SOF, vehicles located at the network extremes begin charging. As the voltage is more sensitive to additional load at these points of the network, the charging rates for these EVs are lower and less energy can be delivered. The same restrictions are not as severe using the WOF as the energy delivered to the EVs is more evenly distributed across the network, resulting in more energy being delivered towards the end of the charging period.

Fig. 4.12 shows the voltage profile for the same CPOC as shown in Fig. 4.8, as a result of the WOF optimisation technique. Once again, it is apparent that the voltage at this CPOC is a binding constraint. However, the EV begins charging much earlier and the BSOC by the end of the charging period has reached 100%, as compared with a figure of 75% using the SOF method.

The distribution function of the BSOC for the EVs by the end of the charging period is given in Fig. 4.13, and shows an increase in the number of EVs with a full BSOC for

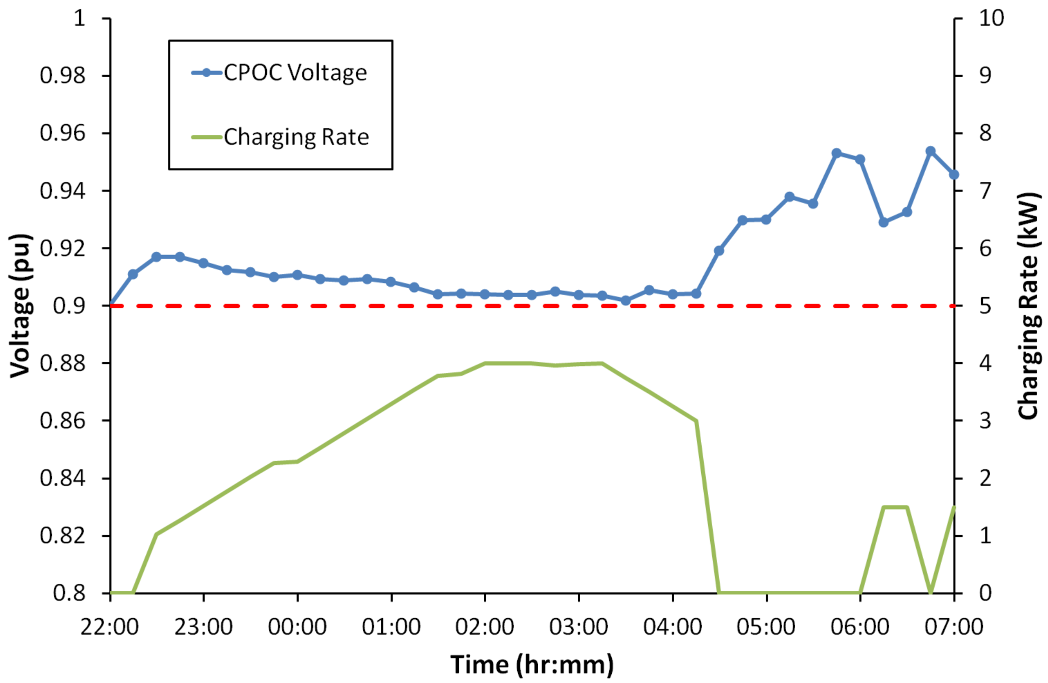

Figure 4.12: Voltage profile for a CPOC at node 6 and charge profile for EV charging at the same CPOC with optimised charging employing the weighted objective function (winter scenario)

both charging period scenarios when compared to the previous method. Specifically, 67 EVs have a full BSOC by the end of the summer charge period, while 66 of the 67 EVs have a full BSOC in the winter scenario. This compares favourably to the SOF method where the lowest BSOC of all the EVs was 68% and 58% for the summer and winter charging periods respectively. As was the case for the previous method, the EV that was not fully charged was connected to phase c and is located near the end of the feeder branches.

It should be noted that the particular allocation of EVs in this work resulted in there being a greater number of EVs connected to one phase compared to the others. As this work has shown, even an optimal method for maximising the energy that can be delivered to charging EVs may be insufficient if a large number of the EVs are connected to the same phase of the network at the same time. Such scenarios may require that the DSO reconfigure the distribution of load across the phases.

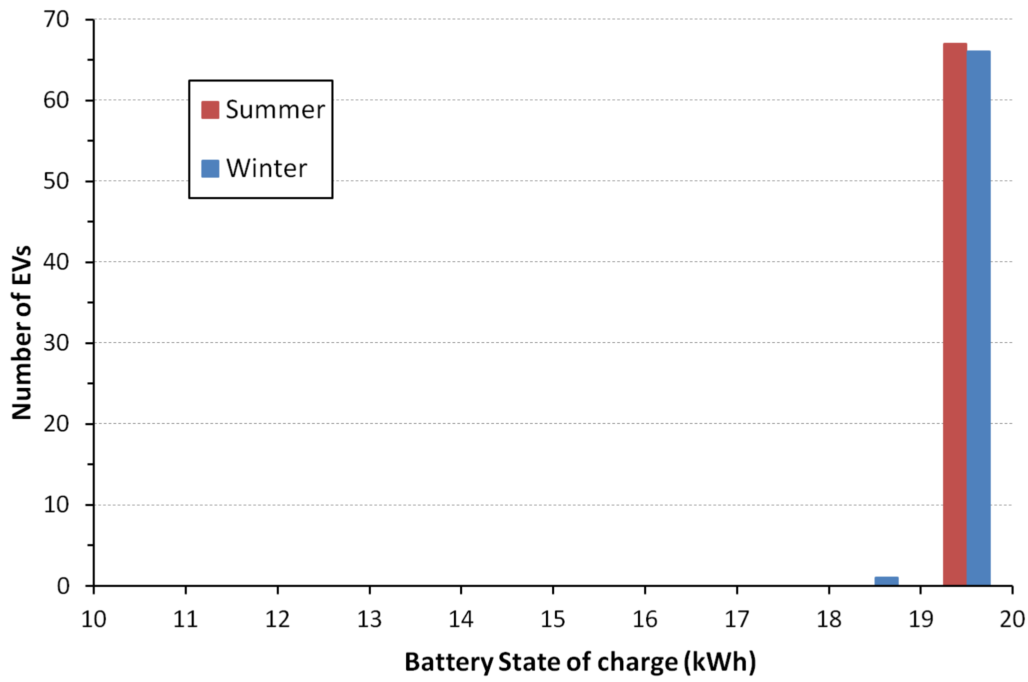

Figure 4.13: Distribution function of the battery state of charge for all EVs at end of the summer and winter charging periods: weighted objective function

4.4.4 Thermal Loading of Network Components

Thermal loading constraints of certain feeder components are also taken into account by the optimisation technique. Fig. 4.14 shows the loading of the LV transformer over the charging period for the winter scenario, while Fig. 4.15 shows the loading for the 3-phase mains cable (Line 1-2 in Fig. 4.3) that supplies the feeder from the transformer for the same scenario. In both cases, it is evident that neither the transformer nor the mains cable loading are the binding constraint on this network. Clearly, the network equipment is more than adequately rated for accommodating the additional load that would be demanded by this high penetration of EVs, assuming that the majority of charging occurs at off-peak times of day. This may not be the case for all residential distribution feeders, many of which may experience overloading of network components due to large numbers of EVs charging simultaneously at both peak and off-peak times of day. Without some form of controlled charging for EVs, a significant increase in the number of overloading incidences will impact on the lifetime of these network compo-

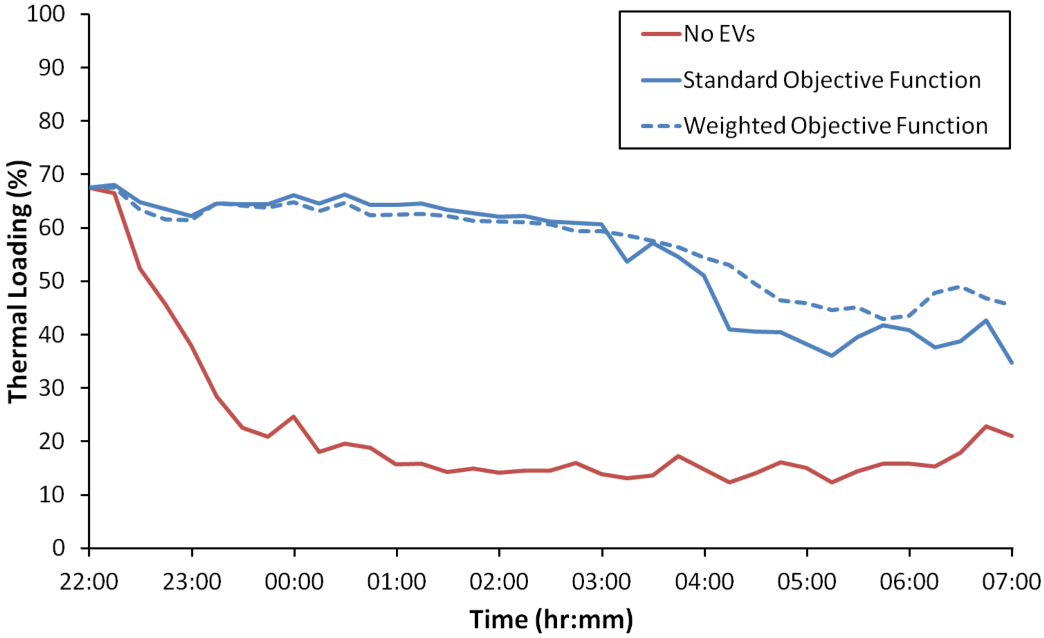

Figure 4.14: Thermal loading of LV transformer for winter charging period

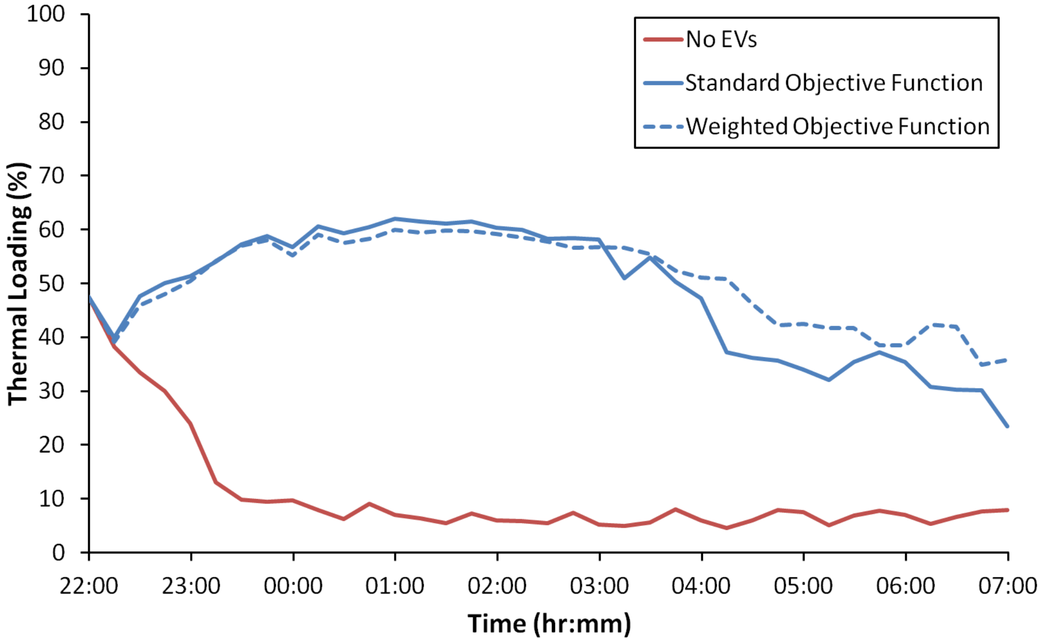

Figure 4.15: Thermal loading of 3-phase mains cable supplying feeder for winter charging period

nents (Taylor et al., 2009). By employing a controlled charging technique, like the one described in this chapter, the overloading of network components due to EV charging can be avoided by incorporating certain constraints, (4.8), (4.9). While this would result in increased loading levels during the off-peak period, a flatter transformer load profile would impact less on the transformer lifetime than a profile with large overloads due to on-peak EV charging (IEEE, 1995). Together with the introduction of other DSM schemes, many forms of residential load could be controlled in a manner which would allow networks to be utilised to their fullest extent while not impacting on component lifetimes.

4.4.5 Network Losses

The network losses as a percentage of the total energy delivered to the network are presented in Fig. 4.16. For each of the cases studied, the losses ratio is greater in the winter charging period than in the summer period due to the increased residential demand in the winter. The added demand from EVs charging causes the losses ratio to increase significantly. This is evident for both the standard (SOF) and weighted (WOF) objective function methods. For the SOF case the losses ratio increases from 0.3% to 4.1% in the summer and 1% to 4.5% in the winter. For the WOF method these values increase to 4.6% in the summer and to 4.8% in the winter scenario due to the increased total energy delivered on the network.

4.4.6 Stochastic Scenario Analysis

A stochastic analysis of the network loading is carried out in order to provide insight into the effects of the optimisation technique while accounting for the variability associated with a high penetration of charging EVs. The optimisation technique using the WOF was simulated for 500, 9-hour charging periods (i.e. 18,500 time steps). Residential load profiles for typical mid-week, winter scenarios were generated based on the associated PDFs.

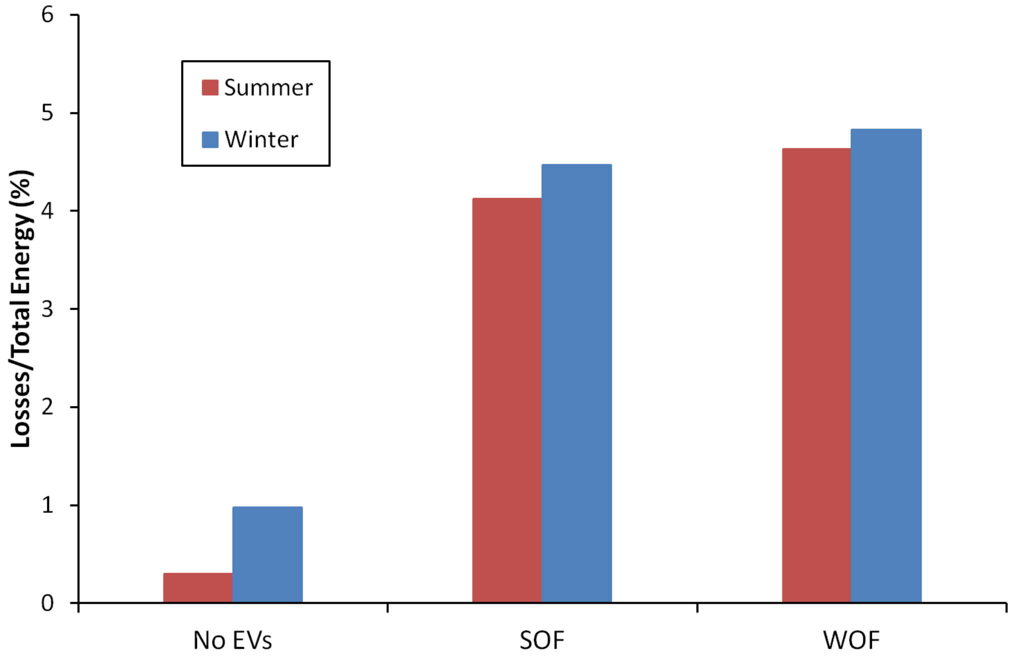

Figure 4.16: Network losses for standard objective function (SOF) and weighted objective function (WOF) cases

Fig. 4.17 shows the distribution of measured voltages for all CPOCs over all charging periods for the scenario with no EVs on the network and the scenario with 50% EV penetration with optimised vehicle charging. This graph shows that the majority of pre-optimisation voltage measurements are near or above 1 pu with reduced occurrences for decreasing voltage levels. Following the application of the optimisation technique, the majority of voltage measurements are recorded between 0.91 and 0.95 pu indicating that the optimisation technique was able to maintain CPOC voltages above the low voltage limit for the network. Any occurrence of voltage levels below the lower voltage limit, in both the case with no EVs and the optimised case, is due to the household demand alone. As a result, these voltages remain unaffected in the optimised case as the technique does not allow EV charging if the network is already exceeding limits.

The distribution of thermal loading results for the transformer during the analysis is presented in Fig. 4.18. Prior to the addition of EVs, the majority of loading measurements were found to lie between 10% and 30% of rated loading. Following the introduction of EVs, charged according to the optimisation method, the majority of

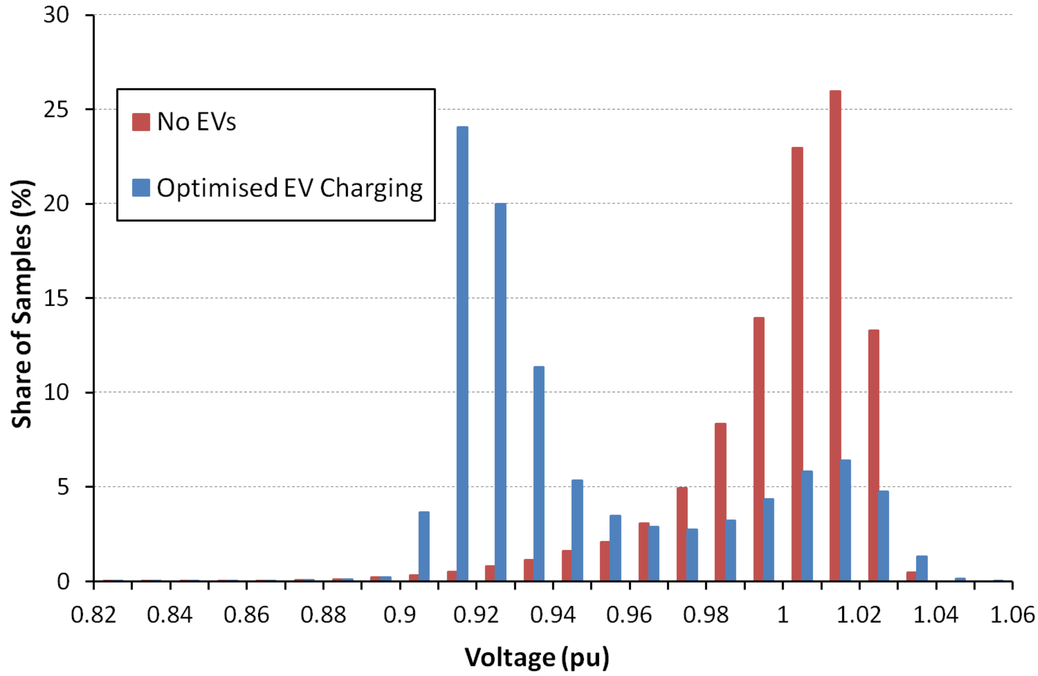

Figure 4.17: Distribution of measured voltages at network CPOCs

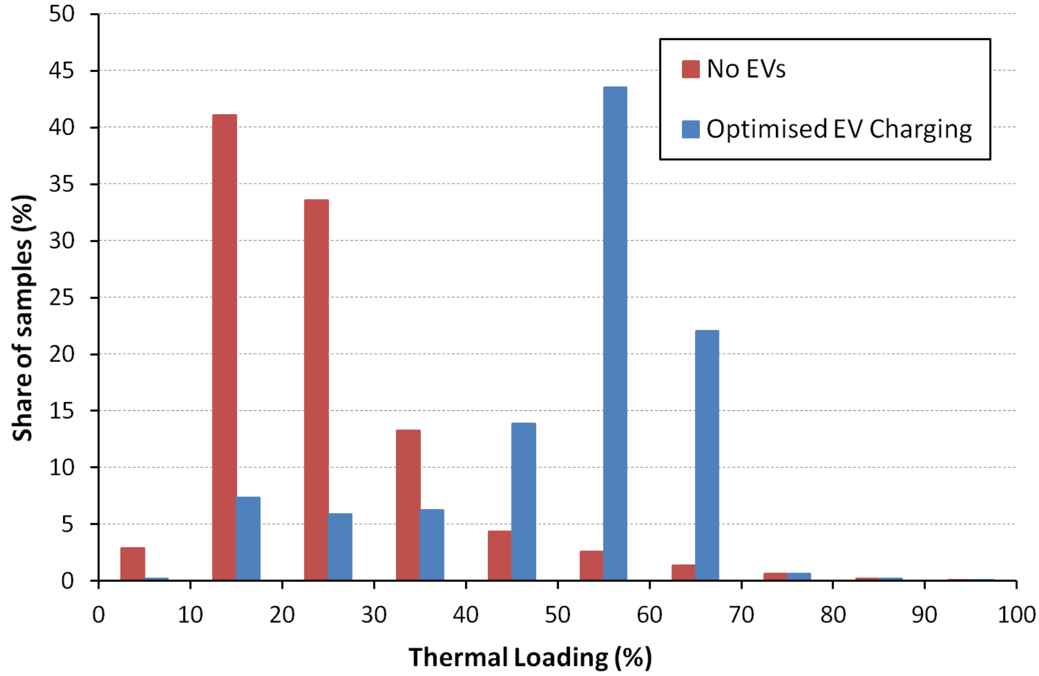

Figure 4.18: Distribution of measured thermal loading levels for the network transformer

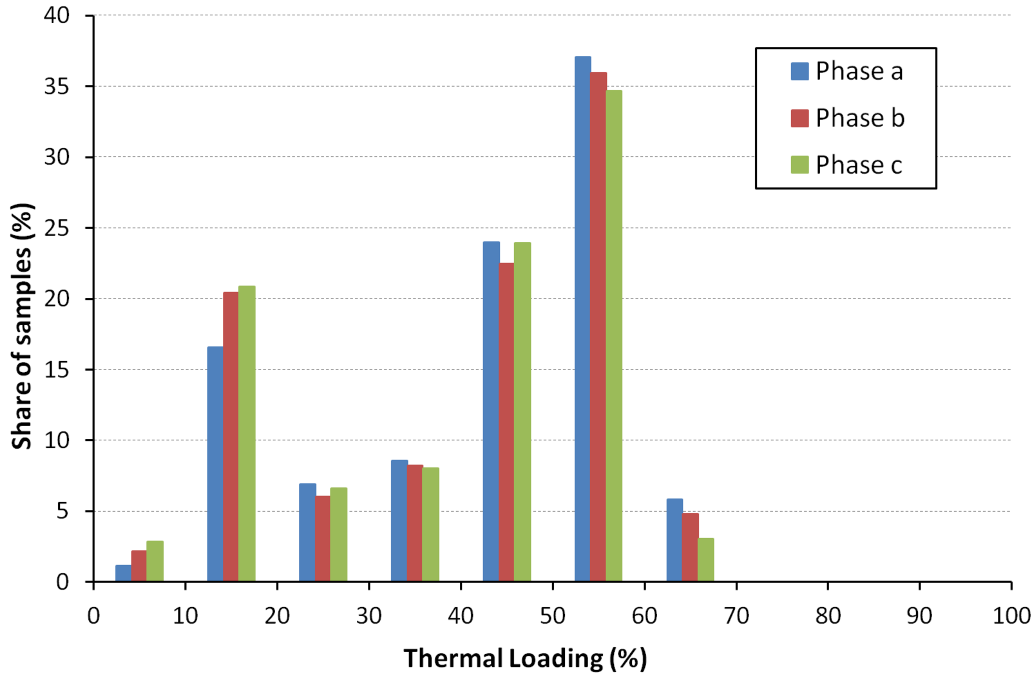

Figure 4.19: Distribution of measured loading levels on each phase of the 3-phase mains cable supplying the network from the transformer (optimised EV charging)

recorded measurements were found to be in the region of 50-70% of rated loading.

Fig. 4.19 shows the distribution of measured thermal loading for each phase of the 3-phase mains cable supplying the feeder from the LV transformer. These measurements are from the optimised case only. As can be seen from the loading results for both the transformer and the mains cable, the rated loading limit for either component is never the constraining factor for the optimisation method. It is apparent that, for this particular network, the electrical components are more than adequately rated to accept the increased loading due to a high penetration of charging EVs. Instead, the voltage limits are more likely to be an issue with off-peak EV charging and, as a result, are typically the constraining factor in the optimisation method.

Fig. 4.20 shows results for the final BSOC of all EVs after each charging period, representing the BSOC of the EV with the lowest BSOC, as well as the average BSOC of all EVs. For the high penetration level of charging EVs examined, the optimisation technique results in an average BSOC of 99.9%. While it is possible that not every

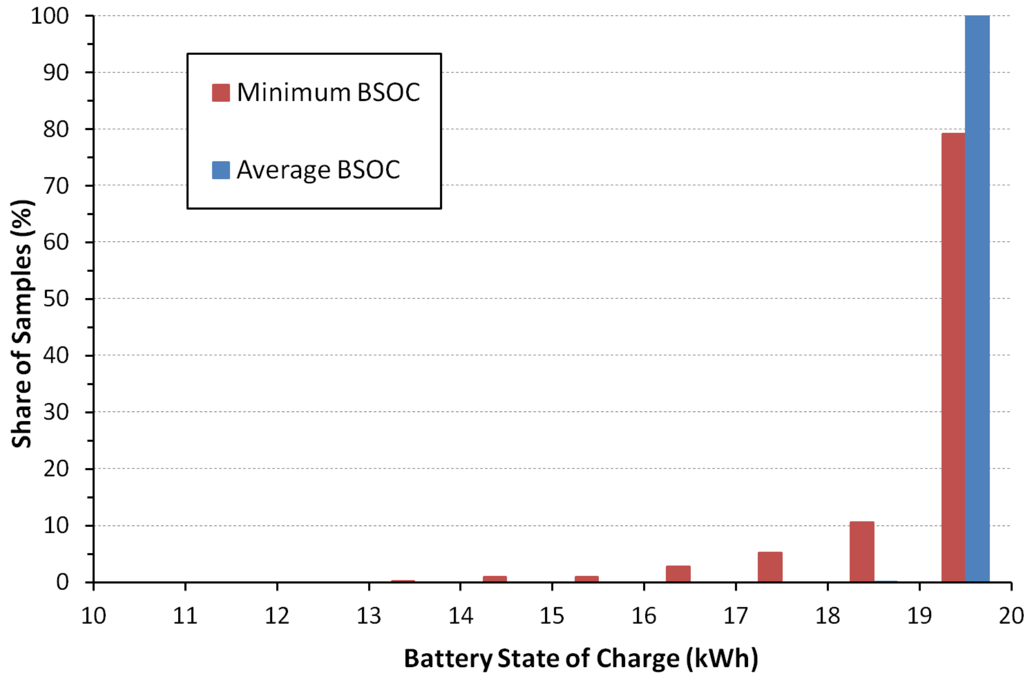

Figure 4.20: Distribution of minimum and average BSOCs for all EVs recorded at the end of each charging period

EV will have a full BSOC by the end of the charging period, such cases occur far less frequently. The lowest final BSOC recorded over the analysis was 13.3 kWh (66.5%).

The average losses on the LV feeder over all charging periods was found to be 11 kWh for the case with no EVs and 80 kWh for the optimised charging case using the WOF method.

4.5 Conclusion

The introduction of high penetrations of EVs will have significant impacts on the operating conditions of distribution networks. If they are to be charged in a passive, uncontrolled manner then major infrastructural upgrades may be required. Controlled charging by the DSO could help to alleviate some of these issues and allow EV owners to charge their vehicles while maintaining the network within acceptable operating limits. This chapter demonstrated how the charging rates of a high penetration of EVs on a test network can be optimised in order to deliver the maximum amount of energy to the EVs within a set charging period subject to network constraints, while ensuring that the underlying residential load remains unaffected.

Results have shown that maximising the total power to all EVs according to network constraints will favour those EVs that are connected near to the transformer, rather than those connected towards the extremes of the radial network. Therefore, a WOF was studied, which optimised the EV charging rates according to both the impact on the network operating conditions and the BSOC of the EVs. Results show that the modified objective function increases the total energy delivered to the EVs. This objective function was also tested for various charging period scenarios and was shown to return an average BSOC of 99.9% for all EVs over all periods examined.

The linear programming based technique proposed in this study is not computationally intense nor does it require storage of historical load data for subsequent use, and therefore could be easily incorporated into a coordinated charging scheme. Determining the various network sensitivities to additional load provides insight into the condition of the network and could prove very useful for DSOs employing such schemes in the future. Assuming the use of AMI within residential households and sufficient communication links between the DSO and the AMI, practical implementation of the optimal charging method would provide significant benefits in terms of accommodating high penetrations of not only EVs, but any form of DER into distribution systems.

CHAPTER 5

Local vs. Centralised Control Strategies

5.1 Introduction

IN Chapter 4, a method for coordinating the operation of DER on LV residential networks was proposed. The technique controls the operation of specific DER units in order to make optimal use of available network capacity while maintaining network operating levels within acceptable limits. A central controller uses real-time information of network conditions as well as the status of each DER unit in order to determine the optimal operating set point to be issued to the individual units. Previous work in this area has investigated the benefits from the implementation of control strategies for DER devices such as EVs (Sortomme and El-Sharkawi, 2011; Dyke et al., 2010; Clement-Nyns et al., 2010). While these studies demonstrate the benefits of controlled EV charging, in terms of reduced network losses, voltage deviations and component overloading, they are all based on a centralised control approach. The implementation of such a strategy would require the installation of an adequate communications system together with a central control centre. Such infrastructure requirements could be costly to put in place and may only make economic sense for networks with very high penetrations of DER units (Dimeas and Hatziargyriou, 2005).

An alternative approach to coordinating multiple dispersed units on a network is through the use of a decentralised or local control approach. In contrast to the work mentioned above, this chapter proposes a strategy for optimising the operation of DER units in LV distribution networks based on a local control charging (LCC) method. The benefits of decentralised control compared to centralised control strategies have been previously explored for large-scale variable DG. In Vovos et al. (2007), both strategies are compared in terms of the capacity of DG that could be accommodated in existing distribution networks by means of voltage control. Results show that while the centralised method allows for a greater penetration of DG, the total capacity is only marginally greater than that from using the decentralised method.

The LCC method proposed in this chapter allows for the optimal operation of DER units to be determined individually based solely on local network conditions and their current operating status. For example, optimal operation can be defined as maximising the total energy delivered to flexible load or maximising the total generation from micro-generation units. As a result, there is no need for bi-directional communication capability between each DER unit and a third-party controller. The main difference between the LCC and the centralised control charging (CCC) strategies is the calculation of the sensitivity values that are used in determining the optimal operating set points for the units. The CCC method has the ability to update these values in real-time based on the loading conditions of the network. This is not possible when using the LCC method as individual units have no intercommunication capabilities. Therefore, DER units participating in a LCC scheme must utilise predetermined sensitivity values to calculate their optimal operating set point. The calculation of these values is described in Section 5.2.4.

As was the case in the previous chapter, the method is demonstrated using EV technology. The objective of the strategy is to deliver the maximum amount of energy to the EVs while maintaining the network within acceptable operating limits. The potential advantages and disadvantages of the LCC strategy are investigated in terms of network capacity utilisation and total energy delivered to the EVs. Results are compared to both an uncontrolled charging scenario and the WOF CCC method of Chapter 4.

The methodology of this chapter is presented in Section 5.2 where the LCC method is outlined. A description of the calculation of the sensitivity values and network constraints are also included. Section 5.3 describes the modelling of the test network, the residential load and the electricity demand profiles of the EVs used in the simulations. Results and discussion for a sample charging period using the LCC method are presented in Section 5.4 along with generalised results for a wide range of network scenarios. Results from the CCC method are also presented here for comparison with the LCC strategy. Conclusions are presented in Section 5.5.

5.2 Methodology

5.2.1 Assumptions

In order to implement any type of active control at the LV distribution system level, it is assumed that EV charging units with load control capability are present in each household with an EV present. AMI, which is also assumed to be present in each household, enables time-of-day electricity tariffs which incentivise customers to avoid the more expensive peak load time-of-day. Each EV can charge at any rate between zero and the charger's maximum rated charge, subject to certain restrictions, which are outlined later in this section. It is assumed that each of the EV charging units on the network has the same charging capabilities. The ability to vary the charge rate of individual EVs in a continuous manner for use in optimal charging strategies has been studied previously in Brooks et al. (2010); Clement-Nyns et al. (2010); Sortomme and El-Sharkawi (2011). While the possibility exists for fast, 3-phase charging, it is assumed that each EV will be connected to the network via a standard single-phase AC connection. Although the concept of vehicle-to-grid for local system support or otherwise exists (Kempton and Tomić, 2005; Tomić and Kempton, 2007), bi-directional flow of electricity to and from an EV battery is not considered in this work. For the CCC method, it is assumed that the load control capability of the EV charging units can be utilised by the DSO, or a third-party controller, from a remote location.

5.2.2 Local Control Charging

Local control charging of EVs is achieved by each individual EV charging unit maximising the charge rate of their connected EV, subject to the voltage at its own CPOC and the loading of its own single-phase service cable. For each LCC unit, the sensitivity of the CPOC voltage and service cable loading to the addition of EV load at its charger unit is predetermined and fixed for all time steps of the simulation. Further details are given in Section 5.2.4. With the predetermined sensitivity value, along with information about the instantaneous voltage at the CPOC and loading of the service cable, the charging unit maximises the rate of charge of the EV without exceeding either the local voltage or single-phase loading limits.

The objective of the charging units in the LCC strategy is to maximise the amount of power delivered to their individual EV at each 15 minute time step, subject to certain constraints. Each charging unit aims to maximise its own charge rate and cannot communicate with any other charger unit on the feeder. The process is performed using a linear programming tool (MATLAB, 2009) and the optimisation occurs for each EV connected to the feeder and available for charging. The optimisation is calculated at each time step t. In this case, the objective function, F_{LCC}, is given as

$$F_{\mathrm{LCC}} = xP_{\mathrm{EV}} \tag{5.1}$$

where P_{EV} is the power delivered to the particular EV. It is assumed that P_{EV} is a continuous control variable that can vary between 0 kW and the maximum power output of the charger. x is zero when an EV is not connected at the CPOC or the EV battery is fully charged, while x equals one when the EV at the CPOC is connected and the EV battery is not fully charged.

5.2.3 Constraints

In Chapter 4, the CCC method incorporated constraints relating to node voltages and component loading across the entire feeder in order to optimally determine the charging rate for each EV. Similar constraints are applied when using the LCC method. However, as each controller has knowledge of local network conditions only, the constraints used in the LCC are specifically defined for the controller itself. A summary of the constraints are outlined below.

Each of the charging units has the ability to vary their output in a continuous manner. The charging rate limits are defined in (5.2), where $P_{\mathrm{EV}_{\mathrm{max}}}$ is the rated output of each charging unit.

$$0 \leq P_{\mathrm{EV}} \leq P_{\mathrm{EV}_{max}} \tag{5.2}$$

As was the case for the CCC method of Chapter 4, a rate of change constraint is also imposed (5.3). The constraint is included in order to avoid large variations in the charging rate over consecutive time steps, which can be undesirable for current battery technology as it may reduce battery cycle life (Hoffart, 2008).

$${P_{\mathrm{EV}}}^{t-1} - \Delta \ \leq \ {P_{\mathrm{EV}}}^{t} \ \leq \ {P_{\mathrm{EV}}}^{t-1} + \Delta \tag{5.3}$$

Here, t is the current time step and Δ is a defined limit, in kW, by which the charging rate can vary, compared to the charging rate at the previous time step, excluding on/off transitions.

For the LCC method, the EV charger unit has the capability to monitor the voltage at its own CPOC and the loading on the service cable supplying the customer residence only. The addition of EV loads, for the most part, will cause the voltage at various points of the network to drop. The extent of the voltage drop can vary depending on a number of factors, which include the location of the EV on the network and the rate of charge. The voltage at each CPOC must be maintained within the rated voltage range specified for the network, (5.4).

$$V_{min} \leq V_{\mathrm{CPOC}} \leq V_{max} \tag{5.4}$$

Here, V_{CPOC} (V) is the voltage at the CPOC, while V_{min} and V_{max} are the minimum and maximum allowable network voltage levels respectively. The thermal loading of the service cable refers to the total current flowing through the cable. This constraint is summarised in (5.5).

$$L_{\mathrm{SC}} \leq L_{\mathrm{SC}_{max}} \tag{5.5}$$

Here, L_{SC} is the thermal loading of the service cable and $L_{\mathrm{SC}_{max}}$ is the current rating for the fuse at the CPOC for the household.

5.2.4 Network Sensitivities

As stated in Section 5.2.2, for the LCC method, the network voltage and loading sensitivities to the addition of EV load are predetermined as the controllers do not have the capability to update them in real-time. One set of sensitivities is used for all time steps, which allows the charging unit at each household to determine an optimal charge rate without the need to calculate a new set of sensitivities at each time step. However, these sensitivity values cannot be expected to match the constantly varying load on the feeder. In order to determine the set of voltage and loading sensitivities for the LCC method, a series of unbalanced, 3-phase load-flow calculations were performed on the test network using power system simulation software (DIgSILENT GmbH, 2011).

These load-flow calculations determine the change in voltage and loading levels at all points on the network subject to the addition of EV load at each CPOC. In order to model the expected residential load during charging periods, each household was assigned a 2 kW load, which approximates the maximum average household demand over all time steps in winter. The sensitivity values for the voltage and loading assigned to a charging unit are the summation of all the voltage and loading sensitivities at all other CPOCs on the feeder respectively. This takes account of the impact that all of the EV loads, charging simultaneously, can have on a particular node and service cable on the feeder. This fixed sensitivity value was used in conjunction with the CPOC voltage and service cable loading measurements at each time step in order to determine the optimal charging rate for the EV. The constraint equations for the CPOC voltage and service cable loading are summarised as,

$$V_{min} \leq V_{init} + \mu P_{\mathrm{EV}} \leq V_{max} \tag{5.6}$$

$$L_{\mathrm{SC}_{init}} + \beta P_{\mathrm{EV}} \leq L_{\mathrm{SC}_{max}} \tag{5.7}$$

where, in (5.6), V_{init} is the initial voltage at the CPOC prior to the optimisation calculation. μ (V/kW) is the summation of the voltage sensitivities at each CPOC due to power demanded by that EV. For (5.7), $L_{\mathrm{SC}_{init}}$ is the initial loading on the service cable supplying the EV prior to the optimisation calculation, and β (A/kW) is the summation of the loading sensitivities for each service cable due to power demanded by that EV. These values would be determined by the charger units at the beginning of each time step.

5.2.5 Centralised Control

The centralised control method used here is based on the weighted objective function CCC method of Chapter 4. In summary, the centralised control of EV charging involves monitoring the voltage at each CPOC, the thermal loading of each household's single-phase service cable, the loading of the LV transformer and the 3-phase mains cable supplying the feeder, and also the BSOC for each connected EV. This information is sent to a centralised controller which incorporates additional network information to determine dispatch signals at each time step for the individual EV charger units accordingly. The sensitivities of the voltage and thermal loading of the network to EV load are calculated in advance for each time step. The centralised controller is also aware of all network voltages and line flows, which allows for a more accurate insight into the instantaneous network condition than is possible with the local control method. The controller then optimises the charge rate of each vehicle in order to deliver the maximum amount of power delivered to all EVs on the feeder, and thereby making best use of the network capacity. The process occurs at each time step and is independent of all other time steps with the exception of the rate of change of charge constraint (5.3).

The objective function for the centralised control method, F_{CCC}, is given by

$$F_{\text{CCC}} = \sum_{i=1}^{N} x_i \left(1 - \left(\frac{\text{BSOC}_i}{\text{BSOC}_{max_i}} \right) \right) P_{\text{EV}_i} \tag{5.8}$$

where N is the number of customers being served by the network, and P_{EV_i} is the power delivered, measured in kW, to the EV connected at the ith CPOC. x_i is zero when an EV is not connected at the ith CPOC or the EV battery is fully charged, while x_i equals one when the EV at the ith CPOC is connected and the EV battery is less than fully charged. BSOC_i is the current BSOC (kWh) for the EV connected at the ith CPOC and BSOC_{max_i} is the maximum battery capacity of that EV. The objective function is weighted according to the current BSOC of each individual EV. This weighting provides a more even distribution of energy to charging EVs and prioritises EVs with a low BSOC (Chapter 4).

The CCC technique considers the same constraints as the local control method (i.e. (5.2),(5.3),(5.4) and (5.5)), along with constraints ensuring that the rated loading of the network transformer and the mains cable supplying the feeder from the transformer are not exceeded. It is assumed that the necessary monitoring and communication equipment is installed on the feeder and that the data collected, along with the data from the AMI of the customers, can be utilised in determining the optimal charging rates for the EVs on the feeder. A full description of the method and constraints for the weighted CCC method can be found in Chapter 4.

5.3 Modelling of Test Network

5.3.1 Distribution Network

The test network is based on a LV residential distribution feeder in a suburban area of Dublin, Ireland, previously described as test network 2, described in Section 3.4.2. Test network 2 was chosen here to demonstrate the capability of the control charging method on a different network to test network 1. A simplified representation of the feeder is given in Fig. 5.1. In the actual test feeder, each household, EV and service cable are modelled separately. To recap, the model incorporates a 400 kVA, 10/0.4 kV step-down transformer supplying a feeder of 74 residential customers. The transformer has no tap-changing capability. A lumped load model, representing a similar number of residential customer loads with no EV loads, is included to represent another feeder being supplied from the same transformer. The nominal voltage of the network is 230/400 V with a voltage range tolerance of +/-10% (ESB Networks, 2007). In order to account for voltage drop along network feeders, the sending end voltage of the MV network is set at 1.05 pu. This ensures that voltage levels at the extremities of the LV network remain within acceptable limits under typical loading conditions. Specifications for the network model are given in Appendix B.

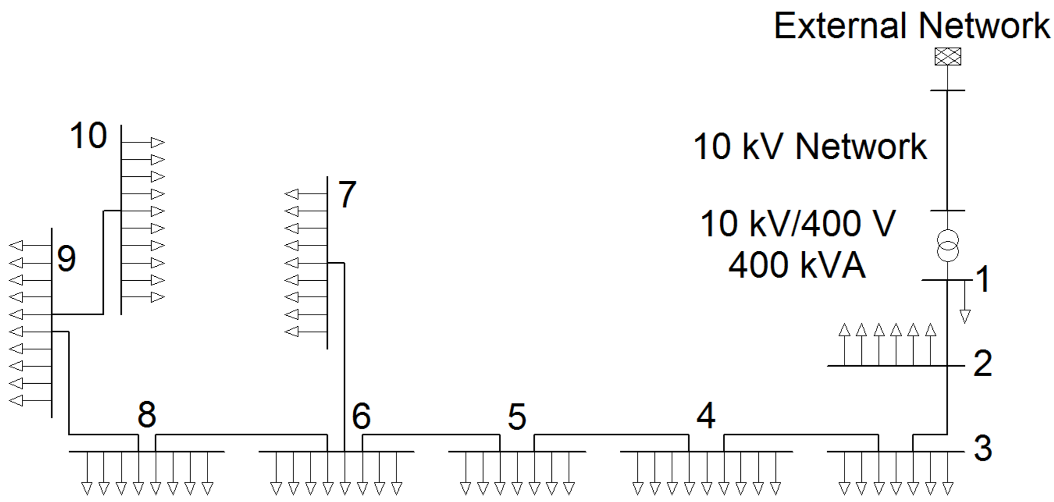

Figure 5.1: Single line diagram of test network

5.3.2 Residential Customer Load Modelling

Load data for domestic electricity demand customers was obtained from the DSO consisting of 15-minute time-series demand data for high, medium and low use customers. These profiles were subject to time-of-day pricing whereby the cheaper, off-peak tariff begins at 11 pm each day and ends at 8 am the following day. Different electricity demand profiles were randomly assigned to each of the houses in the test network based on annual energy demand figures for each household. As was the case in Chapter 4, in order to confirm that these load profiles portrayed an accurate representation of the power demanded by a real distribution feeder, the coincidence factor of the test network was determined. From assessing the yearly load profiles for each of the households on the network, the coincidence factor was found to be 0.36, which compares favourably with networks serving a similar number of customers (Willis, 2004). For modelling purposes, the power factor for each household load was set at 0.95 inductive. The load is modelled as a combination of 50% constant power (P) and 50% constant impedance (Z).

5.3.3 Electric Vehicle Load Modelling

EVs are modelled in a similar manner to that adopted in the CCC method of Chapter 4. To recap, it is assumed that each EV is connected at the same CPOC as the household load through a single-phase connection. Charging profiles for EVs can vary depending on battery type, charging equipment and the electricity supply network. For this work, all EV batteries are modelled with a capacity of 20 kWh. The EV charging equipment is assumed to have a maximum charging rate of 4 kW with a 90% efficiency rating. The charging rate of 4 kW is appropriate in terms of the power delivery capabilities of existing LV distribution networks in Ireland (ESB Networks, 2007). The EV batteries are modelled as constant power loads at unity power factor.

5.3.4 Time Periods for Investigation

5.3.4.1 Sample 24-hour Period

In order to demonstrate each of the charging strategies, a sample 24-hour time period within the one year period of residential load data was chosen. The time period selected is from 12 noon to 12 noon the following day and spans two weekdays in January. Due to the assumption that all customers are subject to a time-of-day tariff scheme, a large residential demand is experienced on the feeder once the cheaper off-peak period begins. The maximum demand on the feeder during this period is 270 kW.

In both cases, a 50% penetration of EVs on the feeder was examined, which means that 37 of the 74 households had exactly one EV charging at certain stages of the 24-hour period. While a 50% penetration of EVs on a distribution feeder may not be experienced for many years to come, it was deemed appropriate to examine such a scenario in order to fully capture the benefits of controlled charging strategies compared to uncontrolled charging. For the simulations, the EVs were allocated to the network in a random manner and the locations remained fixed for each of the charging strategy cases examined. The potential combined maximum demand from a 50% penetration

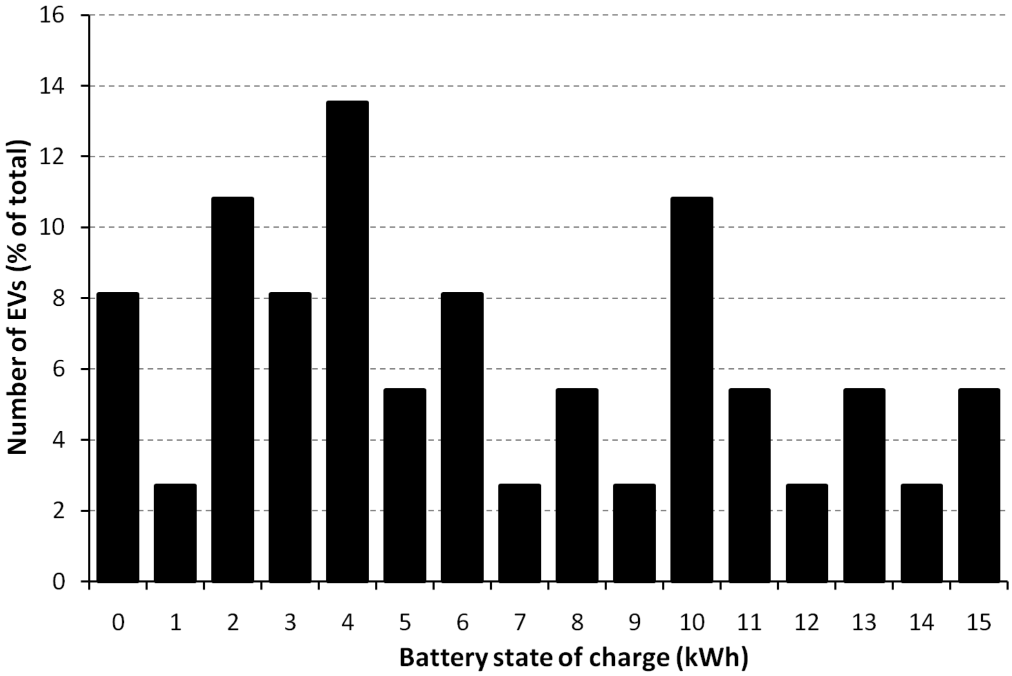

Figure 5.2: Distribution of the initial BSOC for EVs

of EVs is 148 kW. EV usage data was obtained from DSO led vehicle trials in order to determine a plausible range of connection times, durations of connection, and initial BSOC levels for the EVs in the simulations (ESB Ecars, 2011). Based on this data, the connection time for each EV was randomly assigned within a time frame of +/-3 hours of 11 pm, which is the start of the off-peak period. The duration of connection for each EV was also randomly assigned, whereby a vehicle remains connected for anywhere between 6 and 15 hours. Each EV is also assigned an initial BSOC, independent of the connection time, at the beginning of the charge period, determined as a random value between 0% and 75% of the maximum battery capacity of 20 kWh, which ensures that each EV has a charge requirement of at least 25% of their battery capacity upon connection. The distribution of the initial BSOC for each EV is shown in Fig. 5.2. Table 5.1 shows the breakdown of EVs allocated on the feeder along with the total energy requirement of these vehicles on a phase by phase basis.

Table 5.1: Initial EV Conditions

	Number of EVs	**Combined Battery Capacity (kWh)**	**Combined Initial BSOC (kWh)**	**Total Energy Required (kWh)**
Phase a	12	240	86	154
Phase b	13	260	84	176
Phase c	12	240	53	187
Total	37	740	223	517

5.3.4.2 Stochastic Scenario Analysis

The charging period identified above examines the LCC and CCC optimisation techniques for a specific network scenario. In order to investigate a wider range of scenarios, a stochastic tool, similar to the one developed in Chapter 3, was used to generate different residential load scenarios with probabilistic conditions for varying residential load, EV location, initial BSOC and duration of connection.

PDFs for the household load were created based on the residential load data provided by the DSO, with PDFs for low, medium and high use customers. 15-minute household load profiles were then generated for each house for a 24-hour period from 12 noon on a winter weekday to 12 noon the following day, similar to the example 24-hour period. At the beginning of each 24-hour period the EV locations on the network were randomly selected with each EV then assigned an initial BSOC and duration of connection time. The duration of connection is randomly determined between 6-15 hours. The load model and power factor for both the residential and EV load remain the same as for the example 24-hour period analysis.

5.4 Results and Discussion

Both controlled charging strategies are tested for the sample 24-hour period, with the results compared to cases with no EVs charging and with uncontrolled EV charging.

5.4.1 Uncontrolled EV Charging

In a scenario where no active control of EV charging is present, an EV, once connected, will charge at a maximum rate of 4 kW until it reaches a full BSOC. With distribution networks not rated to accommodate high penetrations of this type of load, a limit on the number of EVs allowed would have to be put in place to ensure that the network always remains within acceptable operating limits.

For the purposes of comparison, an example uncontrolled charging scenario was created whereby there was a limit to the number of EVs that were allowed to charge simultaneously. This number was determined by incrementally adding EVs, charging at their maximum rate of charge, to the feeder up to the point before the feeder exceeds an allowable operating limit. This test was performed with the residential load at the maximum expected demand for the example 24-hour period. For the test network utilised in this work, the predetermined number of EVs that could be allowed to charge in an uncontrolled scenario was found to be 7 ($\approx$ 10% of households).

Fig. 5.3 shows a profile of the lowest recorded CPOC voltage on the feeder for each time step for both the base case with no EVs and an uncontrolled case with a 10% penetration level. The total power delivered to the EVs at each time step is also shown. EV charging is assumed to commence once the off-peak period begins (i.e. 11 pm), although a number of EVs connect after this time also. As the figure shows, the introduction of EV charging during this time period pushes the lowest CPOC voltage towards the lower acceptable limit. Any further increase in the number of charging EVs at the beginning of the off-peak time period would likely result in the lower voltage limit being exceeded. The amount of energy delivered to the EVs in this scenario was 80.1 kWh.

5.4.2 Controlled EV Charging

The LCC method described in Section 5.2 is employed to optimise the charging rate of the EVs connected to the network. The rate at which each EV charges is now optimised

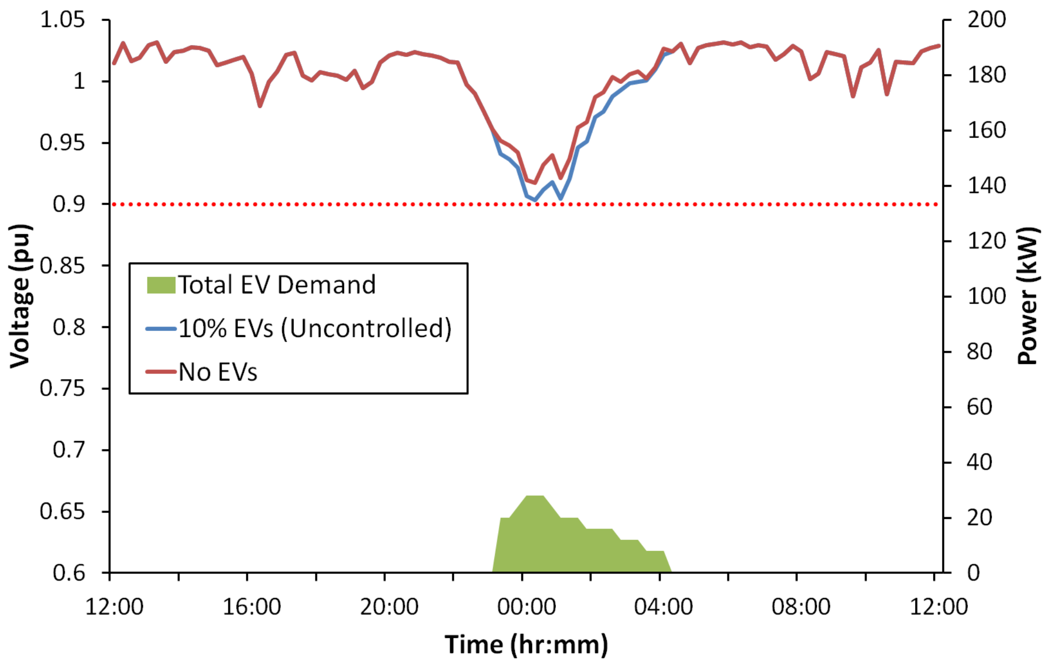

Figure 5.3: Lowest CPOC voltage for base case and uncontrolled charging case, including the power demand from the EVs for the uncontrolled case

individually in order to deliver the maximum power to the EVs while maintaining the voltage and service cable loading within acceptable operating limits for each time step. At the beginning of the charging period, the total energy required to return all EVs to 100% BSOC is 517 kWh. For the optimisation process, the lower voltage limit is set at 0.92 pu, which allows for a margin of safety with respect to the lower voltage limit (0.9 pu) defined in the Irish distribution network code (ESB Networks, 2007). This ensures that any unexpected short term variation in the demand will not cause the network to exceed its operating limits. For convenience, the lower limit is rounded up from the value used in Chapter 4, i.e. 0.913 pu. The maximum variation allowable for the rate of charge between time steps, i.e. Δ in (5.3), is set at 1 kW. This value was chosen to be greater than the corresponding value used in Chapter 4 in order to relax the impact of the constraint and allow for better comparison of the optimisation methods. Values for the voltage sensitivities, μ in (5.6), were calculated to be in the range -0.02 to -0.045 V/kW. CPOCs located at the extremities of the feeder were found to be more sensitive to the addition of EV load than those located near the start of the feeder.

This characteristic is to be expected of a radial feeder. The loading sensitivities, β in (5.7), of the single-phase service cables were calculated to be in the range 8.2 to 8.7 A/kW.

The sample 24-hour time period was tested utilising the controlled charging method for an EV penetration level of 50%. Fig. 5.4 shows the lowest recorded CPOC voltage on the feeder for the base case and the LCC case, and shows that the control method has maintained the lowest voltage above the lower voltage limit of 0.9 pu. The method has achieved this by curtailing EV charging during periods of high residential demand and shifting it to a later stage of the night. However, due to the inability of individual charging units to know the network conditions at the other CPOCs on the network, each unit is unaware of how many EVs are charging at the same time step. This can potentially lead to network conditions exceeding values determined by the individual charger units in their optimisation calculations. An example of this can be seen in Fig. 5.4, where the lowest CPOC voltage has reached a value closer to the network limit of 0.9 pu, rather than the specified limit of 0.92 pu. At the following time step, individual charger units recognise that a limit has been exceeded and automatically attempt to rectify the situation by adjusting their charging rate accordingly.

Fig. 5.5 shows the results for the lowest CPOC voltage recorded for the case employing the centralised control method. When compared to the LCC method, it can be seen that the centralised control technique results in the lowest recorded CPOC being much tighter to the specified voltage limit. Due to the calculation of a new set of sensitivities and knowledge of current network conditions at each time step, the network controller has a much greater insight to the condition of the network at all CPOCs. This allows for a far more accurate dispatch of EV charge rates, resulting in more charge being delivered to the EVs while maintaining acceptable network operating conditions. An example of this can be seen in the EV demand profile for both methods. In Fig. 5.4, even though the base case lowest voltage is already at the specified lower limit just after midnight, the local control technique leads to some EVs requesting charge, which results in a further voltage drop. At the same instant, using the centralised control technique, the controller switches off all EV charging on the network until the lowest

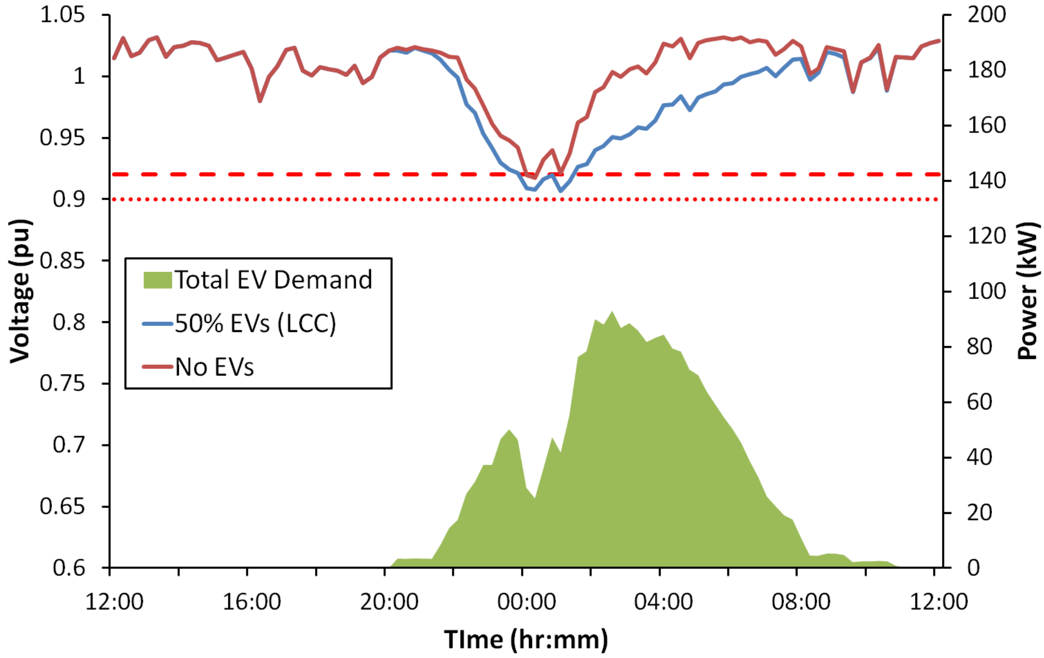

Figure 5.4: Lowest CPOC voltage for base case and local control charging case, including the associated power demand from the EVs

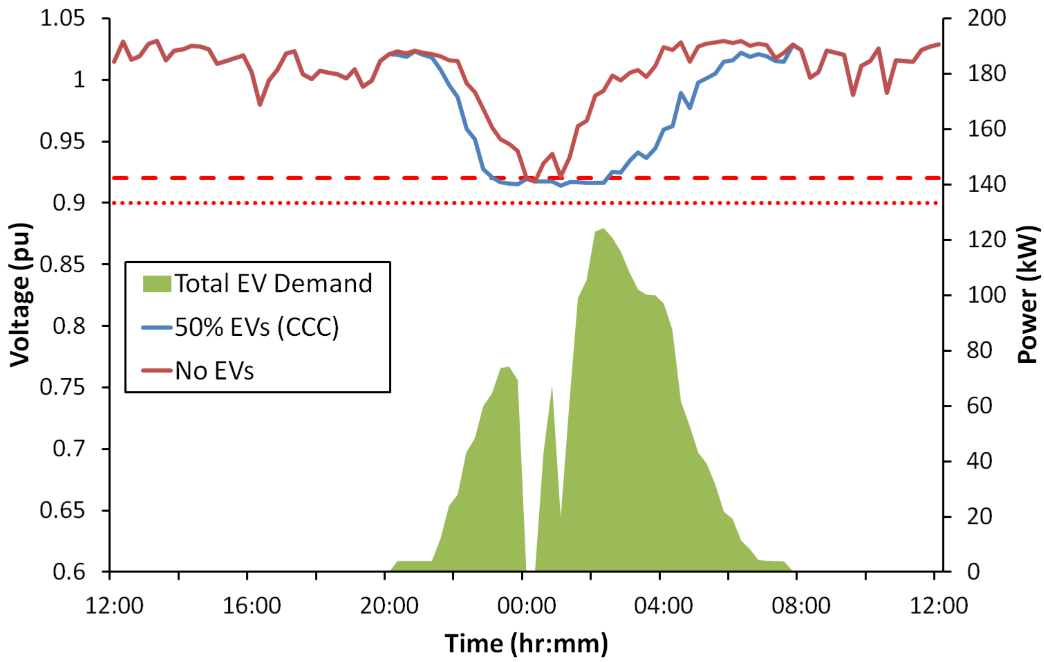

Figure 5.5: Lowest CPOC voltage for base case and centralised control charging case, including the associated power demand from the EVs

base case voltage increases above the specified limit. As the controller required each EV to stop charging during this time, the rate of change of charge constraint (5.3) was relaxed to ensure acceptable network operating conditions were maintained.

The centralised control method's ability to update the set of sensitivities and measure all network conditions at each time step allows it to deliver the maximum amount of power to the EVs, which results in the network capacity being utilised to the fullest extent at each time step. However, in the local control case the sensitivities are fixed, which results in less power being dispatched to the EVs even though the network is not at any of the specified limits. This results in the LCC method taking longer to charge all of the EVs, as shown in Fig. 5.6, where the black area represents the electricity demand from the EVs. In some cases, this can result in EVs finishing their charge period with less than 100% BSOC due to the charger units not utilising the network capacity to its fullest. For both methods, the BSOC upon disconnection from the network is shown in Fig. 5.7. It can be seen that the local control case results in 3 of the 37 EVs having a final BSOC of less than 100%, with the lowest being 90%. Because the centralised control method can deliver more power earlier in the charging period it results in all 37 EVs having a full BSOC by the end of the period. Details of the total energy delivered to the EVs for both control charging methods are given in Table 5.2.

Table 5.2: Total Energy Delivered to EV Batteries

	Total Energy Delivered (kWh)	**% Energy Requirement (for 50% EVs)**
10% EVs (Uncontrolled)	80.1	15.5
50% EVs (LCC)	513	99.2
50% EVs (CCC)	517	100

For both of the methods tested, the lowest CPOC voltage was found to be the binding constraint for the optimisation. Fig. 5.8 shows the greatest loading for all service cables at each time step. While the service cable loading is considered by both methods it is clear that it is never a binding constraint for the 24-hour period examined.

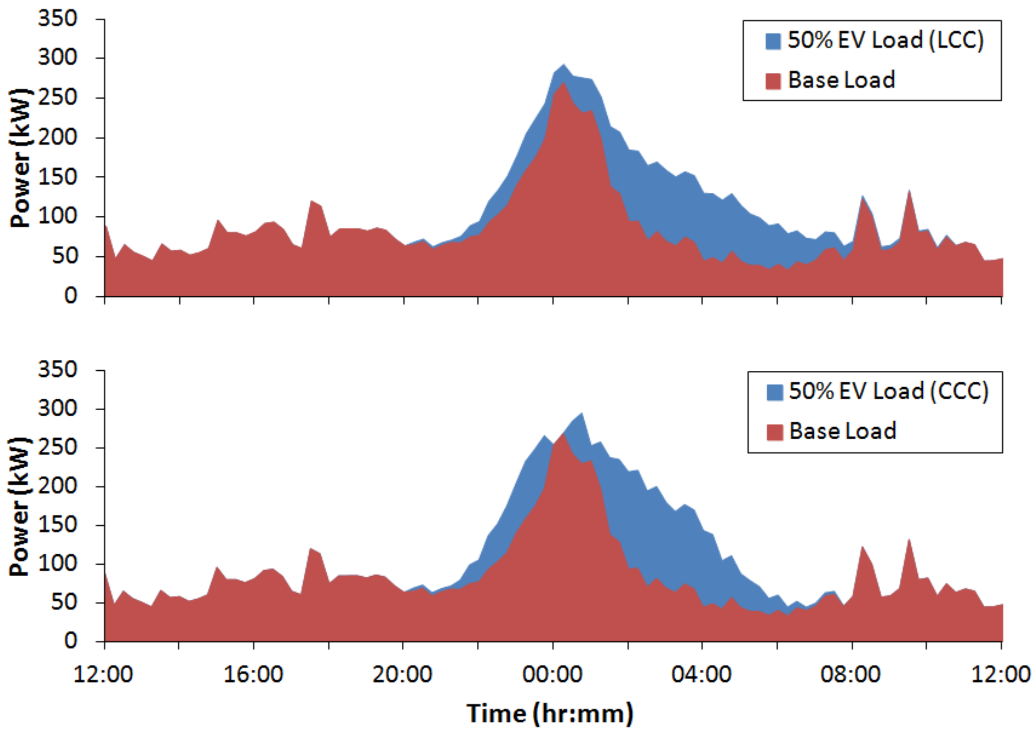

Figure 5.6: Network demand profiles for the local control and centralised control charging scenarios

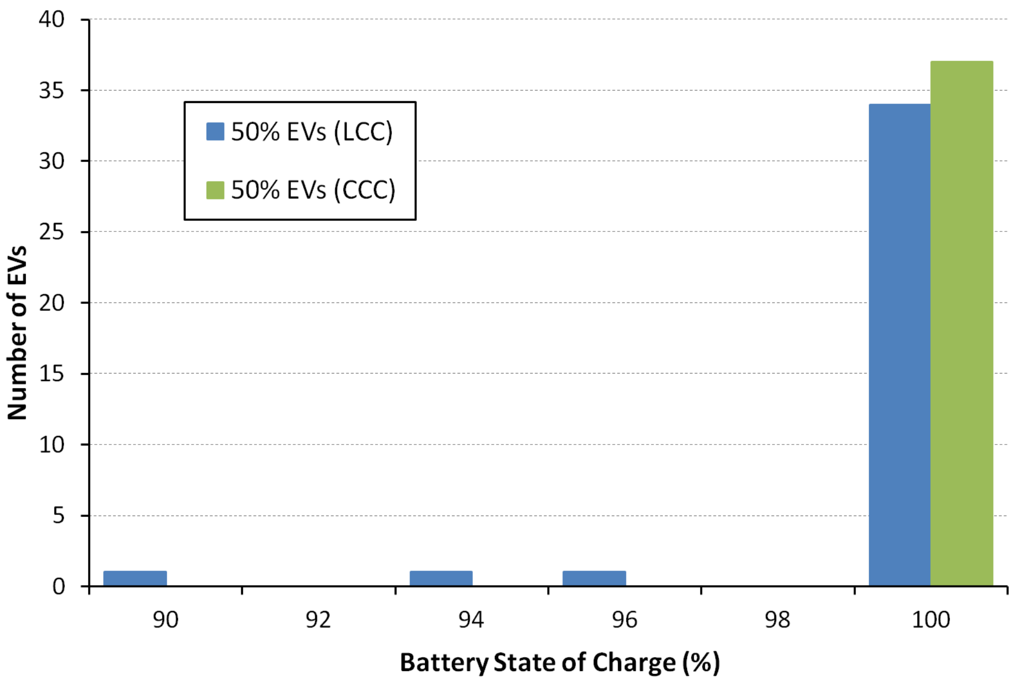

Figure 5.7: Final BSOC for EVs for local and centralised control charging scenarios

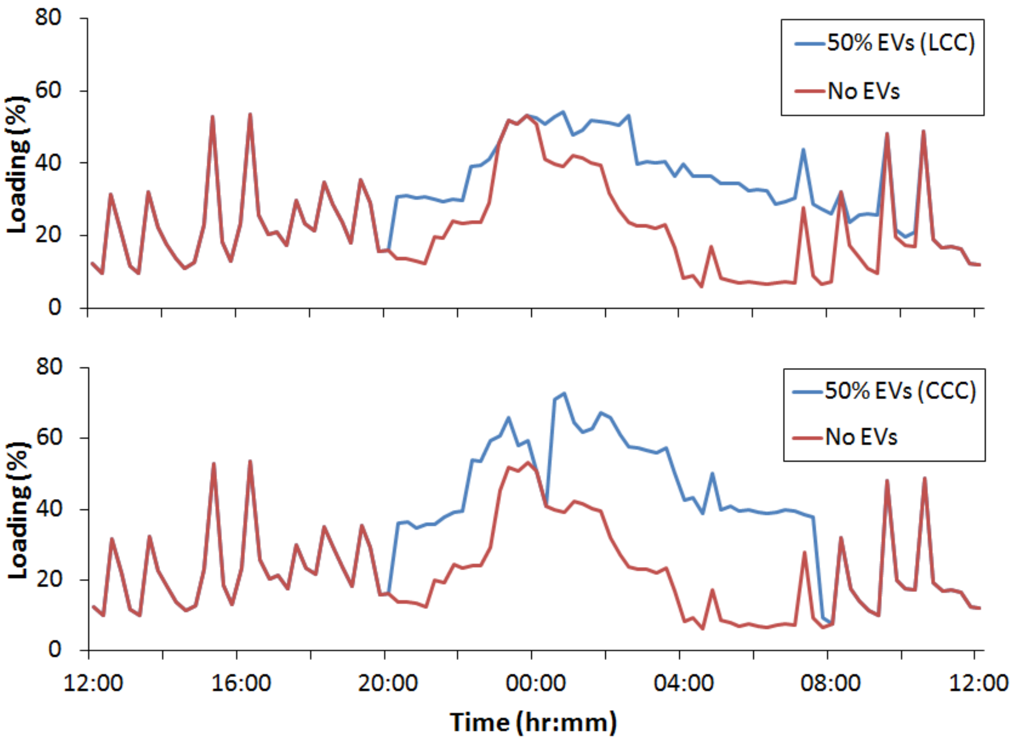

Figure 5.8: Loading of service cable with greatest loading for each time step for the local control and centralised control charging scenarios

The CCC technique also considers the loading on the network transformer and the loading on the 3-phase mains cable supplying the feeder from the transformer. For the 24-hour period examined here, neither the transformer nor the mains cable loading are ever the binding constraint, as shown in Table 5.3.

Table 5.3: Maximum Network Component Loading

		Mains Cable		
	Transformer (%)	**Phase a** (%)	**Phase b** (%)	**Phase c** (%)
No EVs	75.7	55.2	37.1	53.6
10% EVs	81.9	59.4	52.1	57.8
50% EVs (LCC)	82.1	61.8	55.5	69.3
50% EVs (CCC)	80.1	68.9	64.0	71.5

Network losses as a percentage of the total energy delivered to the network over the 24-hour period were also recorded. The increased demand from EV charging causes the losses ratio to increase slightly for all cases compared to the base case (1.1%). For the 10% EV penetration with uncontrolled charging the losses ratio was found to be 1.3%. The local control case (1.8%) incurs less losses on the network when compared to the centralised case (2.1%) but has delivered less energy to the EVs over the charging period.

5.4.3 Stochastic Scenario Analysis

A stochastic analysis of both charging strategies was performed in order to provide insight into operation of the optimisation process while accounting for the variability and uncertainties associated with EV charging, as described in Section 5.3.4.2. Each of the charging techniques were simulated on the test network for 300 distinct 24-hour periods (i.e. 28,800 time steps) during winter.

Fig. 5.9 shows the distribution of measured voltages for all CPOCs over all charging periods for the scenario with no EVs on the network and the scenarios for both controlled charging methods. There is a significant increase in the frequency of voltage levels nearer to the specified lower voltage limit (0.92 pu), with a small increase in the number of occurrences below this limit for both controlled charging methods. There are also more occurrences, using the CCC method, when the lowest CPOC voltage is at the specified limit, which demonstrates better utilisation of the network capacity. As explained in Section 5.4.2, this is due to the LCC method operating on a fixed set of sensitivity values and utilising local network information only, as opposed to the CCC method which updates the sensitivities at each time step and has exact knowledge of all network voltages and line flows.

The distribution of thermal loading levels measured on each of the single-phase service cables is shown in Fig. 5.10. For the majority of recorded values the loading is below 60% of the rating. The service cable loading is only a binding constraint for a very small fraction of the measured samples (i.e. less than 0.01%).

Finally, the distribution of the final BSOC for all the EVs for each charging period

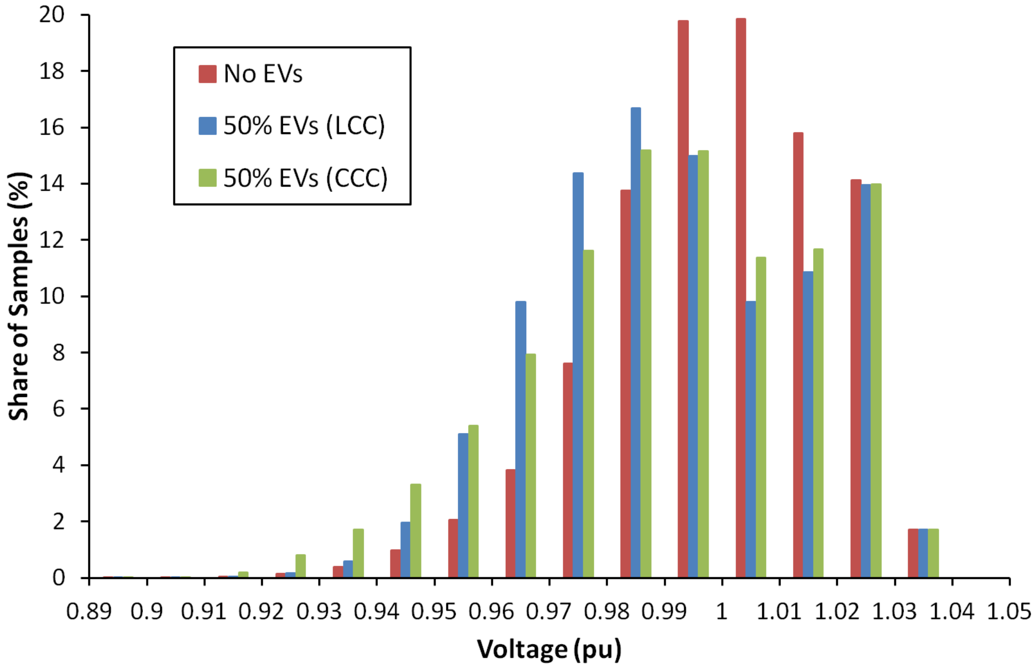

Figure 5.9: Distribution of measured voltages at network CPOCs

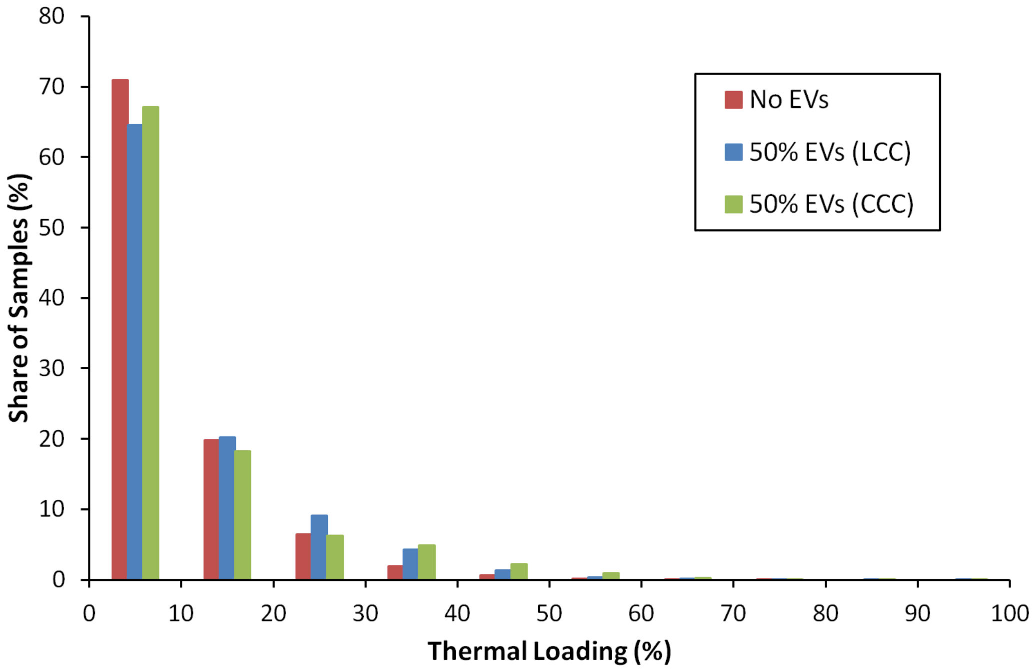

Figure 5.10: Distribution of measured thermal loading levels of single-phase service cables

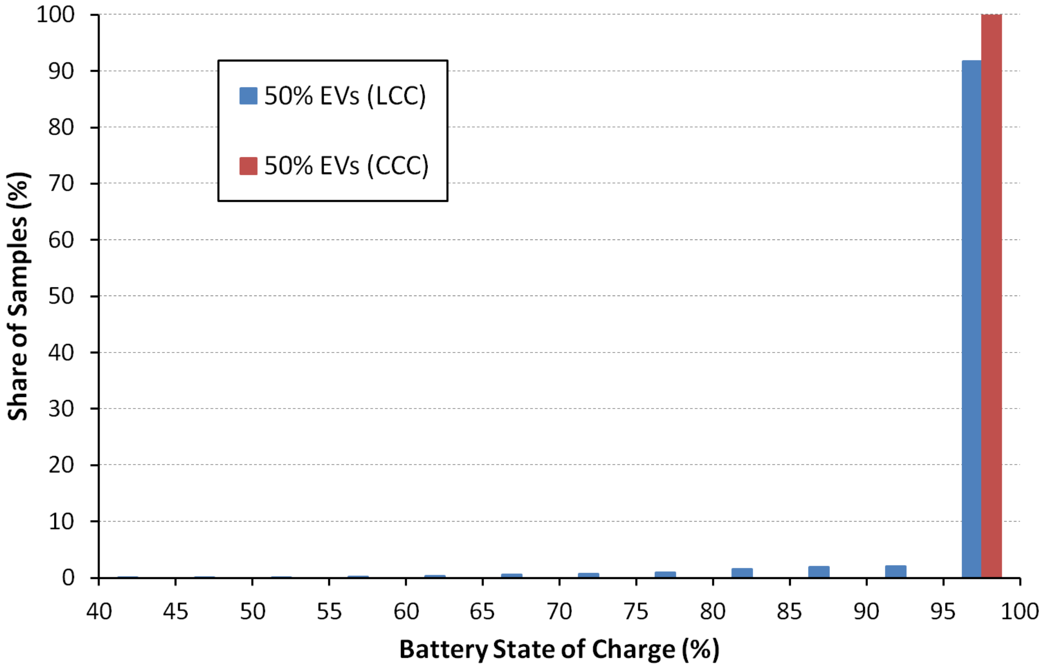

Figure 5.11: Distribution of final BSOC levels for all charging periods

is shown in Fig. 5.11. The LCC method resulted in over 90% of all final BSOC values being within 95-100%, with 97% of all values above 80%. For each charging period using the weighted CCC method, 100% of the final BSOC values were found to be within 95-100% of the maximum capacity.

5.5 Conclusion

This chapter has demonstrated the benefits of controlled charging for a high penetration of EVs charging on a LV network. A local control method was proposed whereby each individual EV charger maximises the charging rate of its EV while maintaining the CPOC voltage and service cable loading within acceptable limits. The method was tested on a LV test network and the results were compared to those employing a centralised control method.

The results indicate that the local control method allows a far greater penetration of EV charging on a feeder than that which could be accommodated with uncontrolled charging. While the technique can deliver a similar amount of energy to the EVs within a certain time period when compared to the centralised control method, it is not as capable at maintaining network parameters within specified limits and may require larger safety margins. However, introducing a number of predefined sets of sensitivities, each calculated based on the expected residential load for a given scenario (e.g. day/night, weekday/weekend, seasonal, etc.), could improve the performance of the local control method.

The network and communications infrastructure required to implement the local control method would be far less than that required for the centralised control case (Dimeas and Hatziargyriou, 2005). Individual controllers would also be able to act independently and not be reliant on external controller signals in order to operate. As such, investing in a centralised control technique may not be required until very high penetrations of EVs on LV networks become a reality. With the introduction of AMI, a local control technique may be sufficient for accommodating initial penetrations of EV charging while maintaining network limits within the desired operating regions.

CHAPTER 6

Conclusion

WITH grid connected DER technology likely to become more prevalent in the coming years, understanding how such devices will potentially affect network operating conditions will be critical to their successful integration. As existing distribution systems were not originally designed to accommodate DER technology, it may become necessary for power system operators to take a more proactive approach in managing the operation of distribution networks. As such, this thesis has presented novel methodologies for maximising the utilisation of network capacity in a secure manner by coordinating the operation of DER units in distribution systems.

In Chapter 3, a study of the potential impact of DER devices in the distribution system was conducted. The study modelled the impact from high penetrations of DER devices on test LV distribution networks, in terms of network voltage levels and thermal loading of feeder components. The analysis comprised of two parts. Firstly, a deterministic analysis was performed, whereby the test feeder was modelled for a worst case scenario in terms of the residential load demand. For micro-generation

DER, this meant that the minimum total residential load was modelled, whereas for flexible load DER, the residential load was at its maximum. For both scenarios, DER units, operating at maximum load/output, were incrementally added to the network in order to determine the maximum DER penetration that could be reached without exceeding acceptable network limits. The analysis showed that, for the worst case scenario of minimum load, a penetration level of up to 90% for micro-generation DER was attainable. However, in a scenario of maximum residential demand, the highest acceptable penetration of flexible load DER, in this case EVs, was found to be as low as 20%. The results of such an analysis are very much dependent on the characteristics of the network that is being assessed. However, they still provide a good indication that high penetrations of electricity demanding DER would have a greater impact on network operating conditions than micro-generation DER.

The second part of the impact study was developed a stochastic scenario analysis method. The method generated household load profiles together with operational profiles for the DER units based on real network data obtained from DSO led field trials. These profiles were then used in a time-series load-flow analysis in order to determine the likely impact of DER devices on network operating conditions over certain time periods. The method takes account of uncertainties such as varying levels of coincident operation and possible locations for DER units on the feeder. The results shown in Chapter 3 indicate that the potential number of occurrences where the operating limits are exceeded is relatively small. These results are, however, only representative of the test network used in the study. In general, the characteristics of distribution networks can vary quite substantially. Therefore, the level of DER that could be successfully accommodated will also vary greatly from network to network. Using deterministic and stochastic tools, like those demonstrated in Chapter 3, will prove to be beneficial in predicting the potential for particular networks to adapt DER technology.

In Chapter 4, a method for coordinating the operation of DER units on a distribution feeder was proposed. High penetrations of DER units operating simultaneously may lead to certain network limitations being exceeded, e.g. voltage limits, thermal overloading. By exploiting the sensitivities of the network voltage and loading levels to the addition of DER units, the control technique optimises the operating set point of each unit in order to maximise its output/demand, while maintaining acceptable operating levels on the network. By doing so, the method allows for more efficient use of existing network capacity, thus deferring the need for costly network reinforcement. The method was demonstrated on a test LV network with a high penetration of EVs connected for charging. At each time step, load-flow analyses determined the sensitivity of the network node voltage and loading levels to the addition of EV load. These sensitivity values were then employed within a linear programming algorithm to determine the optimal rate of charge for each EV. In doing so, the total power delivered to the network is maximised while maintaining network operating conditions within acceptable limits, thereby utilising the network capacity to its fullest. However, due to the radial topology of the network, it was found that the method tended to specify higher charging rates to EVs located nearer the sending end of the feeder than to those located at the extremities. In order to provide a more even distribution of energy across the feeder, the optimisation objective function was modified to account for the charge requirement of each EV. By doing so, the total energy delivered to the EVs was greater than that which was achieved by using the non-weighted objective function method.

The method used for the coordination of DER devices in Chapter 4 is based on centralised control of DER units, whereby a controller has real-time knowledge of network conditions and the operating status of each DER unit. The implementation of such a control scheme would require sufficient communications infrastructure to be installed across the distribution system, which may be costly for DSOs to install and operate. In Chapter 5 a method based on a decentralised, local control approach was proposed. In this method, each individual DER unit determines its own operating set point according to the voltage and cable loading at its connection point to the network. Therefore, there is no requirement for a widespread communication infrastructure to implement the technique. Predetermined sensitivity values for the voltage and loading were implemented in a linear programming algorithm to optimise the operating set point according to the particular objective, e.g. maximise EV charging rate. As was the case in Chapter 4, the method was implemented on a test network with a high penetration of EVs and the results were compared to those of the centralised control method. The local control method could deliver a similar amount of total energy to the EVs as the centralised method. However, it was not as accurate at maintaining voltage and loading levels within the specified limits and may require larger safety margins to ensure acceptable network operation. Overall, the cost savings from implementing a local control strategy may outweigh the loss of accuracy with regard to maintaining acceptable network operating levels, especially so for initial penetrations of DER devices.

6.1 Future Work

The method used for coordinating the operation of DER units in Chapter 4 was tested using EV technology. In the analysis, the EVs were considered to have a flexible load capability only. The concept of using EVs to supply energy either back into the distribution network (Vehicle-to-Grid (V2G)) or for supplying household load (Vehicle-to-Home (V2H)) has been the focus of much recent research (Clement-Nyns et al., 2011; Haines et al., 2009; Kempton and Tomić, 2005; Tomić and Kempton, 2007). The impact of exporting energy from EVs would have much the same impact on network operating conditions as that of micro-generation units with a similar rated export capacity. By utilising the export capability of DER technology (i.e. controllable micro-generation and/or EVs with V2G capability) in the coordinated control method of Chapter 4, it may be possible to increase the total energy deliverable to the load on the network. While investigating the potential for increasing the load capacity of existing networks in this manner would be an interesting topic for future research, such studies must also consider the impact on the DER devices themselves, e.g. the impact on the life cycle of EV batteries (Zhou et al., 2011).

For the most part, loads at the LV level of the distribution system are connected via a single-phase connection to the network. This normally causes an unequal flow of current on each of the phases of a distribution feeder. Maximum levels of permissable unbalance are normally specified in DSO grid codes. Typically, the level of unbalance across the phases of distribution networks is small due to the coincident use of load by customers on each phase (Willis, 2004). The introduction of DER to certain households on a network will potentially increase the levels of unbalance at certain times on the network, and in some cases may exceed permissable limits. The control method proposed in Chapter 4 accounts for the impact on each phase of the network from the connection of a DER unit to a particular phase. Incorporating a similar methodology for use in an unbalanced optimal power flow tool may be beneficial in future impact studies for DER on unbalanced networks.

In Chapter 5, a method for operating DER devices on a feeder using a local control method was proposed. This method relies on robust values for network sensitivities to the addition of DER. In the method, a conservative approach was taken in calculating the sensitivities in order to reduce the potential for network conditions to exceed acceptable limits. Allowing local controllers to select sensitivity values from a number of predefined sets, based on expected residential loading conditions (i.e. time-of day, weekday/weekend, seasonal), may improve utilisation of network capacity by the controllers and, thus, the method itself.

The work presented in this thesis investigates the impact on certain technical aspects of distribution system operation and proposes methods to mitigate those impacts through intelligent control techniques. With the introduction of micro-generation, flexible load and new DSM schemes in future years, customers will have the ability to take a more active approach in managing their energy usage. For example, with the implementation of time-of-day tariffs along with reimbursements for exporting electricity back into the grid, customers may alter their energy usage in order to maximise their financial gain/minimise costs. Future work could consider incorporating time-of-day tariffs together with the DER control techniques proposed in this thesis to schedule the operation of DER units. By doing so, customers could avail of cheaper electricity tariffs while, at the same time, utilisation of network capacity could be maximised. However, some degree of load prediction capability for the household demand may be necessary in order to make optimal use of spare network capacity while satisfying customer energy requirements. Understanding the potential changes in customer behaviour and how price signals will affect their demand/DER usage will be crucial to the successful integration of DER technology in the future.

References

Acha, S., Green, T., Shah, N., April 2010. Effects of optimised plug-in hybrid vehicle charging strategies on electric distribution network losses. In: Proceedings IEEE Power and Energy Society Transmission and Distribution Conference, New Orleans, LA, USA, 2010.

Akmal, M., Fox, B., Morrow, D., Littler, T., June 2011. Impact of high penetration of heat pumps on low voltage distribution networks. In: Proceedings IEEE PowerTech, Trondheim, Norway, 2011.

Alarcon-Rodriguez, A., Ault, G., Galloway, S., 2010. Multi-objective planning of distributed energy resources: a review of the state-of-the-art. Renewable and Sustainable Energy Reviews 14 (5), 1353–1366.

Beddoes, A., Gosden, M., Povey, I., May 2007. The performance of an LV network supplying a cluster of 500 houses each with an installed 1 kW_e domestic combined heat and power unit. In: Proceedings CIRED 19^{th} International Conference on Electricity Distribution, Vienna, Austria, 2007.

Bradley, T., Frank, A., 2009. Design, demonstrations and sustainability impact assessments for plug-in hybrid electric vehicles. Renewable and Sustainable Energy Reviews 13 (1), 115–128.

Brooks, A., Lu, E., Reicher, D., Spirakis, C., Weihl, B., May/June 2010. Demand dispatch: using real-time control of demand to help balance generation and load. IEEE Power and Energy Magazine.

Camus, C., Silva, C., Farias, T., Esteves, J., March 2009. Impact of plug-in hybrid electric vehicles in the Portuguese electric utility system. In: Proceedings International Conference on Power Engineering, Energy and Electrical Drives, Lisbon, Portugal, 2009.

CER, 2010. Commission for Energy Regulation. ESB CS domestic microgenerator export tariff decision.
URL http://www.cer.ie

CER, 2011a. Commission for Energy Regulation. Press release on national roll-out of energy smart meters in Ireland.
URL http://www.cer.ie/

CER, 2011b. Commission for Energy Regulation. Smart metering project.
URL http://www.cer.ie/

Clement-Nyns, K., Haesen, E., Driesen, J., May 2009. Analysis of the impact of plug-in hybrid electric vehicles on residential distribution grids by using quadratic and dynamic programming. In: Proceedings EVS24 International Battery, Hybrid and Fuel Cell Electric Vehicle Symposium, Stavanger, Norway, 2009S.

Clement-Nyns, K., Haesen, E., Driesen, J., February 2010. The impact of charging plug-in hybrid electric vehicles on a residential distribution grid. IEEE Transactions on Power Systems 25 (1), 371–380.

Clement-Nyns, K., Haesen, E., Driesen, J., 2011. The impact of vehicle-to-grid on the distribution grid. Electric Power Systems Research 81 (1), 185–192.

DCENR, 2009. Department of Communications, Energy and Natural Resources, The National Energy Efficiency Action Plan 2009-2020.
URL http://www.dcenr.gov.ie

Deilami, S., Masoum, A., Moses, P., Masoum, M., September 2011. Real-time coordination of plug-in electric vehicle charging in smart grids to minimize power losses and improve voltage profile. IEEE Transactions on Smart Grid 2 (3), 456–467.

Denholm, P., Short, W., 2006. National Renewable Energy Laboratory Report. An evaluation of utility system impacts and benefits of optimally dispatched plug-in hybrid electric vehicles.
URL http://www.nrel.gov

DIgSILENT GmbH, 2011. DIgSILENT PowerFactory.
URL http://www.digsilent.de

Dimeas, A., Hatziargyriou, N., August 2005. Operation of a multiagent system for microgrid control. IEEE Transactions on Power Systems 20 (3), 1447–1455.

Doucette, R., McCulloch, M., July 2011. Modeling the prospects of plug-in hybrid electric vehicles to reduce CO_2 emissions. Applied Energy 88 (7), 2315–2323.

DTI, 2003. Department of Trade and Industry. The impact of small scale embedded generation on the operating parameters of distributed networks.

DTI, 2004. Department of Trade and Industry. System integration of additional microgeneration.

Dyke, K., Schofield, N., Barnes, M., December 2010. The impact of transportation electrification on electrical networks. IEEE Transactions on Industrial Electronics 57 (12), 3917–3926.

EC, 2004. European Commission. European distributed energy resources projects.
URL http://ec.europa.eu/research/energy/pdf/dis_energy_en.pdf

EEI, 2011. Edison Electric Institute. History of the electric power industry.
URL http://www.eei.org

EirGrid, 2011. Demand Side Management Schemes.
URL http://www.eirgrid.com

EirGrid, SONI, 2010. EirGrid and SONI, All-Island Generation Capacity Statement 2011-2020.
URL http://www.eirgrid.com

Ekman, C., 2011. On the synergy between large electric vehicle fleet and high wind penetration - an analysis of the Danish case. Renewable Energy 36 (2), 546–553.

Electric Ireland, 2011. Electric Ireland. Electricity Price Plans.
URL http://www.esb.ie/esbcustomersupply

Element Energy, 2009. Strategies for the uptake of electric vehicles and associated infrastructure implications.
URL http://www.theccc.org.uk

EPRI, July 2007. Electric Power Research Institute. Environmental assessment of plug-hybrid electric vehicles. Volume 1: Nationwide greenhouse gas emissions.
URL http://www.epri.com

ESB, 2011. Electric Vehicle Charging Point Installation Targets.
URL http://www.esb.ie/electric-cars

ESB Ecars, 2011. Electric Car Research and Trials.
URL http://www.esb.ie/electric-cars

ESB Networks, 2007. ESB Networks. Distribution Grid Code.
URL http://www.esb.ie/esbnetworks

EU, 2009. European Union, Directive 2009/28/EC of the European Parliament and of the Council, on the promotion of the use of energy form renewable sources.
URL http://www.europa.eu

EU, 2010. European Union, Directive 2010/31/EU of the European Parliament and of the Council, on the energy performance of buildings.
URL http://www.europa.eu

Fluhr, J., Ahlert, K.-H., Weinhardt, C., January 2010. A stochastic model for simulating the availability of electric vehicles for services to the power grid. In: Proceedings 43rd Hawaii International Conference on System Sciences (HICSS), Honolulu, HI, USA, 2010.

Garcia, P., Pereira, J., Carneiro, S., J., da Costa, V., Martins, N., May 2000. Three-phase power flow calculations using the current injection method. IEEE Transactions on Power Systems 15 (2), 508–514.

Gerkensmeyer, C., Kintner-Meyer, M., DeSteese, J., 2010. Pacific Northwest National Laboratory Report. Technical challenges of plug-in hybrid electric vehicles and impacts to the US power system: distribution system analysis.
URL http://www.pnl.gov/main/publications

Gomes, A., Pires, L., May 2010. Demand modeling for assessing the impacts of micro-generation in a low voltage radial distribution network. In: Proceedings 10th International Conference on Environment and Electrical Engineering (EEEIC), Rome, Italy, 2011.

Hadley, S., 2006. Oak Ridge National Laboratory Report. Impact of plug-in hybrid vehicles on the electric grid.
URL http://ornl.gov/info/ornlreview/v40_2_07/2007_plug-in_paper.pdf

Hadley, S., Tsvetkova, A., 2008. Oak Ridge National Laboratory Report. Potential impacts of plug-in hybrid electric vehicles on regional power generation.
URL http://ornl.gov/info/ornlreview/v41_1_08/regional_phev_analysis.pdf

Haines, G., McGordon, A., Jennings, P., March 2009. The simulation of vehicle-to-home systems - using electric vehicle battery storage to smooth domestic electricity demand. In: Proceedings Ecological Vehicles and Renewable Energies Conference (EVER), Monaco, 2009.

Hatziargyriou, N., Asano, H., Iravani, R., Marnay, C., July-August 2007. Microgrids. IEEE Power and Energy Magazine 5 (4), 78–94.

Heydt, G., May 1983. The impact of electric vehicle deployment on load management strategies. IEEE Transactions on Power Apparatus and Systems PAS-102 (5), 1253–1259.

Hoffart, F., April 2008. Power Electronics Technology. Proper care extends Li-ion battery life.
URL http://powerelectronics.com

IEA, 2008. International Energy Agency. Integration of demand side management, distributed generation, renewable energy sources and energy storages.
URL http://www.ieadsm.org

IEA, 2011a. International Energy Agency, Key World Energy Statistics.
URL http://www.iea.org

IEA, 2011b. International Energy Agency. Technology roadmap: electric and plug-in hybrid electric vehicles.
URL http://www.iea.org/roadmaps/plug_in_electric_vehicles.asp

IEEE, 1995. IEEE Standard C57.91. Guide for loading mineral-oil-immersed transformers.

Katiraei, F., Iravani, R., Hatziargyriou, N., Dimeas, A., May-June 2008. Microgrids management. IEEE Power and Energy Magazine 6 (3), 54–65.

Kempton, W., Tomić, J., 2005. Vehicle-to-grid power implementation: from stabilizing the grid to supporting large-scale renewable energy. Journal of Power Sources 144 (1), 280–294.

Kersting, W., 2002. Distribution system modeling and analysis. CRC Press, London.

Kintner-Meyer, M., Schneider, K., Pratt, R., 2007. Pacific Northwest National Laboratory Report. Impacts assessment of plug-in hybrid vehicles on electric utilities and regional U.S. power grids. Part 1: Technical analysis.
URL http://www.pnl.gov/publications

Kiviluoma, J., Meibom, P., March 2010. Influence of wind power, plug-in electric vehicles, and heat storages on power system investments. Energy 35 (3), 1244–1255.

Maitra, A., Kook, K., Taylor, J., Giumento, A., April 2010. Grid impacts of plug-in electric vehicles on Hydro Quebec's distribution system. In: Proceedings IEEE Power and Energy Society Transmission and Distribution Conference and Exposition, Minneapolis, MN, USA, 2010.

MATLAB, 2009. The Mathworks, Inc. MATLAB R2009a.
URL http://www.mathworks.com

Mullan, J., Harries, D., Bräunl, T., Whitely, S., 2011. Modelling the impacts of electric vehicle recharging on the Western Australian electricity supply system. Energy Policy 39 (7), 4349–4359.

NHBC, 2008. NHBC Foundation. A review of microgeneration and renewable energy technologies.
URL http://www.nhbcfoundation.org/Researchpublications

Papadopoulos, P., Skarvelis-Kazakos, S., Grau, I., Awad, B., Cipcigan, L., Jenkins, N., August-September 2010. Impact of residential charging of electric vehicles on distribution networks, a probabilistic approach. In: Proceedings 45th International Universities Power Engineering Conference (UPEC), Cardiff, Wales, 2010.

Parks, K., Denholm, P., Markel, T., 2007. National Renewable Energy Laboratory Report. Costs and emissions associated with plug-in hybrid electric vehicle charging in the Xcel Energy Colorado service territory.
URL http://www.nrel.gov

Peças Lopes, J., Moreira, C., Madureira, A., May 2006. Defining control strategies for microgrids islanded operation. IEEE Transactions on Power Systems 21 (2), 916–924.

Peças Lopes, J., Polenz, S., Moreira, C., Cherkaoui, R., August 2010. Identification of control and management strategies for LV unbalanced microgrids with plugged-in electric vehicles. Journal of Electric Power Systems Research 80 (8), 898–906.

Peças Lopes, J., Soares, F., Almeida, P., January 2011. Integration of electric vehicles in the electric power system. Proceedings of the IEEE 99 (1), 168–183.

Pehnt, M., Cames, M., Fischer, C., Praetorius, B., Schneider, L., Schumacher, K., Voß, J.-P., 2006. Micro cogeneration: towards decentralized energy systems. Springer, Berlin.

Perujo, A., Ciuffo, B., 2010. The introduction of electric vehicles in the private fleet: potential impact on the electric supply system and on the environment. A case study for the Province of Milan, Italy. Energy Policy 38 (8), 4549–4561.

Pillai, J., Bak-Jensen, B., January 2011. Integration of vehicle-to-grid in the Western Danish power system. IEEE Transactions on Sustainable Energy 2 (1), 12–19.

PSERC, 2009. Power Systems Engineering Research Center. Power system level impacts of plug-in hybrid vehicles.
URL http://www.pserc.wisc.edu

Pudjianto, D., Ramsay, C., Strbac, G., March 2007. Virtual power plant and system integration of distributed energy resources. IET Renewable Power Generation 1 (1), 10–16.

Putrus, G., Suwanapingkarl, P., Johnston, D., Bentley, E., Narayana, M., September 2009. Impact of electric vehicles on power distribution networks. In: Proceedings IEEE Vehicle Power and Propulsion Conference, Dearborn, MI, USA, 2009.

RAE, 2010. The Royal Academy of Engineering. Electric vehicles: charged with potential.
URL http://www.raeng.org.uk/ev

Rahman, S., Shrestha, G., April 1993. An investigation into the impact of electric vehicle load on the electric utility distribution system. IEEE Transactions on Power Delivery 8 (2), 591–597.

Sæle, H., Grande, O., March 2011. Demand response from household customers: experiences from a pilot study in Norway. IEEE Transactions on Smart Grid 2 (1), 102–109.

Schneider, K., Gerkensmeyer, C., Kintner-Meyer, M., Fletcher, R., July 2008. Impact assessment of plug-in hybrid vehicles on Pacific Northwest distribution systems. In: Proceedings IEEE Power and Energy Society General Meeting, Pittsburgh, PA, USA, 2008.

SEAI, 2005. Sustainable Energy Authority of Ireland. A scoping study: demand side measures for small business and residential customers on Ireland's electrical system.
URL http://www.seai.ie/Publications

SEAI, 2008. Sustainable Energy Authority of Ireland. Demand side management in Ireland. Evaluating the energy efficiency opportunities.
URL http://www.seai.ie/Publications

SEAI, 2010. Sustainable Energy Authority of Ireland. A report on micro-generation in Ireland.
URL http://www.seai.ie/Renewables/Microgeneration

SEAI, 2011a. Sustainable Energy Authority of Ireland. Better Energy Homes Scheme.
URL http://www.seai.ie

SEAI, 2011b. Sustainable Energy Authority of Ireland. History of Wind Energy.
URL http://www.seai.ie/Renewables/Wind_Energy/History_of_Wind_Energy

SEAI, 2011c. Sustainable Energy Authority of Ireland. Power of One Scheme.
URL http://www.seai.ie

Shahnia, F., Majumder, R., Ghosh, A., Ledwich, G., Zare, F., 2011. Voltage imbalance analysis in residential low voltage distribution networks with rooftop PVs. Electric Power System Research. (In Press).

Shao, S., Pipattanasomporn, M., Rahman, S., July 2009. Challenges of PHEV penetration to the residential distribution network. In: Proceedings IEEE Power and Energy Society General Meeting, Calgary, AB, Canada, 2009.

Short, W., Denholm, P., 2006. National Renewable Energy Laboratory Report. A preliminary assessment of plug-in hybrid electric vehicles on wind energy markets.
URL http://www.nrel.gov

Shortt, A., O'Malley, M., September 2009. Impact of optimal charging of electric vehicles on future generation portfolios. In: IEEE PES/IAS Conference on Sustainable Alternative Energy (SAE), Valencia, Spain, 2009.

Silva, N., Strbac, G., June 2008. Optimal design policy and strategic investment in distribution networks with distributed generation. In: Proceedings CIRED Smart Grids for Distribution Seminar, Frankfurt, Germany, 2008.

Sortomme, E., El-Sharkawi, M., March 2011. Optimal charging strategies for unidirectional vehicle-to-grid. IEEE Transactions on Smart Grid 2 (1), 131–138.

Sortomme, E., Hindi, M., MacPherson, S., Venkata, S., March 2011. Coordinated charging of plug-in hybrid electric vehicles to minimize distribution system losses. IEEE Transactions on Smart Grid 2 (1), 198–205.

STAR, 2011. EirGrid. Short Term Active Response.
URL http://www.eirgrid.com/operations

Su, W., Chow, M.-Y., 2011. Performance evaluation of an EDA-based large-scale plug-in hybrid electric vehicle charging algorithm. IEEE Transactions on Smart Grid. (In Press).

Taylor, J., Maitra, A., Alexander, M., Brooks, D., Duvall, M., July 2009. Evaluation of the impact of plug-in electric vehicle loading on distribution system operations. In: Proceedings IEEE Power and Energy Society General Meeting, Calgary, AB, Canada, 2009.

Thomson, M., Infield, D., March 2007a. Impact of widespread photovoltaics generation on distribution systems. IET Renewable Power Generation 1 (1), 33–40.

Thomson, M., Infield, D., August 2007b. Network power-flow analysis of a high penetration of distributed generation. IEEE Transactions on Power Systems 22 (3), 1157–1162.

Tomić, J., Kempton, W., 2007. Using fleets of electric-drive vehicles for grid support. Journal of Power Sources 168 (2), 459–468.

UNFCCC, 1997. United Nations Framework Convention on Climate Change, Kyoto protocol to the United Nations framework convention on climate change.
URL http://www.unfccc.int

Vovos, P., Kiprakis, A., Wallace, A., Harrison, G., February 2007. Centralized and distributed voltage control: Impact on distributed generation penetration. IEEE Transactions on Power Systems 22 (1), 476–483.

Wang, J., Liu, C., Ton, D., Zhou, Y., Kim, J., Vyas, A., 2011. Impact of plug-in hybrid electric vehicles on power systems with demand response and wind power. Energy Policy 39 (7), 4016–4021.

Willis, H., 2004. Power distribution planning reference book. Marcel Dekker, Basel.

WPDRS, 2011. EirGrid. Winter Peak Demand Reduction Scheme.
URL http://www.eirgrid.com/operations

Zhou, C., Qian, K., Allan, M., Zhou, W., December 2011. Modeling of the cost of EV battery wear due to V2G application in power systems. IEEE Transactions on Energy Conversion 26 (4), 1041–1050.

Appendix A: Test Network 1

Table A.1: Test Network 1 Cable Characteristics

Line	Length (m)	R_1 (Ω)	X_1 (Ω)	R_0 (Ω)	X_0 (Ω)	C (μF)	I_{rated} (A)
MV	10,000	20.8	4	10	12	0.01	1000
1-2	190	0.032	0.014	0.095	0.041	0.053	510
2-3	27.5	0.008	0.002	0.024	0.006	0.008	368
3-4	85	0.024	0.006	0.073	0.018	0.026	368
4-5	97.5	0.028	0.007	0.084	0.021	0.029	368
5-6	154	0.062	0.011	0.185	0.033	0.046	300
4-7	119	0.048	0.009	0.143	0.026	0.036	300
2-8	32.5	0.009	0.002	0.028	0.007	0.01	368
8-9	59	0.017	0.004	0.051	0.013	0.018	368
9-10	106	0.03	0.008	0.091	0.023	0.032	368
10-11	95	0.027	0.007	0.082	0.021	0.029	368
9-12	217.5	0.087	0.016	0.261	0.047	0.065	368
Service Cable (per km)		0.8	0.07	-	-	0.4	80

R_1 Positive sequence resistance
X_1 Positive sequence reactance
C Capacitance
R_0 Zero sequence resistance
X_0 Zero sequence reactance
I_{rated} Rated current

Figure A.2: Geographical topology of Network 1[1]

[1]Image source: Google Maps (Jan. 2012)

Appendix B: Test Network 2

Table B.1: Test Network 2 Cable Characteristics

Line	Length (m)	R_1 (Ω)	X_1 (Ω)	R_0 (Ω)	X_0 (Ω)	C (μF)	I_{rated} (A)
MV	11,000	18.9	4.4	11	13.2	2.75	1000
1-2	24	0.005	0.002	0.003	0.005	0.006	425
2-3	36	0.008	0.002	0.003	0.007	0.01	425
3-4	45	0.01	0.003	0.005	0.009	0.013	425
4-5	46	0.01	0.003	0.005	0.01	0.013	425
5-6	59	0.013	0.004	0.006	0.012	0.017	425
6-7	49	0.028	0.004	0.014	0.011	0.014	245
6-8	59	0.013	0.004	0.006	0.012	0.017	425
8-9	60	0.03	0.004	0.015	0.013	0.045	212
9-10	54	0.027	0.004	0.014	0.012	0.041	212
Service Cable (per km)		1.18	0.037	-	-	0.28	130

R_1 Positive sequence resistance
X_1 Positive sequence reactance
C Capacitance
R_0 Zero sequence resistance
X_0 Zero sequence reactance
I_{rated} Rated current

Figure B.2: Geographical topology of Network 2[2]

[2]Image source: Google Maps (Jan. 2012)

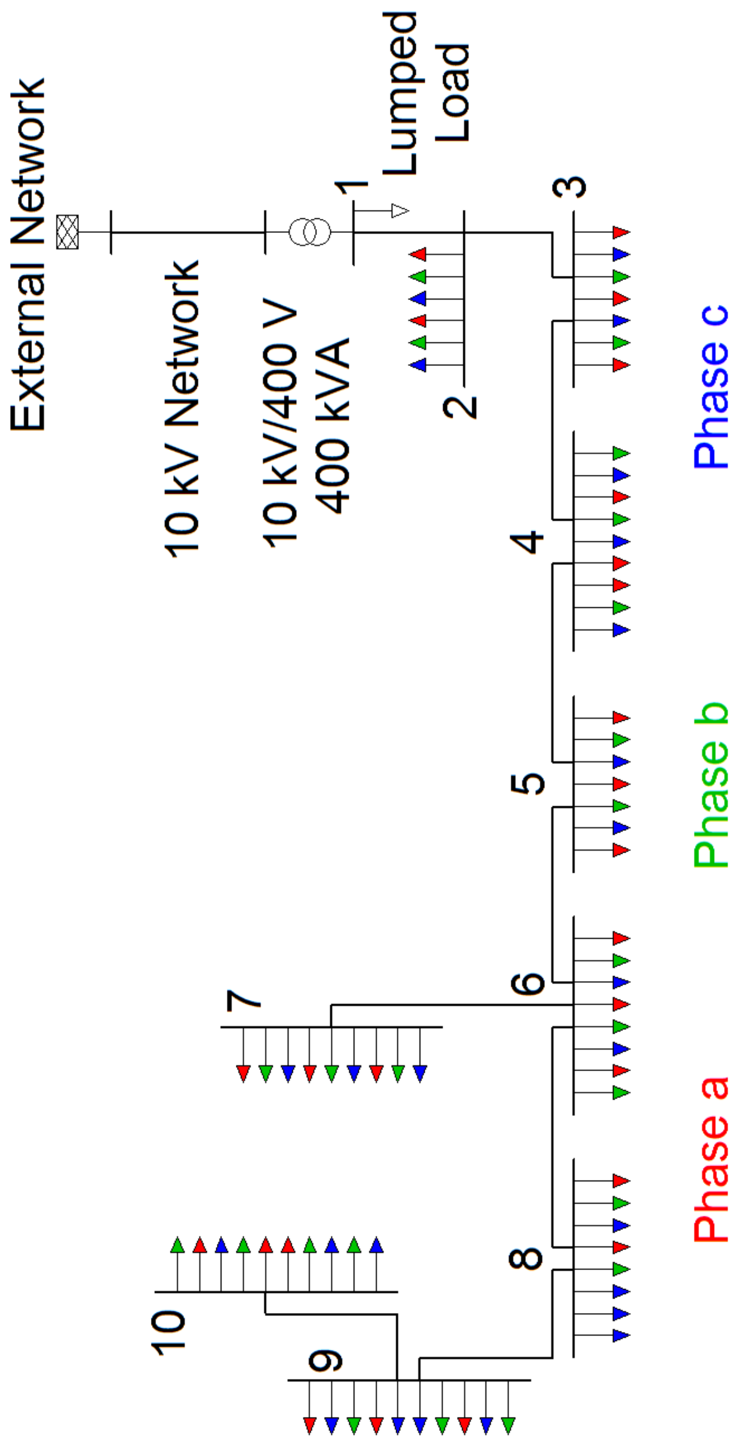

Figure B.3: Customer phase connections for Network 2

Appendix C: Publications Arising

1. P. Richardson, D. Flynn, and A. Keane, "Optimal charging of electric vehicles in low voltage distribution systems," *IEEE Transactions on Power Systems,* vol. 27, no. 1, pp. 268-279, February 2012.

2. P. Richardson, D. Flynn, and A. Keane, "Local vs. centralised charging strategies for electric vehicles in low voltage distribution systems," *IEEE Transactions on Smart Grid,* Special issue on "Applications of smart grid technologies on power distribution systems". In press.

Optimal Charging of Electric Vehicles in Low Voltage Distribution Systems

Peter Richardson, *Student Member, IEEE,* Damian Flynn, *Member, IEEE* and Andrew Keane, *Member, IEEE*

***Abstract*—Advances in the development of electric vehicles, along with policy incentives will see a wider uptake of this technology in the transport sector in future years. However, the widespread adoption of electric vehicles could lead to adverse effects on the power system, especially for existing distribution networks. These effects would include excessive voltage drops and overloading of network components, which occur mainly during periods of simultaneous charging of large numbers of electric vehicles. This paper demonstrates how controlling the rate at which electric vehicles charge can lead to better utilisation of existing networks. A technique based on linear programming is employed, which determines the optimal charging rate for each electric vehicle in order to maximise the total power that can be delivered to the vehicles while operating within network limits. The technique is tested on a section of residential distribution network. Results show that, by controlling the charging rate of individual vehicles, high penetrations can be accommodated on existing residential networks with little or no need for upgrading network infrastructure.**

***Index Terms*—road vehicle electric propulsion, linear programming, load flow analysis, optimisation methods, power distribution**

I. Introduction

ELECTRIC vehicle technology is seen by many countries as a key component in the effort to reduce harmful greenhouse gas emissions, while also reducing the dependence on imported petroleum within the transport sector. As a result, many automotive manufacturers have begun to place increased emphasis on the development of various types of electric vehicle (EV). These include battery electric vehicles, which operate purely from battery power, and plug-in hybrid electric vehicles, which operate on power from a combination of an on-board battery and a combustion engine. The batteries for both technologies can be recharged from external energy sources, e.g. an electricity network. Ambitious targets and incentives for introducing EVs into the transport sector have been proposed in many countries [1]–[3]. Such targets, along with the likely increase in the cost of fossil fuels over the coming years, will see EV technology become more widespread.

Distribution networks are rated (kVA limit) to deliver electricity depending on the number of customers in a given area and the historical electricity demand data for each of those customers. The widespread adoption of EVs will introduce new customer demand patterns, and large vehicle penetrations could result in adverse effects on the network. Investigations into the potential impact of EVs on load patterns and the need for load management at the distribution network level have been conducted since as early as the 1980s [4], [5]. More recent work in this area has sought to investigate the limitations from large numbers of EVs on network infrastructure in terms of increased loading, impacts on efficiency and loss of life for network assets [6]–[10]. These studies examined varying scenarios, such as unrestricted charging, peak and off-peak charging, diversified charging, and charging at varying power levels. The general consensus from these studies is that existing distribution networks should be able to accommodate substantial penetration levels of EVs if the majority of charging is restricted to low charging rates at off-peak times. Uncoordinated charging, especially fast, 3-phase charging, will lead to an increase in the number of occurrences of component overloading and excessive voltage deviations if it coincides with existing peaks from the residential load. Staggering the charging start times for localised groups of EVs is also shown to help avoid these adverse effects, as well as spikes in demand due to simultaneous commencement of charging. The impact on voltage levels from high penetrations of EVs is also investigated in [11] and shows how high levels of coincident charging can cause voltages to drop beyond acceptable limits during times of high residential demand.

The introduction of advanced metering infrastructure (AMI) systems in residential housing, be it for real-time pricing or active demand side management, or both, will aid the control/predictability of the load patterns on residential networks. AMI could potentially have the ability to control certain loads within the household (including EVs) and allow DSOs or demand side aggregators to manage these loads in a coordinated manner. Such concepts have been investigated previously. The work described in [12] proposes management strategies for EV charging/discharging in LV microgrids. By allowing network control devices to respond to voltage and frequency levels, it is shown that the EV load can enable LV microgrids to be operated in a stable manner. In [13], a technique is employed to minimise power losses and on-load tap changes for the network transformer, mainly due to the charging/discharging of EVs located far from the slack bus.

In [14], various techniques are utilised to investigate the impact of varying penetrations of EVs on residential networks. Quadratic and dynamic programming techniques minimise the impact from EV charging on network losses and voltage de-

P. Richardson (peter.richardson@ucd.ie), D. Flynn (damian.flynn@ucd.ie) and A. Keane (andrew.keane@ucd.ie) are all with the School of Electrical, Electronic and Mechanical Engineering, University College Dublin, Ireland.

This work was conducted in the Electricity Research Centre, University College Dublin, Ireland, which is supported by the Commission for Energy Regulation, Bord Gáis Energy, Bord na Móna Energy, Cylon Controls, EirGrid, the Electric Power Research Institute (EPRI), ESB Energy International, ESB Energy Solutions, ESB Networks, Gaelectric, Siemens, SSE Renewables, SWS Energy and Viridian Power & Energy.

This publication has emanated from research conducted with the financial support of Science Foundation Ireland under Grant Number 06/CP/E005.

viation in particular. By controlling and optimising individual EV charging rates, network losses and voltage deviations are reduced for all penetration levels examined. The methodology is examined using both deterministic and stochastic methods and concludes that while the difference in the results obtained using the quadratic or dynamic technique is negligible, the dynamic technique is more computationally intense. Work in [15] investigated the use of voltage control on EVs with charge/discharge capabilities. Here the objective was to minimise the charging cost to the EV owner while maintaining network voltage levels within acceptable limits. Results were shown to vary significantly depending on the initial state of charge of the EV batteries, with high dependence on the tariffs associated with charging and discharging.

The work in this paper differs in its approach to the coordinated charging of EVs described above. Instead of minimising power losses and/or voltage deviations, the objective of the optimisation technique employed here is to maximise the total amount of energy that can be delivered to all EVs over a charging period while ensuring that network limits are never exceeded due to high levels of coincident EV charging. Such an approach ensures that optimal use is made of available network capacity while avoiding excessive voltage drop and component overloading, which have been shown, in work cited above, to be potential issues with high levels of EV charging. The technique employs linear programming that takes advantage of the approximately linear characteristics of both the network voltages and component loading sensitivities to the addition of EV load.

The methodology for this work is presented in Section II. Section III describes the modelling of the test network, the residential load and the electricity demand profiles of EVs. Results and discussion for two specific charging periods are presented in Section IV along with generalised results for a wide range of network scenarios. Conclusions are presented in Section V.

II. Methodology

A. Assumptions

Coordinated charging of EVs could be achieved in a variety of ways. It is assumed here that EV owners are incentivised to charge their vehicles at off-peak times of day. Once the off-peak period has begun, no additional EVs will connect for charging and no EVs will disconnect before reaching a full battery state of charge (BSOC). Smart metering technology with load control capability is also assumed to be present in each household. It is assumed that this load control capability can be utilised by the DSO (or a third-party aggregator), from a remote location, in order to manage certain loads on the consumer side of the meter. Such a scheme would be subject to prior agreement by both the consumer and the DSO. For the purposes of this work, the ability to control the load extends to EV charging only and allows the operator to vary the charging rate of each EV on the feeder. Each EV can charge at any rate between zero and the maximum rated output, subject to certain restrictions, which are outlined later in this section. The ability to vary the charge rate of individual EVs in a continuous manner has been studied for use in optimal charging strategies previously [14], [16], [17]. While the possibility exists for fast, 3-phase charging, it is assumed that each EV will be connected to the network via a standard single-phase AC connection. Although the concept of vehicle-to-grid for local system support or otherwise exists [12], [13], [15], [17], bi-directional flow of electricity to and from an EV battery is not considered in this work.

B. Standard Objective Function

The objective of the method is to maximise the energy delivered to all EVs within a set period of time. This is achieved by optimising the charging rate of each connected EV in order to maximise the total power that can be delivered for each 15 minute time interval, subject to network constraints. Coordinating the charging of EVs ensures that the network is utilised to its fullest extent in terms of energy delivered.

The standard objective function, F, is given as

$$F = \sum_{i=1}^{N} P_{\mathrm{EV}_i} x_i \tag{1}$$

where N is the number of customers being served by the network, and P_{EV_i} is the power delivered, measured in kW, to the EV connected at the ith customer point of connection (CPOC). It is assumed that P_{EV_i} is a continuous control variable that can vary between 0 kW and the maximum power output of the charger at node i. x_i is zero when an EV is not connected at the ith CPOC or the EV battery is fully charged, while x_i equals one when the EV at the ith CPOC is connected and the EV battery is less than fully charged.

C. Constraints

At each time step, the objective function, F, is maximised subject to certain constraints. The first of these is that the power demand of an EV cannot exceed the rated power output of the charger supplying that vehicle, (2).

$$0 \leq P_{\mathrm{EV}_i} \leq {P_{\mathrm{EV}_i}}^{max} \tag{2}$$

In order to avoid large variations in the charging rate over consecutive time steps, which is undesirable for current battery technology [18], a rate of change constraint is also imposed (3).

$$ {P_{\mathrm{EV}_i}}^{t-1} - \Delta \ \leq \ {P_{\mathrm{EV}_i}}^{t} \ \leq \ {P_{\mathrm{EV}_i}}^{t-1} + \Delta \tag{3}$$

Here, t is the current time step and Δ is a defined limit, in kW, by which the charging rate can vary, compared to the charging rate at the previous time step, excluding on/off transitions.

The next constraint relates to the acceptable voltage range for the LV network. The addition of EV loads, for the most part, will cause the voltage at various points of the network to drop. The extent of the voltage drop can vary depending on a number of factors, which include the location of the EV and the rate of charge. The voltage at each CPOC must be maintained within the rated voltage range specified for the network, (4).

$$V_{min_i} \leq V_i \leq V_{max_i} \qquad i \forall N \tag{4}$$

Here, V_i (V) is the voltage at the *i*th CPOC, while V_{min_i} and V_{max_i} are the minimum and maximum allowable network voltage levels respectively.

The thermal loading of network components refers to the ratio of the apparent power flowing through the component to its rated capacity. For this study, the thermal loading of both the network transformer and the mains cable connecting the transformer to the network are considered. These constraints are summarised in equations (5) and (6) respectively.

$$L_{\mathrm{TX}} \leq L_{\mathrm{TX}_{max}} \tag{5}$$

$$L_{\mathrm{MC}} \leq L_{\mathrm{MC}_{max}} \tag{6}$$

where L_{TX} and L_{MC} are the thermal loading (kVA) for the transformer and mains cable respectively, while $L_{\mathrm{TX}_{max}}$ and $L_{\mathrm{MC}_{max}}$ are the associated maximum loading of the components.

D. Network Sensitivities

A time-series, unbalanced, 3-phase load flow analysis of the test network is performed in order to determine the network voltage and thermal loading levels as a result of the residential household load. This is performed using power system analysis software [19] and applying residential load information. The voltage sensitivities at each CPOC are also calculated for both the addition of EV load at their own terminal and at each of the other household terminals on the network, i.e. the change in voltage due to charging demand from the EVs. For each time step, EV load is added incrementally at each CPOC in turn and the change in voltage at each CPOC is recorded. This data is then used to calculate the voltage sensitivities of the network to the addition of EV load. The addition of EV load to any CPOC on the network causes variations in the voltage at each of the other CPOCs. Thermal loading sensitivities for the network components of interest are calculated in the same manner. The addition of EV load at any point of the network causes an increase in the thermal loading experienced by the transformer. Analysis of the load flow results shows that the assumption of linearity for both the voltage and thermal loading sensitivity characteristics is adequate [11]. The constraint for the voltage level can be summarised as,

$$V_{min_i} \leq V_{init_i} + \mu_i P_{\mathrm{EV}_i} + \sum_{j=1}^{N} \mu_{ji} P_{\mathrm{EV}_j} \leq V_{max_i} \qquad i \forall N \quad , \quad i \neq j \tag{7}$$

where V_{init_i} is the initial voltage at the *i*th CPOC of the network with no EVs charging, μ_i (V/kW) is the sensitivity of the voltage at the *i*th CPOC due to power demanded by the EV connected at the same CPOC, μ_{ji} is the sensitivity of the voltage at the *i*th CPOC due to power demanded by an EV connected at the *j*th CPOC.

The thermal loading constraints are summarised as

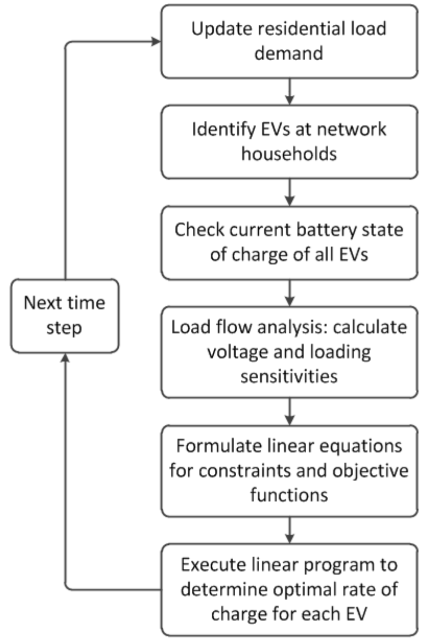

Fig. 1. Methodology for optimising the charging rates of EVs.

$$L_{\mathrm{TX}_{init}} + \sum_{k=1}^{N} \delta_k P_{\mathrm{EV}_k} \leq L_{\mathrm{TX}_{max}} \qquad k \forall N \tag{8}$$

$$L_{\mathrm{MC}_{init}} + \sum_{k=1}^{N} \beta_k P_{\mathrm{EV}_k} \leq L_{\mathrm{MC}_{max}} \qquad k \forall N \tag{9}$$

where $L_{\mathrm{TX}_{init}}$ and $L_{\mathrm{MC}_{init}}$ are the initial thermal loading levels of the network transformer and mains cable respectively, and δ_k (kVA/kW) and β_k (kVA/kW) are the sensitivities of the transformer and mains cable loading to power demand (P_{EV_k}) of an EV at the *k*th CPOC.

The voltage and thermal loading sensitivities are determined for each time step of the analysis. Subsequently, a linear programming tool in [20] determines the optimal charging rate for each connected EV for each time step, in order to maximise the total amount of energy that can be delivered over the considered period. A summary of the methodology is outlined in the flow chart presented in Fig. 1.

E. Weighted Objective Function

Due to the radial layout of the majority of LV residential networks, the standard optimisation technique tends to charge EVs connected near to the transformer at a higher rate than those located far from the transformer. This is due to the voltage levels being less sensitive to the addition of EV load near to the transformer. In order to provide a more even distribution of energy to the charging EVs and prioritise batteries with a low BSOC, a modified objective function is applied to the optimisation algorithm, which applies a weighting according to each individual EV's BSOC at the previous time step. It is assumed that the BSOC of each EV

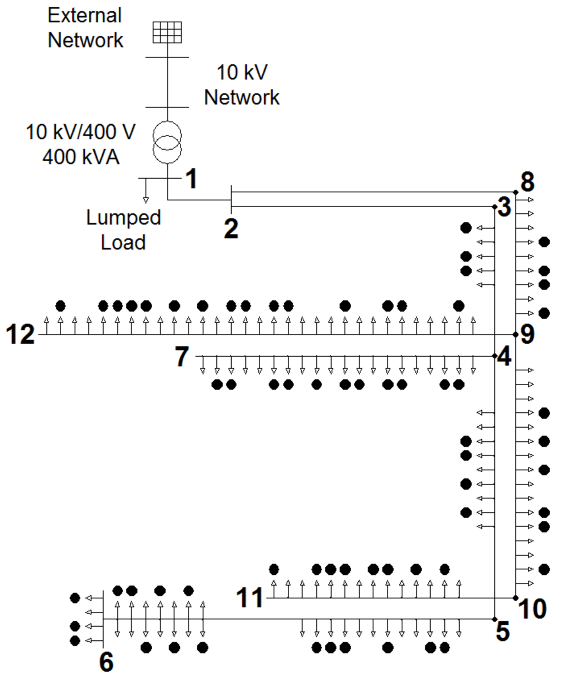

Fig. 2. Single line diagram of test network. Circles show houses where EVs are connected for charging.

is known at the beginning of each optimisation time step. The modified objective function, F, is summarised as follows:

$$F = \sum_{i=1}^{N} \left(1 - \left(\frac{\text{BSOC}_i}{\text{BSOC}_{max_i}}\right)\right) P_{\text{EV}_i} x_i \qquad (10)$$

where BSOC_i is the current battery state of charge (kWh) of the EV connected at the ith CPOC and BSOC_{max_i} is the maximum battery capacity of that EV.

III. Modelling of Test Network

A. Distribution Network

The test network is based on a LV residential distribution feeder in a suburban area of Dublin, Ireland. A simplified representation of the feeder is given in Fig. 2. In the actual test feeder, each household, EV and service cable are modelled separately. The model incorporates a 400 kVA, 10/0.4 kV step-down transformer supplying a feeder of 134 residential customers through 1.2 km of 3-phase copper mains cables and 980 m of single-phase copper service cables. A lumped load model, representing a similar number of residential customer loads with no EV loads, is included to represent another feeder being supplied from the same transformer.

In Ireland, the LV distribution network is operated at a nominal voltage of 230/400 V with a voltage range tolerance of +/-10% [21]. For the most part, LV substation transformers in Ireland do not have tap-changing capabilities, which is the case for the transformer modelled in the test network. As such, the medium voltage (MV) network supplying the LV transformer is included in the model as an equivalent impedance in order to take account of the voltage drop at this network level. The MV network is modelled such that at maximum residential load (with no EV charging), the voltage at all points of the network does not exceed -10% of nominal. Specifications for the network model components were supplied by Electricity Supply Board (ESB) Networks, who are the DSO in the Republic of Ireland, and are given in Table III in the Appendix.

B. Residential Customer Load Modelling

Typical load data for domestic electricity demand customers was obtained from the DSO consisting of 15-minute time-series demand data for high, medium and low use customers over a one year period. Different electricity demand profiles were randomly assigned to each of the houses in the test network. However, in order to confirm that these load profiles portrayed an accurate representation of the power demanded by a real distribution feeder, the coincidence factor of the test network was determined. The coincidence factor is defined as the ratio of the maximum diversified demand divided by the maximum non-coincidental demand [22]. From assessing the yearly load profiles for each of the households on the network, the coincidence factor was found to be 0.32, which compares favourably with similar residential networks [23].

For modelling purposes, the power factor for each household load is set at 0.97 inductive during the day and 0.95 inductive at night. Here, daytime is specified as between 6 am and 10 pm, and nighttime as between 10 pm and 6 am. The load is modelled as a combination of constant power (P) and constant impedance (Z). From April to September inclusive, the load is modelled as 60% constant P, 40% constant Z. From October to March inclusive, the load is modelled as 40% constant P and 60% constant Z, due to an increase in electric heating load. It is common practice to model residential loads in this manner when exact information on the load type is not available [23].

C. Electric Vehicle Load Modelling

It is assumed that each EV is connected at the same CPOC as the household load through a single-phase connection. Charging profiles for EVs can vary depending on battery type, charging equipment and the electricity supply network. For this work, EV batteries are modelled based on lithium-ion battery technology. It is assumed that once connected, an individual EV with no charge controlling capability charges at a rate of 4 kW up to a BSOC of approximately 95%. After this point the vehicle charges at a rate of 1.5 kW until the battery has reached its maximum capacity. For this work, all EV batteries are modelled with a capacity of 20 kWh. The EV charging equipment is assumed to have a 90% efficiency rating. The charging rate of 4 kW is appropriate in terms of the power delivery capabilities of existing LV distribution networks in Ireland [21]. EV batteries are modelled as constant power loads with unity power factor.

D. Time Periods for Investigation

In order to demonstrate the benefits of the optimisation technique, two specific periods of time within the one year period of residential load data were chosen. For this study,

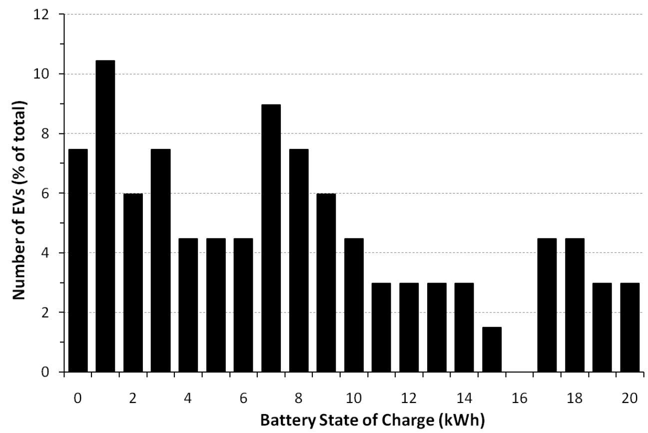

Fig. 3. Distribution of the initial BSOC for each EV.

the charging period occurs from 10 pm to 7 am the next day. One test period was chosen because it contained the highest 15-minute residential demand during the off-peak charging periods (winter scenario). The maximum 15-minute residential demand for this time period was approximately 152 kW. The other test period chosen was a low-demand mid-week charging period in the summer (summer scenario).

For the simulations, half of the residential households were randomly assigned an EV, as shown in Fig. 2. This amounts to 67 EVs on the network with a potential combined maximum demand of 268 kW. It was assumed that all EVs remain connected to the network for the entire charging period, with each EV randomly assigned an initial integer valued BSOC. The distribution of the initial BSOC for each EV is shown in Fig. 3. The average initial BSOC of all the EVs was 7.8 kWh, or 39% of the maximum BSOC.

Table I shows the breakdown of EVs allocated to the network as well as the total energy requirement of these vehicles on a phase-by-phase basis. It is clear from this table that there is a greater number of EVs on phase c, and thus a larger energy requirement, compared to the other phases. While a 50% penetration of EVs on a distribution feeder may not be experienced in reality for many years to come, it was deemed appropriate to examine such a demanding scenario in order to fully capture the main benefits from controlled charging strategies compared to uncontrolled charging.

TABLE I
INITIAL EV CONDITIONS

	Number of EVs	**Combined Battery Capacity (kWh)**	**Combined Initial BSOC (kWh)**	**Total Energy Required (kWh)**
Phase a	19	380	139	241
Phase b	18	360	146	234
Phase c	30	600	236	344
Total	67	1340	521	819

E. Stochastic Scenario Analysis

The charging periods identified above are chosen to examine the optimisation technique for specific network scenarios. However, in order to demonstrate the benefits of the optimisation technique for a wider range of scenarios, a stochastic tool is developed to generate different residential load scenarios with probabilistic conditions for varying residential load, EV location and initial BSOC.

Probability distribution functions (PDFs) for the household load were created based on the residential load data provided by the DSO with PDFs for low, medium and high use customers. 15-minute household load profiles were then generated for each house for a 9 hour period from 10 pm to 7 am the next day, similar to the deterministic analysis. It is assumed that all EVs are connected for charging at the beginning of this period and remain connected until the end. At the beginning of each 9 hour charging period the EV locations on the network were randomly selected with each one then assigned an initial BSOC. As no real charging data was available, a PDF (mean = 10.75 kWh, standard deviation = 6 kWh) for assigning initial BSOC was created. For each charging period time step, network sensitivities are determined which are then used to optimise the charging rate of each EV. The load model and power factor for both the residential and EV load remain the same as for the deterministic analysis.

IV. RESULTS AND DISCUSSION

The optimisation technique is tested with the two different objective functions, (1) and (10). The results for each approach are outlined below and are compared to scenarios with no EV charging present and with uncontrolled EV charging.

A. Network Sensitivities

For each 15-minute time interval, a series of three-phase, unbalanced load flow calculations are performed using the customer demand profiles in order to determine the voltage and thermal loading sensitivities of the network due to the introduction of EVs. These sensitivities inform the optimal charging rate of each EV for each time step of the charging period. The voltage sensitivity at each CPOC is measured for varying charging rates and varying EV charging locations on the network. Fig. 4 demonstrates how the voltages measured at the CPOCs closer to the transformer (i.e. 3 and 8 from Fig. 2) are less sensitive to the addition of EV loads as compared to those located near the end of the feeder (i.e. points 6, 7, 11 and 12).

Since the household loads for this network are connected to individual phases of the network, the addition of EV load to a particular CPOC affects the voltage at that particular CPOC as well as the voltage on the other phases of the network, as demonstrated in Fig. 5. As can be seen, the addition of EV load on phase c only causes the voltage on that phase to decrease while the remaining phase voltages increase slightly. This effect is not uncommon in unbalanced networks [22] and is captured in the voltage constraint equation, (7), where the sensitivity, μ, of the voltage at a particular CPOC can be either

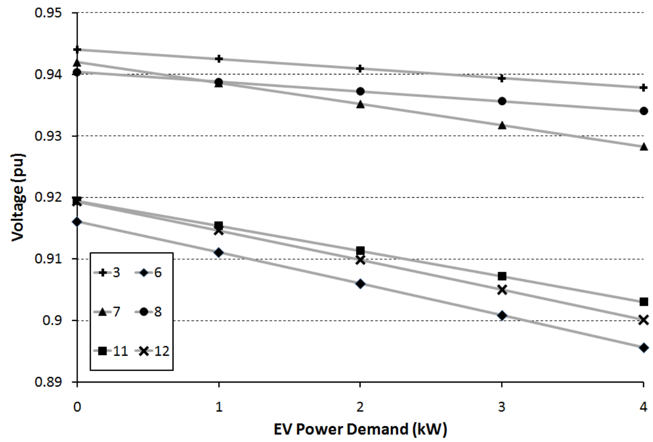

Fig. 4. CPOC voltage sensitivities to charging EVs at 6 network points for the Winter Scenario.

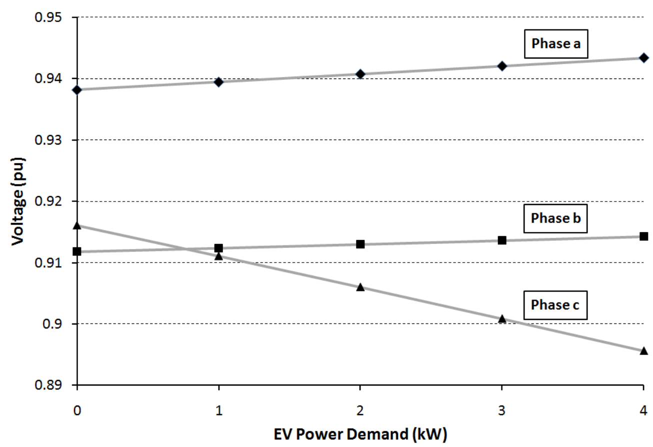

Fig. 5. Interdependence of 3 CPOC voltages with EV charging on phase c for the Winter Scenario.

positive or negative depending on the phase to which an EV is connected.

The voltage sensitivities can vary significantly due to the changes in the domestic household load, and therefore they are calculated for each time step of the analysis. This information is then subsequently used to optimise the EV charging rates, the results of which are outlined in the following sections.

In order to determine the accuracy of the optimisation technique, error margins were calculated based on the difference between the predicted CPOC voltages from the optimsation algorithm and the CPOC voltages recorded from the subsequent load-flow calculations. The average maximum error margin over the summer charging period was found to be 1% for the standard and weighted objective functions. For the winter charging scenarios these values were recorded as 1.4% (standard objective function) and 1.5% (weighted objective function). As can be seen in the results presented below, the accuracy of the sensitivities is adequate to ensure that no operating limits are exceeded due to EV charging.

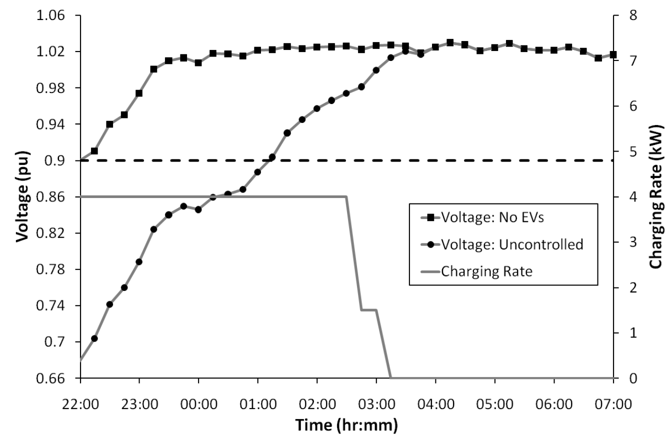

Fig. 6. Voltage level for a CPOC at node 6 for base case and uncontrolled charging scenarios with charge profile for an EV charging at the same CPOC. (Winter scenario)

B. Uncontrolled EV Charging

With no active control over EV charging rates, all of the EVs would be expected to commence charging at the beginning of the charging time period at the maximum rate of charge. As the network is not rated for this high level of demand, the network operating conditions are severely impacted. Fig. 6 shows the voltage level at a CPOC at node 6 for the winter scenario base case. The charge profile for an EV connected at the same CPOC is also displayed. The initial BSOC of this EV was 3 kWh or 15%. While all EVs on the network would be fully charged by the end of the charging period the lower voltage limit at this CPOC, i.e. 0.9 pu, is exceeded for over 3 hours at the start of the charging period. The lowest voltage experienced at this node is approximately 0.68 pu. It is clear that such a scenario could not be permitted to occur and it is likely that the number of EVs on the network would be restricted to a predetermined limit. For the purposes of comparison, an uncontrolled charging scenario was created whereby there is a limit to the number of EVs that are allowed to charge simultaneously. This number was determined by incrementally adding EVs, charging at the maximum rate of charge, to the extremities of the feeder up to the point before the feeder exceeds an allowable operating limit. This test was performed with the residential load at the maximum expected midnight demand. Charging was restricted to begin only after midnight to ensure that the residential load is off-peak. For the test network utilised in this work, the predetermined number of EVs that could be allowed to charge in an uncontrolled scenario was found to be 21.

C. Controlled EV Charging

By employing the methodology described in Section II, the rate at which each EV charges is now optimised in order to deliver the maximum power to the EVs while maintaining all voltages and network flows within acceptable operating limits for each time step. At the beginning of the charging period, the total energy required to return all EVs to 100% BSOC is 819 kWh. For the optimisation, the lower voltage limit is set at 210

V or 0.913 pu, which allows for a margin of safety with respect to the lower voltage limit defined in the Irish distribution network code [21]. This ensures that any unexpected short term variations in the demand, will not cause the network to exceed its operating limits. The maximum variation allowable for the rate of charge between time steps, i.e. Δ in (3), is set at 0.25 kW for each of the control strategies.

1) Standard Objective Function: From Table II it can be seen that using the standard objective function a total of 810 kWh in the summer and 798 kWh in the winter were delivered to the EVs by the end of the respective charging periods. Although this means that the total EV energy requirement (819 kWh) was not met, in both cases the network was maintained within normal operating limits for the entire duration of the charging period.

TABLE II
TOTAL ENERGY DELIVERED TO EV BATTERIES

		Total Energy Delivered (kWh)	% Energy Requirement
Uncontrolled Charging (21 of 67 EVs)	Summer	238	29
	Winter	238	29
Standard Objective Function	Summer	810	98.9
	Winter	798	97.4
Weighted Objective Function	Summer	818	99.9
	Winter	815	99.5

The voltage profile of a CPOC at node 6 with an EV charging and the corresponding EV charge profile is given in Fig. 7. It is evident that the voltage here is a binding constraint for the optimisation technique as it is held just above the lower voltage limit for the majority of the charging period. It can also be seen that the EV connected to this CPOC does not truly begin charging until the third hour of the charging period and does not approach a maximum rate of charge until towards the end of the period. This particular EV had an initial BSOC of 3 kWh (15%) and had reached a BSOC of 15 kWh (75%) by the end of the charging period. Clearly, this would be an unacceptable outcome for an EV owner that desired a full BSOC.

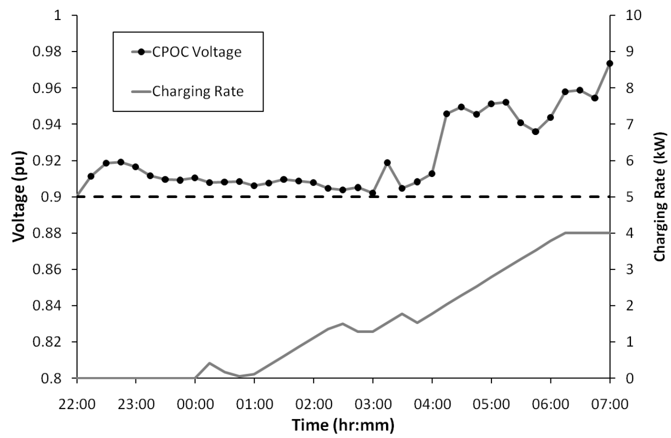

Fig. 7. Voltage profile for a CPOC at node 6 and charge profile for EV charging at the same CPOC with optimised charging employing the standard objective function. (Winter scenario)

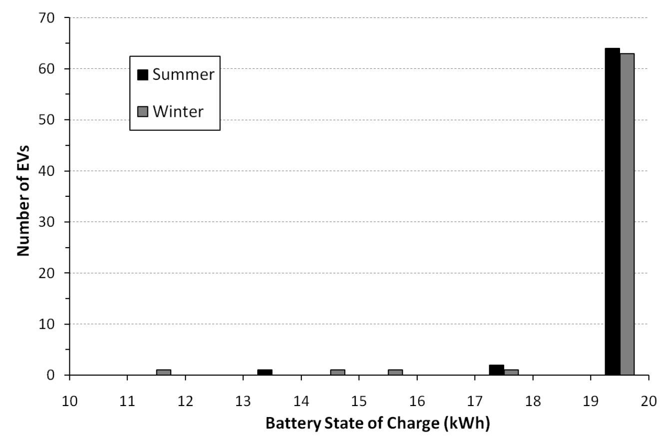

Fig. 8. Distribution function of the battery state of charge for all EVs at end of the summer and winter charging periods: standard objective function.

Fig. 8 shows the distribution function for the BSOC of each EV at the end of both the summer and winter charging periods. It is evident in both cases that a number of EVs, including the one shown in Fig. 7, have not reached a full BSOC by the end of the charging period. In the summer scenario, 64 of the 67 EVs were fully charged, while for the winter charging period, 63 EVs had a full BSOC. In both cases, the EVs with a BSOC of less than 100% are all located near the end of the branches of the feeder and are connected to phase c. From Table I it can be seen that a greater number of EVs are connected to phase c than either of the other phases, which results in a larger energy requirement. Additional load due to EV charging at CPOCs near the end of feeder branches will have a greater effect on network voltage levels than if located closer to the transformer. As a result, the optimisation method allocates low charging rates to these EVs until the other EVs are fully charged. The combination of both factors leads to a number of EVs not receiving a full BSOC by the end of the charging period. This outcome is displayed in Fig. 9, which shows the active power demand, with and without EV charging, on each phase of the network over the charging period. It is clear that, while the EVs connected to phase a and phase b have completed charging, power is still being delivered to some EVs connected to phase c. Also shown in this figure is the lowest CPOC voltage measured on each phase of the feeder for each time step. It is clear that while power is being delivered to the EVs on the feeder, the voltage levels at each of the CPOCs are held above the lower voltage limit.

2) Weighted Objective Function: The standard objective function optimisation technique will consistently tend to assign low charging rates to EVs located further from the transformer. Such a situation would clearly be unacceptable. In order to overcome this, the optimisation process was repeated, as described in Section II, with the objective function weighted according to the current BSOC of each charging EV, (10).

By employing this method, 818 kWh of energy are delivered to the EVs for the summer charging period and 815 kWh are delivered in the winter charging period, which represents 99.9% and 99.5%, respectively, of the total energy required

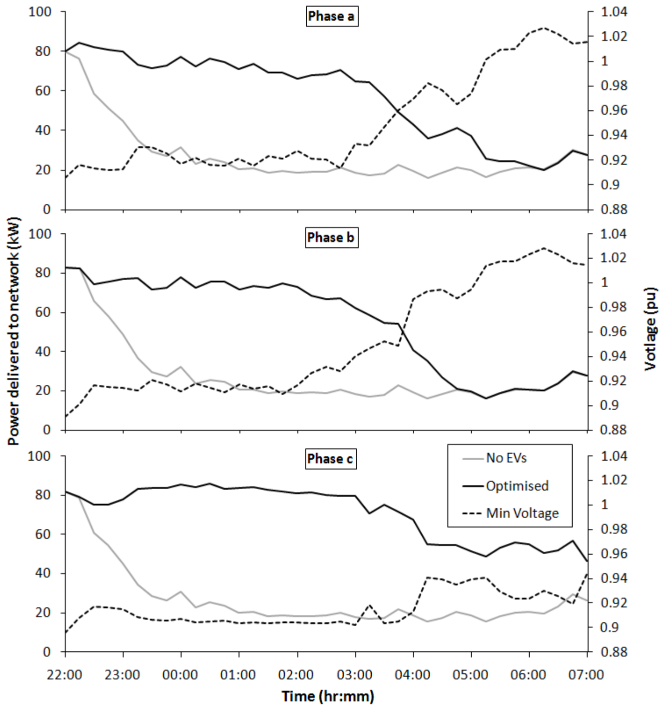

Fig. 9. Power delivered to network on each phase for the case with no EVs charging and the optimised charging case employing the standard objective function (Winter). The lowest CPOC voltage for each phase at each time step for the optimised charging case is also shown.

to return all EV batteries to a full BSOC. The total power delivered to the EVs for the uncontrolled and optimised charging scenarios is shown in Fig. 10. While both objective function methods deliver similar energy totals by the end of the charging period, the individual EV charging patterns vary significantly across the network. During the early stages of the charging period, the SOF prioritises EVs that are located close to the transformer, whereas the WOF assigns higher charging rates to EVs with a low BSOC, wherever they may be located in the network. Later in the charging period, applying the SOF, vehicles located at the network extremes begin charging. As the voltage is more sensitive to additional load at these points of the network, the charging rates for these EVs are lower and less energy can be delivered. The same restrictions are not as severe using the WOF as the energy delivered to the EVs is more evenly distributed across the network, resulting in more energy being delivered towards the end of the charging period (Fig. 13 and 14).

Fig. 11 shows the voltage profile, for the same CPOC as shown in Fig. 7, as a result of the weighted objective function optimisation technique. Once again, it is apparent that the voltage at this CPOC is a binding constraint. However, the EV begins charging much earlier and the BSOC by the end of the charging period has reached 100%, as compared with a figure of 75% using the standard objective function method.

The distribution function of the BSOC for the EVs by the end of the charging period is given in Fig. 12, and shows an increase in the number of EVs with a full BSOC for both charging period scenarios when compared to the previous method. Specifically, 67 EVs have a full BSOC by the end of

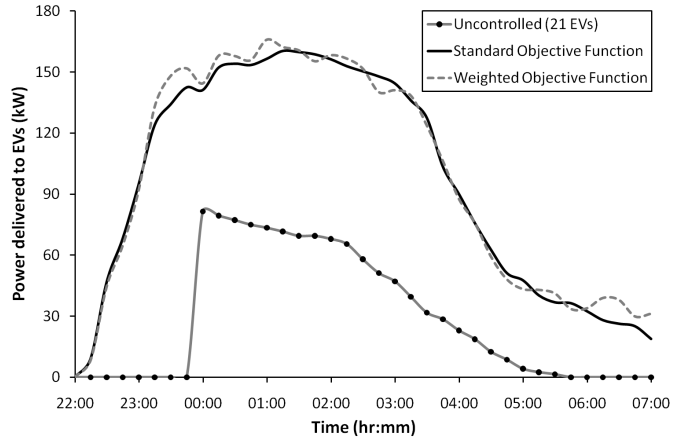

Fig. 10. Total power delivered to EVs for uncontrolled and optimised winter charging scenarios.

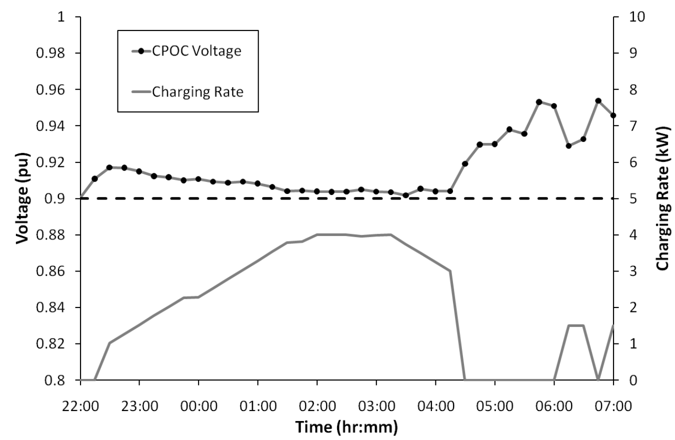

Fig. 11. Voltage profile for a CPOC at node 6 and charge profile for EV charging at the same CPOC with optimised charging employing the weighted objective function. (Winter scenario)

the summer charge period, while 66 of the 67 EVs have a full BSOC in the winter scenario. This compares favourably to the standard objective function method where the lowest BSOC of all the EVs was 68% and 58% for the summer and winter charging periods respectively. As was the case for the previous method, the EV that was not fully charged was connected to phase c and is located near the end of the feeder branches.

It should be noted that the particular allocation of EVs in this work resulted in there being a greater number of EVs connected to one phase compared to the others. As this work has shown, even an optimal method for maximising the energy that can be delivered to charging EVs may be insufficient if a large number of the EVs are connected to the same phase of the network at the same time. Such scenarios may require that the DSO reconfigure the distribution of load across the phases.

D. Thermal Loading of Network Components

Thermal loading constraints of certain feeder components are also taken into account by the optimisation technique. Fig. 13 shows the loading of the LV transformer over the

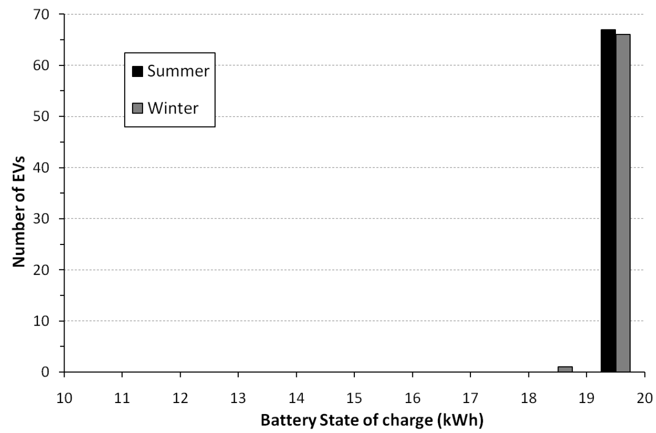

Fig. 12. Distribution function of the battery state of charge for all EVs at end of the summer and winter charging periods: weighted objective function.

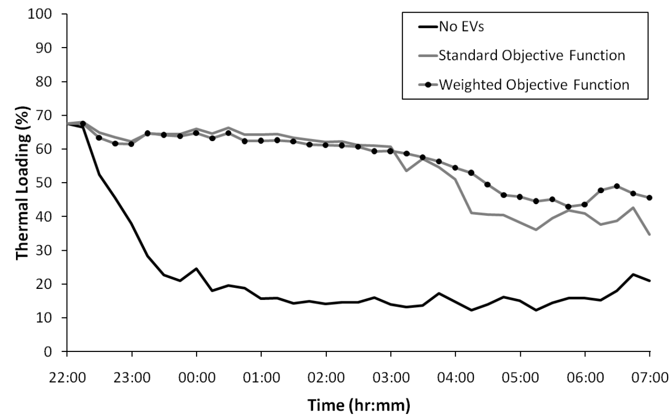

Fig. 13. Thermal loading of LV transformer for winter charging period.

charging period for the winter scenario, while Fig. 14 shows the loading for the 3-phase mains cable (Line 1-2 in Fig. 2) that supplies the feeder from the transformer for the same scenario. In both cases, it is evident that neither the transformer nor the mains cable loading are the binding constraint on this network. Clearly, the network equipment is more than adequately rated for accommodating the additional load that would be demanded by this high penetration of EVs, assuming that the majority of charging occurs at off-peak times of day. This may not be the case for all residential distribution feeders, many of which may experience overloading of network components due to large numbers of EVs charging simultaneously at both peak and off-peak times of day. Without some form of controlled charging for EVs, a significant increase in the number of overloading incidences will impact on the lifetime of these network components [6]. By employing a controlled charging technique, like the one described in this paper, the overloading of network components due to EV charging can be avoided by incorporating certain constraints, (8), (9). While this would result in increased loading levels during the off-peak period, a flatter transformer load profile would impact less on the transformer lifetime than a profile with large overloads due to on-peak EV charging [24]. Together with the introduction of other demand side management schemes, many forms of residential load could be controlled in a manner which would allow networks to be utilised to their fullest extent while not impacting on component lifetimes.

E. Network Losses

The network losses as a percentage of the total energy delivered to the network are presented in Fig. 15. For each of the cases studied, the losses ratio is greater in the winter charging period than in the summer period due to the increased residential demand in the winter. The added demand from EVs charging causes the losses ratio to increase significantly. This is evident for both the standard (SOF) and weighted (WOF) objective function methods. For the SOF case the losses ratio increases from 0.3% to 4.1% in the summer and 1% to 4.5% in the winter. For the WOF method these values increase to 4.6% in the summer and to 4.8% in the winter scenario.

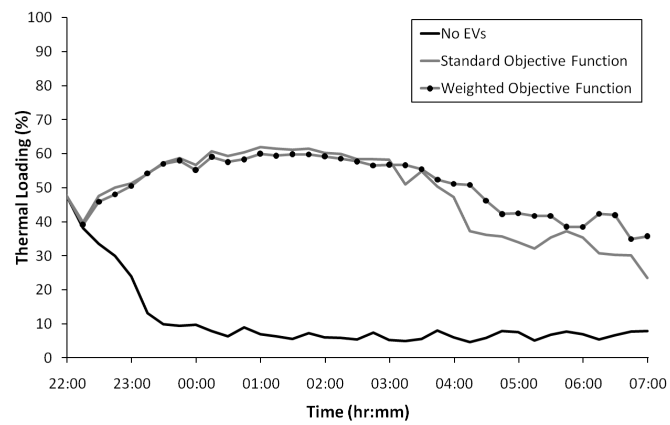

Fig. 14. Thermal loading of 3-phase mains cable supplying feeder for winter charging period.

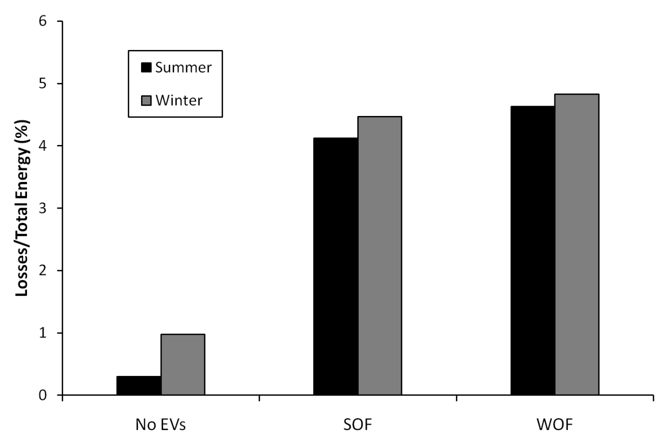

Fig. 15. Network losses for standard objective function (SOF) and weighted objective function (WOF) cases.

F. Stochastic Scenario Analysis

A stochastic analysis of the network loading is carried out in order to provide insight into the effects of the optimisation technique while accounting for the variability associated with a high penetration of charging EVs. The optimisation technique using the weighted objective function was simulated for 500,

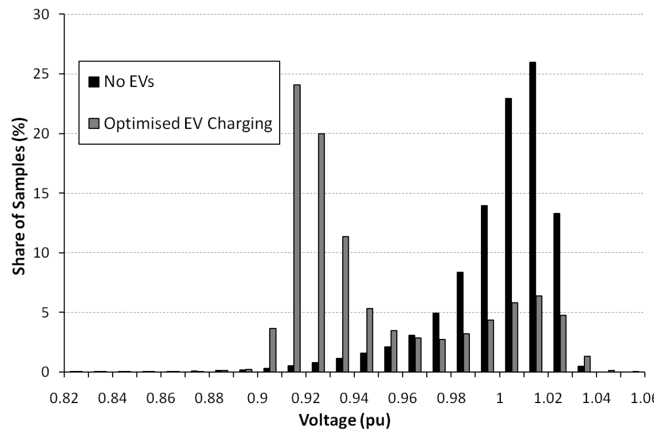

Fig. 16. Distribution of measured voltages at network CPOCs.

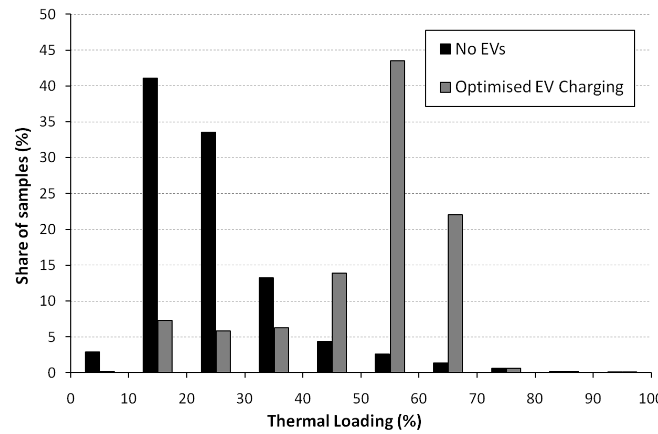

Fig. 17. Distribution of measured thermal loading levels for the network transformer.

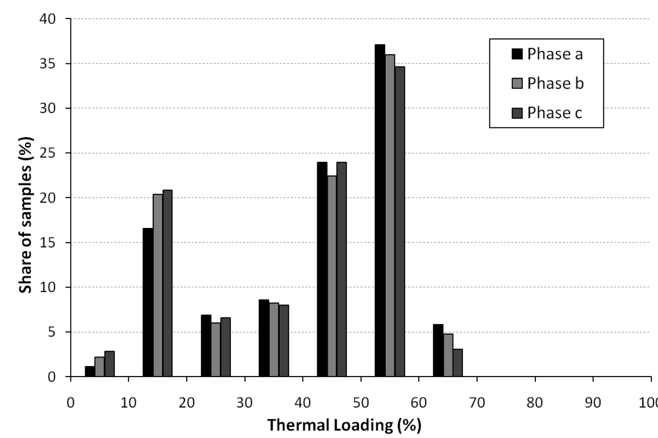

Fig. 18. Distribution of measured loading levels on each phase of the 3-phase mains cable supplying the network from the transformer (optimised EV charging).

9-hour charging periods (i.e. 18,500 time steps). Residential load profiles for typical mid-week, winter scenarios were generated based on the associated PDFs.

Fig. 16 shows the distribution of measured voltages for all CPOCs over all charging periods for the scenario with no EVs on the network and the scenario with 50% EV penetration with optimised vehicle charging. This graph shows that the majority of pre-optimisation voltage measurements are near or above 1 pu with reduced occurrences for decreasing voltage levels. Following the application of the optimisation technique, the majority of voltage measurements are recorded between 0.91 and 0.95 pu indicating that the optimisation technique was able to maintain CPOC voltages above the low voltage limit for the network. Any occurrence of voltage levels below the lower voltage limit, in both the case with no EVs and the optimised case, is due to the household demand. As a result, these voltages remain unaffected in the optimised case as the technique does not allow EV charging if the network is already exceeding limits.

The distribution of thermal loading results for the transformer during the analysis is presented in Fig. 17. Prior to the addition of EVs, the majority of loading measurements were found to lie between 10% and 30% of rated loading. Following the introduction of EVs, charged according to the optimisation method, the majority of recorded measurements were found to be in the region of 50-70% of rated loading.

Fig. 18 shows the distribution of measured thermal loading for each phase of the 3-phase mains cable supplying the feeder from the LV transformer. These measurements are from the optimised case only. As can be seen from the loading results for both the transformer and the mains cable, the rated loading limit for either component is never the constraining factor for the optimisation method. It is apparent that, for this particular network, the electrical components are more than adequately rated to accept the increased loading due to a high penetration of charging EVs. Instead, the voltage limits are more likely to be an issue with off-peak EV charging and, as a result, are typically the constraining factor in the optimsation method.

Fig. 19 shows results for the final BSOC of all EVs after each charging period, representing the BSOC of the EV with the least BSOC, as well as the average BSOC of all EVs. For the high penetration level of charging EVs examined, the optimisation technique results in an average BSOC of 99.9%. While it is possible that not every EV will have a full BSOC by the end of the charging period, such cases occur far less frequently. The lowest final BSOC recorded over the analysis was 13.3 kWh (66.5%).

The average losses on the LV feeder over all charging periods were found to be 11 kWh for the case with no EVs and 80 kWh for the optimised charging case using the weighted objective function method.

V. Conclusion

The introduction of large penetrations of EVs will have significant impacts on the operating conditions of distribution networks. If they are to be charged in a passive, uncontrolled manner then major infrastructure upgrades may be required. Controlled charging by the DSO could help to alleviate some of these issues and allow EV owners to charge their vehicles while maintaining the network within acceptable operating limits. The work presented here has demonstrated how the charging rates of a high penetration of EVs on a test network

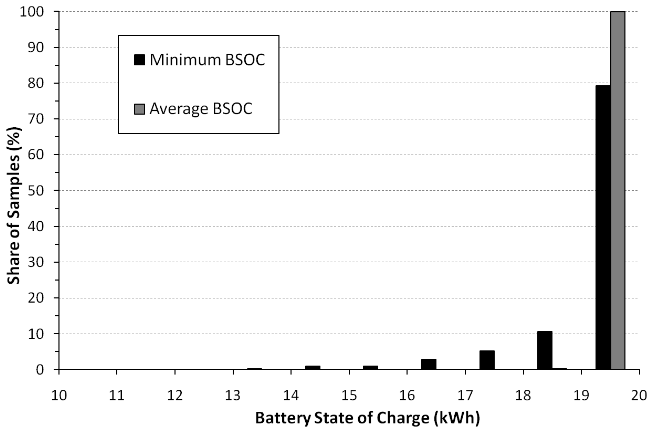

Fig. 19. Distribution of minimum and average BSOCs for all EVs recorded at the end of each charging period.

can be optimised in order to deliver the maximum amount of energy to the EVs within a set charging period subject to network constraints, while ensuring that the underlying residential load remains unaffected.

Results from this work have shown that maximising the total power to all EVs according to network constraints will favour those EVs that are connected near to the transformer, rather than those connected towards the extremes of the radial network. Therefore, a weighted objective function was studied, which optimised the EV charging rates according to both the impact on the network operating conditions and the BSOC of the EVs. Results show that the modified objective function increases the total energy delivered to the EVs. This objective function was also tested for various charging period scenarios and was shown to return an average BSOC of 99.9% for all EVs over all periods examined.

Due to the use of linear programming, large amounts of data are not required by the DSO at each time step in order to find the optimal rate of charge for each EV. The technique is not computationally intense nor does it require storage of historical load data for subsequent use, and therefore could be easily incorporated into a coordinated charging scheme. Determining the various network sensitivities to additional load provides insight into the condition of the network and could prove very useful for DSOs employing such schemes. Assuming the use of AMI within residential households and sufficient communication links between the DSO and the AMI metering, practical implementation of the optimal charging method would provide significant benefits in terms of accommodating high penetrations of EVs.

Acknowledgment

The authors would like to acknowledge ESB Networks for providing the necessary data for carrying out this work.

Appendix

TABLE III
Cable Characteristics

Line	Length (m)	R_1 (Ω)	X_1 (Ω)	R_0 (Ω)	X_0 (Ω)	C (μF)	I_{rated} (A)
MV	10,000	20.8	4	10	12	0.01	1000
1-2	190	0.032	0.014	0.095	0.041	0.053	510
2-3	27.5	0.008	0.002	0.024	0.006	0.008	368
3-4	85	0.024	0.006	0.073	0.018	0.026	368
4-5	97.5	0.028	0.007	0.084	0.021	0.029	368
5-6	154	0.062	0.011	0.185	0.033	0.046	300
4-7	119	0.048	0.009	0.143	0.026	0.036	300
2-8	32.5	0.009	0.002	0.028	0.007	0.01	368
8-9	59	0.017	0.004	0.051	0.013	0.018	368
9-10	106	0.03	0.008	0.091	0.023	0.032	368
10-11	95	0.027	0.007	0.082	0.021	0.029	368
9-12	217.5	0.087	0.016	0.261	0.047	0.065	368
Service Cable (per km)		0.8	0.07	-	-	0.4	80

R_1 Positive sequence resistance
X_1 Positive sequence reactance
C Capacitance
R_0 Zero sequence resistance
X_0 Zero sequence reactance
I_{rated} Rated current

References

[1] Department of Transport, Republic of Ireland. "Smarter travel, a sustainable transport future: a new Transport policy for Ireland 2009-2020". Available: *http://www.transport.ie/upload/general/11284-0.pdf*

[2] Department for Transport, United Kingdom. "Ultra-low carbon cars: next steps on delivering the £250 million consumer incentive programme for electric and plug-in hybrid cars", July 2009. Available: *http://www.dft.gov.uk/adobepdf/163944/ulcc.pdf*

[3] J. Heywood, P. Baptista, I. Berry, K. Bhatt, L. Cheah, F. de Sisternes, V. Karplus, D. Keith, M. Khusid, D. MacKenzie and J. McAulay, "An action plan for cars: the policies needed to reduce U.S. petroleum consumption and greenhouse gas emissions", Massachusetts Institute of Technology Energy Initiative Report, December 2009. Available: *http://web.mit.edu/sloan-auto-lab/research/beforeh2/actionplan/ActionPlan_CombinedFinal_ForPublication_8Feb10.pdf*

[4] G. T. Heydt, "The impact of electric vehicle deployment on load management strategies", *IEEE Transactions on Power Apparatus and Systems*, vol. PAS-102, no. 5, pp. 1253-1259, May 1983.

[5] S. Rahman and G. B. Shrestha, "An investigation into the impact of electric vehicle load on the electric utility distribution system", *IEEE Transactions on Power Delivery*, vol. 8, no. 2, pp. 591-597, April 1993.

[6] J. Taylor, A. Maitra, M. Alexander, D. Brooks and M. Duvall, "Evaluation of the impact of plug-in electric vehicle loading on distribution system operations", *In Proc. IEEE Power and Energy Society General Meeting*, Calgary, Canada, July 2009.

[7] K. Schneider, C. Gerkensmeyer, M. Kintner-Meyer and R. Fletcher, "Impact assessment of plug-in hybrid vehicles on Pacific Northwest distribution systems", *In Proc. IEEE Power and Energy Society General Meeting*, Pittsburgh, Pennsylvania, USA, July 2008.

[8] C. Gerkensmeyer, M. Kintner-Meyer and J.G. DeSteese, "Technical challenges of plug-in hybrid electric vehicles and impacts to the US power system: distribution system analysis", Pacific Northwest National Laboratory Report, January 2010. Available: *http://www.pnl.gov/main/publications/external/technical_reports/PNNL-19165.pdf*

[9] S. Shao, M. Pipattanasomporn and S. Rahman, "Challenges of PHEV penetration to the residential distribution network", *In Proc. IEEE Power and Energy Society General Meeting*, Calgary, Canada, July 2009.

[10] G. A. Putrus, P. Suwanapingkarl, D. Johnston, E. C. Bentley and M. Narayana, "Impact of electric vehicles on power distribution networks", *In Proc. IEEE Vehicle Power and Propulsion Conference*, Dearborn, Michigan, USA, September 2009.

[11] P. Richardson, D. Flynn and A. Keane, "Impact assessment of varying penetrations of electric vehicles on low voltage distribution systems", *In Proc. IEEE Power and Energy Society General Meeting*, Minneapolis, Minnesota, USA, July 2010.

[12] J. A. Peças Lopes, S. A. Polenz, C. L. Moreira and R. Cherkaoui, "Identification of control and management strategies for LV unbalanced microgrids with plugged-in electric vehicles", *J. Electric Power Systems Research*, vol. 80, no. 8, pp. 898-906, August 2010.

[13] S. Acha, T. C. Green, N Shah, "Effects of optimised plug-in hybrid vehicle charging strategies on electric distribution network losses", *In Proc. IEEE Power and Energy Society Transmission and Distribution Conference and Exposition*, New Orleans, Louisiana, USA, April 2010.

[14] K. Clement, E. Haesen and J. Driesen, "The impact of charging plug-in hybrid electric vehicles on a residential distribution grid", *IEEE Transactions on Power Systems*, vol. 25, no. 1, pp. 371-380, February 2010.

[15] K. Clement-Nyns, E. Haesen and J. Driesen, "Analysis of the impact of plug-in hybrid electric vehicles on residential distribution grids by using quadratic and dynamic programming", *EVS24 International Battery, Hybrid and Fuel Cell Electric vehicle Symposium*, Stavanger, Norway, May 2009.

[16] A. Brooks, E. Lu, D. Reicher, C. Spirakis and B. Weihl, "Demand dispatch: using real-time control of demand to help balance generation and load." *IEEE Power and Energy Magazine*, vol. 8, number 3, pp. 20-29, May/June 2010.

[17] E. Sortomme and M. A. El-Sharkawi, "Optimal Charging Strategies for Unidirectional Vehicle-to-Grid", *IEEE Transactions on Smart Grid*, vol. 2, no. 1, pp. 131-138, March 2011.

[18] F. Hoffart, "Proper care extends Li-ion battery life". *Power Electronics Technology*, April 2008. Available: *http://powerelectronics.com/portable_power_management/battery_charger_ics/proper_care_extends-li-ion-battery-0425/index.html*

[19] DIgSILENT PowerFactory. DIgSILENT GmbH. Available: *http://www.digsilent.de/*

[20] MATLAB R2009a. The MathWorks, Inc.

[21] ESB Networks Distribution Code, October 2007. Available: *http://www.esb.ie/esbnetworks/en/downloads/Distribution-Code.pdf*

[22] W. H. Kersting, *Distribution System Modeling and Analysis*. London: CRC Press, 2002.

[23] H. L. Willis, *Power Distribution Planning Reference Book*. Basel: Marcel Dekker, 2004.

[24] *IEEE guide for loading mineral-oil-immersed transformers*, IEEE Standard C57.91, 1995.

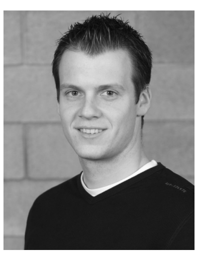

Peter Richardson (S'08) received his B.E. degree in Electrical Engineering from University College Dublin in 2007. He is currently studying for his Ph.D. at University College Dublin with research interests in electric vehicles, distributed energy resources and distribution networks.

Damian Flynn (M'96) is a senior lecturer in power engineering at University College Dublin. His research interests involve an investigation of the effects of embedded generation sources, especially renewables, on the operation of power systems. He is also interested in advanced modelling and control techniques applied to power plant.

Andrew Keane (S'04, M'07) received B.E. and Ph.D. degrees in Electrical Engineering from University College Dublin in 2003 and 2007 respectively. He is currently a lecturer with the School of Electrical, Electronic and Mechanical Engineering, University College Dublin with research interests in power systems planning and operation, distributed energy resources and distribution networks.

Local vs. Centralised Charging Strategies for Electric Vehicles in Low Voltage Distribution Systems

Peter Richardson, *Student Member, IEEE,* Damian Flynn, *Senior Member, IEEE* and Andrew Keane, *Member, IEEE*

***Abstract*—Controlled charging of electric vehicles offers a potential solution to accommodating large numbers of such vehicles on existing distribution networks without the need for widespread upgrading of network infrastructure. Here, a local control technique is proposed whereby individual electric vehicle charging units attempt to maximise their own charging rate for their vehicle while maintaining local network conditions within acceptable limits. Simulations are performed to demonstrate the benefits of the technique on a test distribution network. The results of the method are also compared to those from a centralised control method whereby EV charging is controlled by a central controller. The paper outlines the advantages and disadvantages of both strategies in terms of capacity utilisation and total energy delivered to charging EVs.**

***Index Terms*—linear programming, load flow analysis, optimisation methods, power distribution, road vehicle electric propulsion**

I. Introduction

THERE is growing interest in electric vehicle technology across the world, with many countries setting targets for the integration of electric vehicles (EVs) into their respective transportation sectors. The term "electric vehicle" can cover a number of technologies that employ electrical energy as a means of propulsion. These include battery electric vehicles, which operate purely from battery power, and plug-in hybrid electric vehicles, which operate on power from a combination of an on-board battery and a combustion engine. The batteries for both types of technology can be recharged from external energy sources, in particular an electricity network.

Widespread implementation of plug-in EVs would lead to significant changes to the way in which distribution systems are planned and operated. Recent work in this area has sought to investigate the limitations from large numbers of EVs on network infrastructure in terms of increased loading, impacts on efficiency and loss of life for network assets [1]–[5]. The consensus from these studies is that existing distribution networks should be able to accommodate substantial penetration levels of EVs if the majority of charging is restricted to single-phase charging at off-peak times.

The introduction of advanced metering infrastructure (AMI) systems in residential housing, be it for real-time pricing or active demand side management, or both, will aid the control and predictability of the load patterns on residential networks. In order to accommodate large numbers of EVs in distribution systems, charging strategies could be implemented to control the rate at which individual EVs charge. Previous work has shown that by controlling the charge rates of EVs on a low voltage (LV) residential network, so as to deliver the maximum amount of power while maintaining the network within its acceptable operating limits, many more vehicles can be accommodated for charging than would be possible in an uncontrolled scenario [6].

In [7], quadratic and dynamic programming techniques are utilised to minimise the impact from EV charging on network losses and deviations from nominal voltage on residential networks. By controlling and optimising individual EV charging rates, network losses and voltage deviations are reduced for all penetration levels examined. The work described in [8] and [9] propose management strategies for EV charging/discharging in LV microgrids. By allowing network control devices to respond to voltage and frequency levels, it is shown that the EV load can enable LV microgrids to be operated in a stable manner. In [10], optimal charging strategies are developed whereby aggregated EV load can be used for network regulation purposes. A number of optimisation methods for determining the EV charging rates are examined. Depending on the particular algorithm used, the techniques were shown to provide significant benefits in terms of cost savings for the customer and aggregator, and flexibility for utilities accommodating variable renewable energy sources. The work described in [11] uses an estimation of distribution algorithm to schedule EV charging for large numbers of EVs in a parking deck. The method optimises the energy allocation to the EVs in real time while considering various constraints associated with EV battery limits and utility limits. The method compares favourably to other optimisation techniques in terms of total energy delivered upon departure of the EVs. In [12], the ability of a large number of EVs to smooth the load profile of residential networks is investigated. By controlling the bi-directional flow of energy to and from the EV batteries, it is demonstrated that EVs can supply power to meet residential load peaks while also creating more predictable load profiles.

P. Richardson (peter.richardson@ucd.ie), D. Flynn (damian.flynn@ucd.ie) and A. Keane (andrew.keane@ucd.ie) are all with the School of Electrical, Electronic and Communications Engineering, University College Dublin, Ireland.

This work was conducted in the Electricity Research Centre, University College Dublin, Ireland, which is supported by the Commission for Energy Regulation, Bord Gáis Energy, Bord na Móna Energy, Cylon Controls, EirGrid, Electric Ireland, EPRI, ESB International, ESB Networks, Gaelectric, Intel, SSE Renewables, UTRC, and Viridian Power & Energy.

This publication has emanated from research conducted with the financial support of Science Foundation Ireland under Grant Number 06/CP/E005.

Utilising EVs for the smoothing of load profiles is also shown to be beneficial in terms of accommodating renewable distributed generation.

This paper proposes a strategy for optimising the charging rates of EVs based on a local control charging (LCC) method. The objective of the strategy is to deliver the maximum amount of energy to the EVs while maintaining the network within acceptable operating limits. The LCC method allows the optimal charging rates of the EVs to be determined individually based solely on local network conditions and their battery state of charge. This paper investigates the potential advantages and disadvantages of the LCC strategy in terms of network capacity utilisation and total energy delivered to EVs. The results are compared to those of a centralised control charging (CCC) method whereby a single controller manages the charging rates of all the EVs on the network simultaneously [6].

The methodology for this work is presented in Section II. Section III describes the modelling of the test network, the residential load and the electricity demand profiles of the EVs. Results and discussion for a sample charging period are presented in Section IV along with generalised results for a wide range of network scenarios. Conclusions are presented in Section V.

II. Methodology

A. Assumptions

In order to implement any type of active control at the LV distribution system level, it is assumed that EV charging units with load control capability are present in each household with an EV present. AMI, which is also assumed to be present in each household, enables time-of-day electricity tariffs which incentivise customers to avoid the more expensive peak load time of day. Each EV can charge at any rate between zero and the charger's maximum rated charge, subject to certain restrictions, which are outlined later in this section. It is assumed that each of the EV charging units on the network have the same charging capabilities. The ability to vary the charge rate of individual EVs in a continuous manner for use in optimal charging strategies has been studied previously [7], [10], [13]. While the possibility exists for fast, 3-phase charging, it is assumed that each EV will be connected to the network via a standard single-phase AC connection. Although the concept of vehicle-to-grid for local system support or otherwise exists [8], [10], [14], bi-directional flow of electricity to and from an EV battery is not considered in this work. For the CCC method, it is assumed that the load control capability of the EV charging units can be utilised by the distribution system operator (DSO), or a third-party controller, from a remote location.

B. Local Control Charging

Local control charging of EVs is achieved by each individual EV charging unit maximising the charge rate of their connected EV, subject to the voltage at its own customer point of connection (CPOC) and the loading of its own single-phase service cable. For each distributed control charging unit, the sensitivity of the CPOC voltage and service cable loading to the addition of EV load at its charger unit is predetermined and is not updated at each time step (Section II-D). With the predetermined sensitivity value, along with information about the instantaneous voltage at the CPOC and loading of the service cable, the charging unit maximises the rate of charge of the EV without exceeding either the local voltage or single-phase loading limits.

The objective of the charging units in the LCC strategy is to maximise the amount of power delivered to their individual EV at each 15 minute time step, subject to certain constraints. Each charging unit aims to maximise its own charge rate and cannot communicate with any other charger unit on the feeder. The process is performed using the linear programming tool in [17] and the optimisation occurs for each EV connected to the feeder and available for charging. The optimisation is calculated at each time step *t*. In this case, the objective function, F_{LCC}, is given as

$$F_{\text{LCC}} = P_{\text{EV}} x \tag{1}$$

where P_{EV} is the power delivered. It is assumed that P_{EV} is a continuous control variable that can vary between 0 kW and the maximum power output of the charger. x is zero when an EV is not connected at the CPOC or the EV battery is fully charged, while x equals one when the EV at the CPOC is connected and the EV battery is not fully charged.

C. Constraints

While each of the charging units has the ability to vary their output in a continuous manner, the charging rate limits are defined in (2), where $P_{\text{EV}_{\max}}$ is the rated output of each charging unit.

$$0 \leq P_{\text{EV}} \leq P_{\text{EV}_{max}} \tag{2}$$

In order to avoid large variations in the charging rate over consecutive time steps, which is undesirable for current battery technology [15], a rate of change constraint is also imposed (3).

$$P_{\text{EV}}{}^{t-1} - \Delta \;\leq\; P_{\text{EV}}{}^{t} \;\leq\; P_{\text{EV}}{}^{t-1} + \Delta \tag{3}$$

Here, *t* is the current time step and Δ is a defined limit, in kW, by which the charging rate can vary, compared to the charging rate at the previous time step, excluding on/off transitions.

For the LCC method, the EV charger unit has the capability to monitor the voltage at its own CPOC and the loading on the service cable supplying the customer residence only. The addition of EV loads, for the most part, will cause the voltage at various points of the network to drop. The extent of the voltage drop can vary depending on a number of factors, which include the location of the EV on the network and the rate of charge. The voltage at each CPOC must be maintained within the rated voltage range specified for the network, (4).

$$V_{min} \leq V_{\text{CPOC}} \leq V_{max} \tag{4}$$

Here, V_{CPOC} (V) is the voltage at the CPOC, while V_{min} and V_{max} are the minimum and maximum allowable network voltage levels respectively. The thermal loading of the service cable refers to the total current flowing through the cable. This constraint is summarised in (5).

$$L_{\text{SC}} \leq L_{\text{SC}_{max}} \tag{5}$$

Here, L_{SC} is the thermal loading of the service cable and $L_{\text{SC}_{max}}$ is the current rating for the fuse at the CPOC for the household.

D. Network Sensitivities

As stated in Section II-B, for the LCC method, the network voltage and loading sensitivities to the addition of EV load are predetermined. Only one set of sensitivities is used for all time steps, which allows the charging unit at each household to determine an optimal charge rate without the need to calculate a new set of sensitivities at each time step. However, these sensitivity values cannot be expected to match the constantly varying load on the feeder. In order to determine the set of voltage and loading sensitivities for the LCC method, a series of unbalanced, 3-phase load flow calculations are performed on the test network using power system simulation software [16]. These load flow calculations determine the change in voltage and loading levels at all points on the network subject to the addition of EV load at each CPOC. In order to model the expected residential load during charging periods, each household is assigned a 2 kW load, which approximates the maximum average household demand over all time steps in winter. The sensitivity values for the voltage and loading assigned to a charging unit are the summation of all the voltage and loading sensitivities at all other CPOCs on the feeder respectively. This takes account of the impact that multiple EV loads, charging simultaneously, can have on a particular node and service cable on the feeder. This fixed sensitivity value is used in conjunction with the CPOC voltage and service cable loading measurements at each time step in order to determine the optimal charging rate for the EV. The constraint equations for the CPOC voltage and service cable loading are summarised as,

$$V_{min} \leq V_{init} + \mu P_{\text{EV}} \leq V_{max} \tag{6}$$

$$L_{\text{SC}_{init}} + \beta P_{\text{EV}} \leq L_{\text{SC}_{max}} \tag{7}$$

where, in (6), V_{init} is the initial voltage at the CPOC. μ (V/kW) is the summation of the voltage sensitivities at each CPOC due to power demanded by that EV. For (7), $L_{\text{SC}_{init}}$ is the initial loading on the service cable supplying the EV, and β (A/kW) is the summation of the loading sensitivities for each service cable due to power demanded by that EV.

E. Centralised Control

Centralised control of EV charging involves monitoring the voltage at each CPOC, the thermal loading of each household's single-phase service cable, the loading of the LV transformer and the 3-phase mains cable supplying the feeder, and also the battery state of charge for each connected EV. This information is sent to a centralised controller which incorporates additional network information to determine dispatch signals at each time step for the individual EV charger units accordingly. The sensitivities of the voltage and thermal loading of the network to EV load are calculated in advance for each time step. The centralised controller is also aware of all network voltages and line flows, which allows for a more accurate insight into the instantaneous network condition than is possible with the local control method. The controller then optimises the charge rate of each vehicle in order to deliver the maximum amount of power delivered to all EVs on the feeder, and thereby making best use of the network capacity. The process occurs at each time step and is independent of all other time steps with the exception of the rate of change of charge constraint (3).

The objective function for the centralised control method, F_{CCC}, is given by

$$F_{\text{CCC}} = \sum_{i=1}^{N} \left(1 - \left(\frac{\text{BSOC}_i}{\text{BSOC}_{max_i}} \right) \right) P_{\text{EV}_i} x_i \tag{8}$$

where N is the number of customers being served by the network, and P_{EV_i} is the power delivered, measured in kW, to the EV connected at the *i*th CPOC. x_i is zero when an EV is not connected at the *i*th CPOC or the EV battery is fully charged, while x_i equals one when the EV at the *i*th CPOC is connected and the EV battery is less than fully charged. BSOC_i is the current battery state of charge (kWh) for the EV connected at the *i*th CPOC and BSOC_{max_i} is the maximum battery capacity of that EV.

In (8), the objective function is weighted according to the current BSOC of each individual EV. This weighting provides a more even distribution of energy to charging EVs and prioritises EVs with a low BSOC [6].

The centralised control charging technique considers the same constraints as the local control method (i.e. (2),(3),(4) and (5)), along with constraints ensuring that the rated loading of the network transformer and the mains cable supplying the feeder from the transformer are not exceeded. It is assumed that the necessary monitoring and communication equipment is installed on the feeder and that the data collected, along with the data from the AMI of the customers, can be utilised in determining the optimal charging rates for the EVs on the feeder. A more detailed description of the method and constraints for the centralised control method can be found in [6].

III. Simulation Data

A. Distribution Network

The test network is based on a LV residential distribution feeder in a suburban area of Dublin, Ireland. A simplified representation of the feeder is given in Fig. 1. In the actual test feeder, each household, EV and service cable are modelled separately. The model incorporates a 400 kVA, 10/0.4 kV step-down transformer supplying a feeder of 74 residential customers through 432 m of 3-phase mains cables and 2.16 km of single-phase service cables. A lumped load model, representing a similar number of residential customer loads with no EV loads, is included to represent another feeder being supplied from the same transformer.

In Ireland, the LV distribution network is operated at a nominal voltage of 230/400 V with a voltage range tolerance of

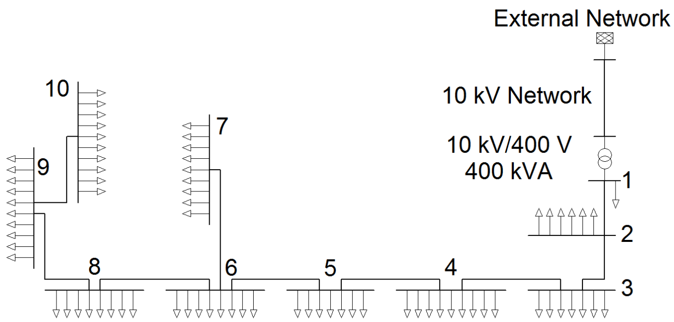

Fig. 1. Single line diagram of test network.

+/-10% [18]. The transformer modelled here does not have any tap-changing capability, which is typical of LV transformers in Ireland. As such, the medium voltage (MV) network supplying the LV transformer is included in the model as an equivalent impedance in order to take account of the voltage drop at this network level. The MV network is modelled such that at maximum residential load (with no EV charging) the voltage at all points of the network does not exceed -10% of nominal. The voltage at the sending end of the MV network is set at 1.05 pu. Specifications for the network model components were supplied by Electricity Supply Board (ESB) Networks, who are the DSO in the Republic of Ireland.

B. Residential Customer Load Modelling

Load data for domestic electricity demand customers was obtained from the DSO consisting of 15-minute time-series demand data for high, medium and low use customers over a one year period. These profiles were subject to time-of-day pricing whereby the cheaper, off-peak tariff begins at 11 pm each day and ends at 8 am the following day. Different electricity demand profiles were randomly assigned to each of the houses in the test network. In order to confirm that these load profiles portrayed an accurate representation of the power demanded by a real distribution feeder, the coincidence factor of the test network was determined. The coincidence factor is defined as the ratio of the maximum diversified demand divided by the maximum non-coincidental demand. From assessing the yearly load profiles for each of the households on the network, the coincidence factor was found to be 0.36, which compares favourably with networks serving a similar number of customers [19]. For modelling purposes, the power factor for each household load is set at 0.95 inductive. The load is modelled as a combination of 50% constant power (P) and 50% constant impedance (Z).

C. Electric Vehicle Load Modelling

It is assumed that each EV is connected at the same CPOC as the household load through a single-phase connection. Charging profiles for EVs can vary depending on battery type, charging equipment and the electricity supply network. For this work, all EV batteries are modelled with a capacity of 20 kWh. The EV charging equipment is assumed to have a maximum charging rate of 4 kW with a 90% efficiency rating. The charging rate of 4 kW is appropriate in terms of the power delivery capabilities of existing LV distribution networks in Ireland [18]. The EV batteries are modelled as constant power loads at unity power factor.

D. Time Periods for Investigation

1) Sample 24-hour Period: In order to demonstrate each of the charging strategies, a sample 24-hour time period within the one year period of residential load data was chosen. The time period selected is from 12 noon to 12 noon the following day and spans two weekdays in January. Due to the assumption that all customers are subject to a time-of-day tariff scheme, a large residential demand is experienced on the feeder once the cheaper off-peak period begins. The maximum demand on the feeder during this period is 270 kW.

In both cases, a 50% penetration of EVs on the feeder was examined, which means that 37 of the 74 households had exactly one EV charging at certain stages of the 24-hour period. While a 50% penetration of EVs on a distribution feeder may not be experienced for many years to come, it was deemed appropriate to examine such a scenario in order to fully capture the benefits of controlled charging strategies compared to uncontrolled charging. For the simulations, the EVs were allocated to the network in a random manner and the locations remained fixed for each of the charging strategy cases examined. The potential combined maximum demand from a 50% penetration of EVs is 148 kW. EV usage data was obtained from DSO led vehicle trials in order to determine a plausible range of connection times, durations of connection, and initial BSOC levels for the EVs in the simulations [20]. Based on this data, the connection time for each EV is randomly assigned within a time frame of +/-3 hours of 11 pm, which is the start of the off-peak period. The duration of connection for each EV is also randomly assigned, whereby a vehicle remains connected for anywhere between 6 and 15 hours. Each EV is also assigned an initial BSOC, independent of the connection time, at the beginning of the charge period, determined as a random value between 0% and 75% of the maximum battery capacity of 20 kWh, which ensures that each EV has a charge requirement of at least 25% of their battery capacity upon connection. The distribution of the initial BSOC for each EV is shown in Fig. 2. Table I shows the breakdown of EVs allocated on the feeder along with the total energy requirement of these vehicles on a phase by phase basis.

TABLE I
INITIAL EV CONDITIONS

	Number of EVs	**Combined Battery Capacity (kWh)**	**Combined Initial BSOC (kWh)**	**Total Energy Required (kWh)**
Phase a	12	240	86	154
Phase b	13	260	84	176
Phase c	12	240	53	187
Total	37	740	223	517

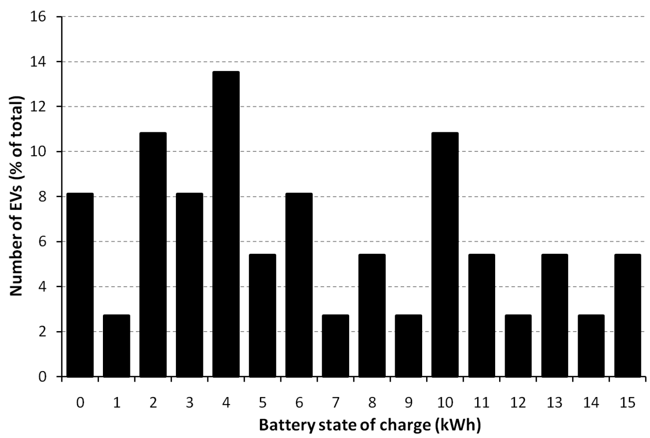

Fig. 2. Distribution of the initial BSOC for EVs.

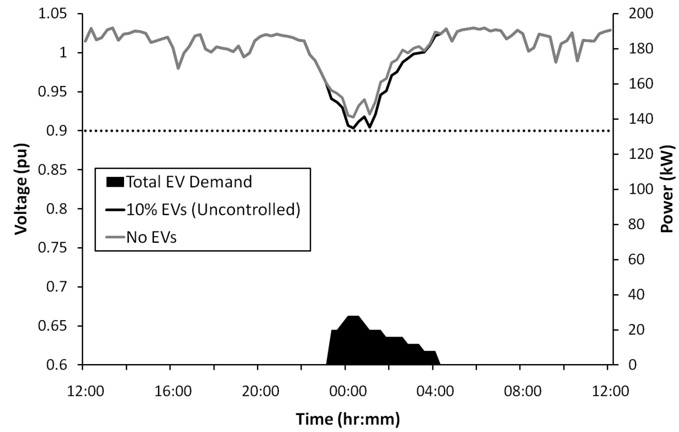

Fig. 3. Lowest CPOC voltage for base case and uncontrolled charging case, including the power demand from the EVs for the uncontrolled case.

2) Stochastic Scenario Analysis: The charging period identified above examines the LCC and CCC optimisation techniques for a specific network scenario. In order to investigate a wider range of scenarios, a stochastic tool, similar to one developed in [21], was used to generate different residential load scenarios with probabilistic conditions for varying residential load, EV location, initial BSOC and duration of connection.

Probability distribution functions (PDFs) for the household load were created based on the residential load data provided by the DSO, with PDFs for low, medium and high use customers. 15-minute household load profiles were then generated for each house for a 24-hour period from 12 noon on a winter weekday to 12 noon the following day, similar to the example 24-hour period. At the beginning of each 24-hour period the EV locations on the network were randomly selected with each EV then assigned an initial BSOC and duration of connection time. The duration of connection is randomly determined between 6-15 hours. The load model and power factor for both the residential and EV load remain the same as for the example 24-hour period analysis.

IV. Results and Discussion

Both controlled charging strategies are tested for the sample 24-hour period, with the results compared to cases with no EVs charging and with uncontrolled EV charging.

A. Uncontrolled EV Charging

In a scenario where no active control of EV charging is present, an EV, once connected, will charge at a maximum rate of 4 kW until it reaches a full BSOC. With distribution networks not rated to accommodate large penetrations of this type of load, a limit on the number of EVs allowed would have to be put in place to ensure that the network always remains within acceptable operating limits.

For the purposes of comparison, an example uncontrolled charging scenario was created whereby there is a limit to the number of EVs that are allowed to charge simultaneously. This number was determined by incrementally adding EVs, charging at their maximum rate of charge, to the feeder up to the point before the feeder exceeds an allowable operating limit. This test was performed with the residential load at the maximum expected demand for the example 24-hour period. For the test network utilised in this work, the predetermined number of EVs that could be allowed to charge in an uncontrolled scenario was found to be 7 ($\approx$ 10% of households).

Fig. 3 shows a profile of the lowest recorded CPOC voltage on the feeder for each time step for both the base case with no EVs and an uncontrolled case with a 10% penetration level. The total power delivered to the EVs at each time step is also shown. EV charging is assumed to commence once the off-peak period begins (i.e. 11 pm), although a number of EVs connect after this time also. As the figure shows, the introduction of EV charging during this time period pushes the lowest CPOC voltage towards the lower acceptable limit. Any further increase in the number of charging EVs at the beginning of the off-peak time period would likely result in the lower voltage limit being exceeded. The amount of energy delivered to the EVs in this scenario was 80.1 kWh.

B. Controlled EV Charging

The LCC method described in Section II is employed to optimise the charging rates of the EVs connected to the network. The rate at which each EV charges is now optimised individually in order to deliver the maximum power to the EVs while maintaining the voltage and service cable loading within acceptable operating limits for each time step. At the beginning of the charging period, the total energy required to return all EVs to 100% BSOC is 517 kWh. For the optimisation process, the lower voltage limit is set at 0.92 pu, which allows for a margin of safety with respect to the lower voltage limit (0.9 pu) defined in the Irish distribution network code [18]. This ensures that any unexpected short term variations in the demand will not cause the network to exceed its operating limits. The maximum variation allowable for the rate of charge between time steps, i.e. Δ in (3), is set at 1 kW for both control strategies. Values for the voltage sensitivities, μ in (6), were calculated to be in the range -0.02 to -0.045 V/kW. CPOCs located at the extremities of the feeder were found to be more sensitive to the addition of EV load than those located near

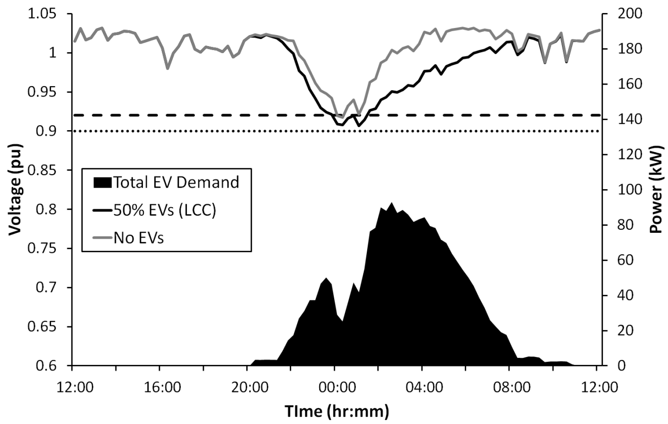

Fig. 4. Lowest CPOC voltage for base case and local control charging case, including the associated power demand from the EVs.

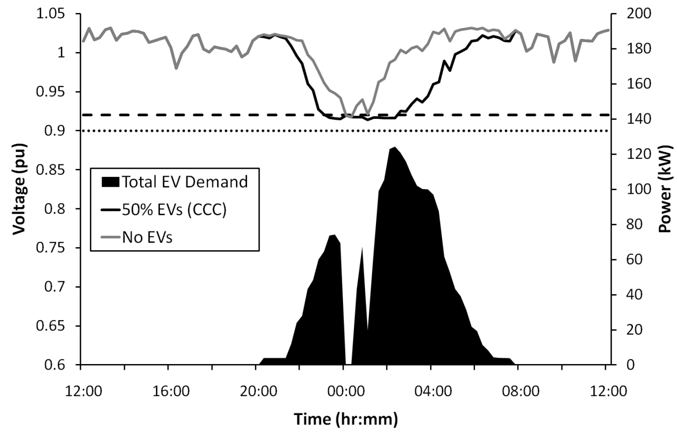

Fig. 5. Lowest CPOC voltage for base case and centralised control charging case, including the associated power demand from the EVs.

the start of the feeder. This characteristic is to be expected of a radial feeder. The loading sensitivities, β in (7), of the single-phase service cables were calculated to be in the range 8.2 to 8.7 A/kW.

The sample 24-hour time period is tested utilising the controlled charging method for an EV penetration level of 50%. Fig. 4 shows the lowest recorded CPOC voltage on the feeder for the base case and the LCC case, and shows that the control method has maintained the lowest voltage above the lower voltage limit of 0.9 pu. The method has achieved this by curtailing EV charging during periods of high residential demand and shifting it to a later stage of the night. However, due to the inability of individual charging units to know the network conditions at the other CPOCs on the network, each unit is unaware of how many EVs are charging at the same time step. This can potentially lead to network conditions exceeding values determined by the individual charger units in their optimisation calculations. An example of this can be seen in Fig. 4, where the lowest CPOC voltage has reached a value closer to the network limit of 0.9 pu, rather than the specified limit of 0.92 pu. At the following time step, individual charger units recognise that a limit has been exceeded and automatically attempt to rectify the situation by adjusting their charging rate accordingly.

Fig. 5 shows the results for the lowest CPOC voltage recorded for the case employing the centralised control method. When compared to the LCC method, it can be seen that the centralised control technique results in the lowest recorded CPOC being much tighter to the specified voltage limit than in the local control case. Due to the calculation of a new set of sensitivities and knowledge of current network conditions at each time step, the network controller has a much greater insight to the condition of the network at all CPOCs. This allows for a far more accurate dispatch of EV charge rates, resulting in more charge being delivered to the EVs while maintaining acceptable network operating conditions. An example of this can be seen in the EV demand profile for both methods. In Fig. 4, even though the base case lowest voltage is already at the specified lower limit just after midnight, the local control technique leads to some EVs requesting charge, which results in a further voltage drop. At the same instant, using the centralised control technique, the controller switches off all EV charging on the network until the lowest base case voltage increases above the specified limit.

The centralised control method's ability to update the set of sensitivities and measure all network conditions at each time step allows it to deliver the maximum amount of power to the EVs, which results in the network capacity being utilised to the fullest extent at each time step. However, in the local control case the sensitivities are fixed, which results in less power being dispatched to the EVs even though the network is not at any of the specified limits. This results in the LCC method taking longer to charge all of the EVs, as shown in Fig. 6, where the black area represents the electricity demand from the EVs. In some cases, this can result in EVs finishing their charge period with less than 100% BSOC due to the charger units not utilising the network capacity to its fullest. For both methods, the BSOC upon disconnection from the network is shown in Fig. 7. It can be seen that the local control case results in 3 of the 37 EVs having a final BSOC of less than 100%, with the lowest being 90%. Because the centralised control method can deliver more power earlier in the charging period it results in all 37 EVs having a full BSOC by the end of the period. Details of the total energy delivered to the EVs for both control charging methods are given in Table II.

TABLE II
TOTAL ENERGY DELIVERED TO EV BATTERIES

	Total Energy Delivered (kWh)	**% Energy Requirement (for 50% EVs)**
10% EVs (Uncontrolled)	80.1	15.5
50% EVs (LCC)	513	99.2
50% EVs (CCC)	517	100

For both of the methods tested, the lowest CPOC voltage was found to be the binding constraint for the optimisation. Fig. 8 shows the greatest loading for all service cables at each time step. While the service cable loading is considered by

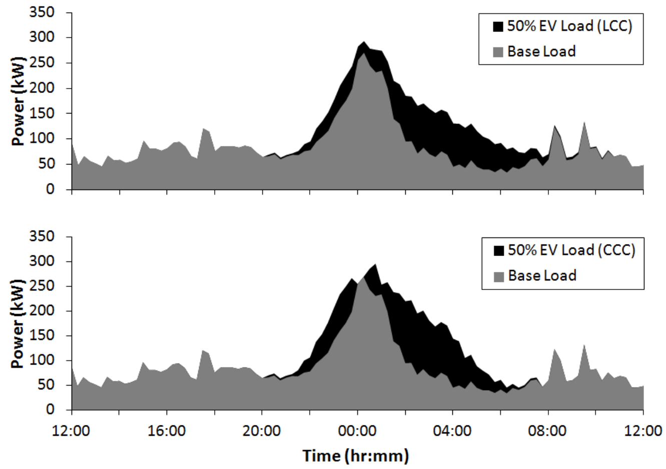

Fig. 6. Network demand profiles for the local control and centralised control charging scenarios.

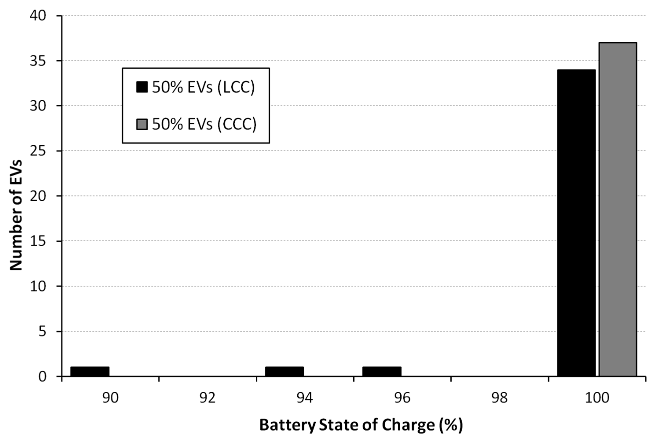

Fig. 7. Final BSOC for EVs for local and centralised control charging scenarios.

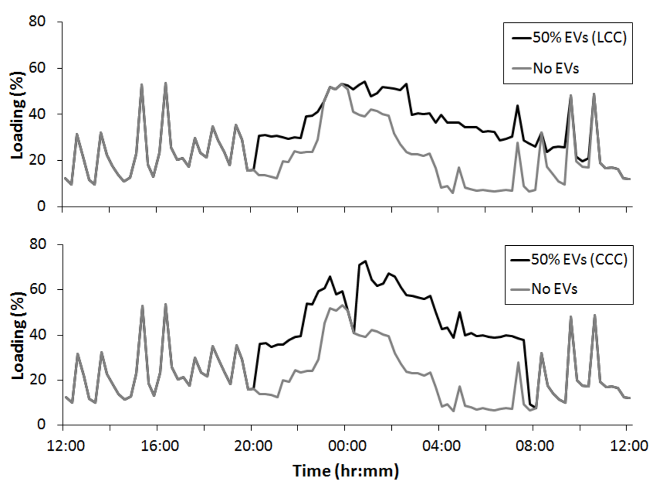

Fig. 8. Loading of service cable with greatest loading for each time step for the local control and centralised control charging scenarios.

both methods it is clear that it is never a binding constraint for the 24-hour period examined.

The CCC technique also considers the loading on the network transformer and the loading on the 3-phase mains cable supplying the feeder from the transformer. For the 24-hour period examined here, neither the transformer nor the mains cable loading are ever the binding constraint, as shown in Table III.

TABLE III
MAXIMUM NETWORK COMPONENT LOADING

	Transformer (%)	Mains Cable Phase a (%)	Mains Cable Phase b (%)	Mains Cable Phase c (%)
No EVs	75.7	55.2	37.1	53.6
10% EVs	81.9	59.4	52.1	57.8
50% EVs (LCC)	82.1	61.8	55.5	69.3
50% EVs (CCC)	80.1	68.9	64.0	71.5

Network losses as a percentage of the total energy delivered to the network over the 24-hour period were also recorded. The increased demand from EV charging causes the losses ratio to increase slightly for all cases compared to the base case (1.1%). For the 10% EV penetration with uncontrolled charging, the losses ratio was found to be 1.3%. The local control case (1.8%) incurs less losses on the network when compared to the centralised case (2.1%) but has delivered less energy to the EVs over the charging period.

C. Stochastic Scenario Analysis

A stochastic analysis of both charging strategies was performed in order to provide insight into operation of the optimisation process while accounting for the variability and uncertainties associated with EV charging, as described in Section III-D2. Each of the charging techniques were simulated on the test network for 300 distinct 24-hour periods (i.e. 28,800 time steps) during winter.

Fig. 9 shows the distribution of measured voltages for all CPOCs over all charging periods for the scenario with no EVs on the network and the scenarios for both controlled charging methods. There is a significant increase in the frequency of voltage levels nearer to the specified lower voltage limit (0.92 pu), with a small increase in the number of occurrences below this limit for both controlled charging methods. There are also more occurrences, using the CCC method, when the lowest CPOC voltage is at the specified limit, which demonstrates better utilisation of the network capacity. As explained in Section IV-B, this is due to the LCC method operating on a fixed set of sensitivity values and utilising local network information only, as opposed to the CCC method which updates the sensitivities at each time step and has exact knowledge of all network voltages and line flows.

The distribution of thermal loading levels measured on each of the single-phase service cables is shown in Fig. 10. For the majority of recorded values the loading is below 60% of the rating. The service cable loading is only a binding constraint for a very small fraction of the measured samples (i.e. less than 0.01%).

Finally, the distribution of the final BSOC for all the EVs for each charging period is shown in Fig. 11. The LCC method

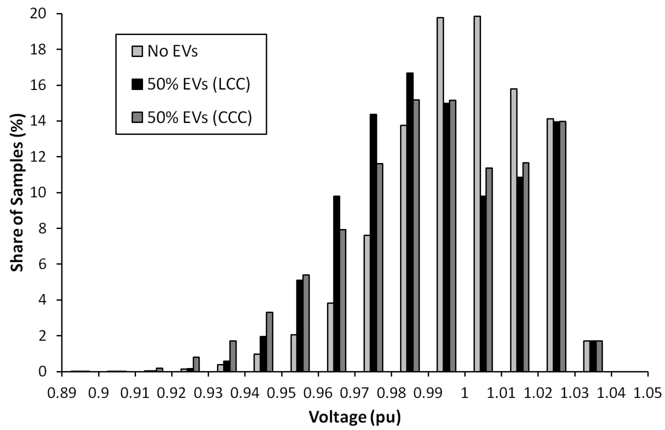

Fig. 9. Distribution of measured voltages at network CPOCs.

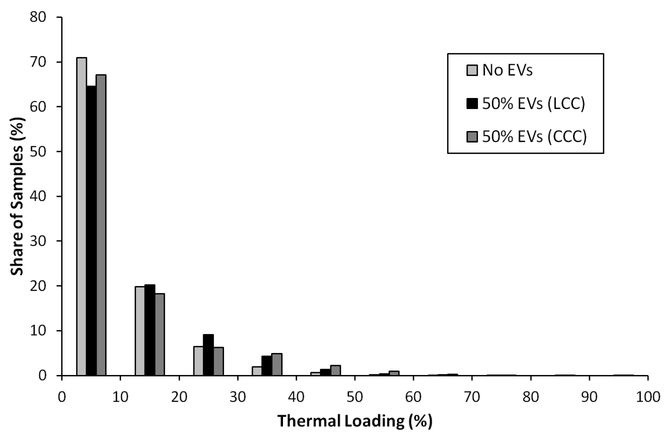

Fig. 10. Distribution of measured thermal loading levels of single-phase service cables.

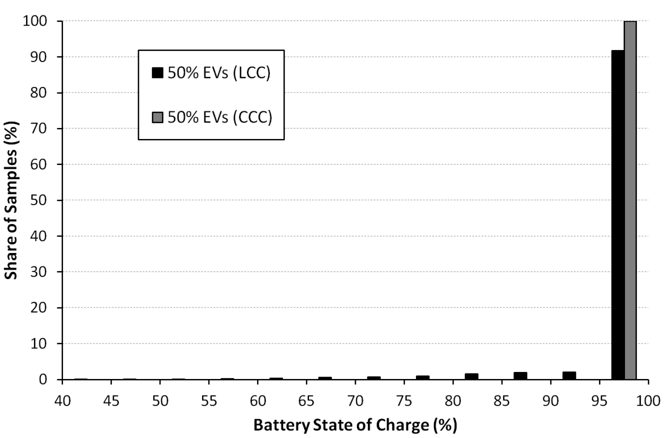

Fig. 11. Distribution of final BSOC levels for all charging periods.

resulted in over 90% of all final BSOC values being within 95-100%, with 97% of all values above 80%. For each of the CCC method charging periods, 100% of the final BSOC values were found to be within 95-100% of the maximum capacity.

V. Conclusion

This work has demonstrated the benefits of controlled charging for a high penetration of EVs charging on a LV network. A local control method was proposed whereby each individual EV charger maximises the charging rate of its EV while maintaining the CPOC voltage and service cable loading within acceptable limits. The method was tested on a LV test network and the results were compared to those employing a centralised control method.

The results indicate that the local control method allows a far greater penetration of EV charging on a feeder than that which could be accommodated with uncontrolled charging. While the technique can deliver a similar amount of energy to the EVs within a certain time period when compared to the centralised control method, it is not as capable at maintaining network parameters within specified limits and may require larger safety margins. However, introducing a number of predefined sets of sensitivities, each calculated based on the expected residential load for a given scenario (e.g. day/night, weekday/weekend, seasonal, etc.), could improve the performance of the local control method.

The network and communications infrastructure required to implement the local control method would be far less than that required for the centralised control case. Individual controllers would also be able to act independently and not be reliant on external controller signals in order to operate. As such, investing in a centralised control technique may not be required until very high penetrations of EVs on LV networks become a reality. With the introduction of AMI, a local control technique may be sufficient for accommodating initial penetrations of EV charging while maintaining network limits within the desired operating regions.

A summary of the advantages and disadvantages for both the LCC and CCC methods is given as follows:

Local Control Charging
Advantages:
· Minimal communications infrastructure required
· Sufficient for lower EV penetration levels
Disadvantages:
· No communication links to rest of network
· Larger safety margin required to maintain operating limits

Centralised Control Charging
Advantages:
· Real time insight into operating conditions at all points on network
· Better utilisation of network capacity
· Option to include BSOC weighting
Disadvantages:
· Requires significant communications infrastructure across network
· Requires 3rd party to control charging rates

Acknowledgment

The authors would like to acknowledge ESB Networks for providing the necessary data to perform this work. Thanks are also due to Jason Taylor of EPRI.

References

[1] K. Schneider, C. Gerkensmeyer, M. Kintner-Meyer and R. Fletcher, "Impact assessment of plug-in hybrid vehicles on Pacific Northwest distribution systems", *In Proc. IEEE Power and Energy Society General Meeting*, Pittsburgh, Pennsylvania, USA, July 2008.

[2] C. Gerkensmeyer, M. Kintner-Meyer and J.G. DeSteese, "Technical challenges of plug-in hybrid electric vehicles and impacts to the US power system: distribution system analysis", Pacific Northwest National Laboratory Report, January 2010.

[3] J. Taylor, A. Maitra, M. Alexander, D. Brooks and M. Duvall, "Evaluation of the impact of plug-in electric vehicle loading on distribution system operations", *In Proc. IEEE Power and Energy Society General Meeting*, Calgary, Canada, July 2009.

[4] S. Shao, M. Pipattanasomporn and S. Rahman, "Challenges of PHEV penetration to the residential distribution network", *In Proc. IEEE Power and Energy Society General Meeting*, Calgary, Canada, July 2009.

[5] G. A. Putrus, P. Suwanapingkarl, D. Johnston, E. C. Bentley and M. Narayana, "Impact of electric vehicles on power distribution networks", *In Proc. IEEE Vehicle Power and Propulsion Conference*, Dearborn, Michigan, USA, September 2009.

[6] P. Richardson, D. Flynn and A. Keane, "Optimal charging of electric vehicles in low voltage distribution systems", *IEEE Transactions on Power Systems*, 2011 (In Press).

[7] K. Clement, E. Haesen and J. Driesen, "The impact of charging plug-in hybrid electric vehicles on a residential distribution grid", *IEEE Transactions on Power Systems*, vol. 25, no. 1, pp. 371-380, 2010.

[8] J. A. Peças Lopes, S. A. Polenz, C. L. Moreira and R. Cherkaoui, "Identification of control and management strategies for LV unbalanced microgrids with plugged-in electric vehicles", *J. Electric Power Systems Research*, vol. 80, issue 8, pp. 898-906, 2010.

[9] J. A. Peças Lopes, F. J. Soares, and P. M. R. Almeida, "Integration of electric vehicles in the electric power system", *Proceedings of the IEEE*, vol. 99, no. 1, pp. 168-183, 2011.

[10] E. Sortomme and M. A. El-Sharkawi, "Optimal charging strategies for unidirectional vehicle-to-grid", *IEEE Transactions on Smart Grid*, vol. 2, no. 1, pp. 131-138, 2011.

[11] W. Su, and M.-Y. Chow,"Performance evaluation of an EDA-based large-scale plug-in hybrid electric vehicle charging algorithm", *IEEE Transactions on Smart Grid*, Special Issue on Transportation Electrification and Vehicle-to-Grid Application, 2011. (In Press)

[12] K. J. Dyke, N. Schofield, and M. Barnes,"The impact of transportation electrification on electrical networks", *IEEE Transactions on Industrial Electronics*, vol. 57, no. 12, pp. 3917-3926, 2010.

[13] A. Brooks, E. Lu, D. Reicher, C. Spirakis and B. Weihl, "Demand dispatch: using real-time control of demand to help balance generation and load." *IEEE Power and Energy Magazine*, vol. 8, no. 3, pp. 20-29, May/June 2010.

[14] S. Acha, T. C. Green and N Shah, "Effects of optimised plug-in hybrid vehicle charging strategies on electric distribution network losses", *In Proc. IEEE Power and Energy Society Transmission and Distribution Conference and Exposition*, New Orleans, Louisiana, USA, April 2010.

[15] F. Hoffart, "Proper care extends Li-ion battery life". *Power Electronics Technology*, April 2008.

[16] DIgSILENT PowerFactory. DIgSILENT GmbH.

[17] MATLAB R2009a. The MathWorks, Inc.

[18] ESB Networks Distribution Code, October 2007. Available: *http://www.esb.ie/esbnetworks/en/downloads/Distribution-Code.pdf*

[19] H. L. Willis, *Power Distribution Planning Reference Book*. Basel: Marcel Dekker, 2004.

[20] ESB and EPRI Smart Grid Demonstration Project Overview. Available: *http://smartgrid.epri.com/DemoProjects.aspx*

[21] P. Richardson, J. Taylor, D. Flynn and A. Keane, "Stochastic analysis of the impact of electric vehicles on distribution networks", *In Proc. CIRED 21^{st} Intl. Conf. on Electricity Distribution*, Frankfurt, Germany, June 2011.

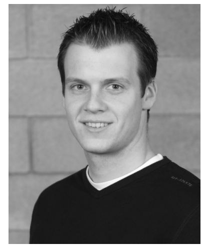

Peter Richardson (S'08, M'12) completed his B.E. and Ph.D. degrees in Electrical Engineering in University College Dublin in 2007 and 2012 respectively. His research interests include electric vehicles, distributed energy resources and distribution systems.

Damian Flynn (M'96, SM'11) is a senior lecturer in power engineering at University College Dublin. His research interests involve an investigation of the effects of embedded generation sources, especially renewables, on the operation of power systems. He is also interested in advanced modelling and control techniques applied to power plant.

Andrew Keane (S'04, M'07) received B.E. and Ph.D. degrees in Electrical Engineering from University College Dublin in 2003 and 2007 respectively. He is currently a lecturer with the School of Electrical, Electronic and Communications Engineering, University College Dublin with research interests in power systems planning and operation, distributed energy resources and distribution networks.